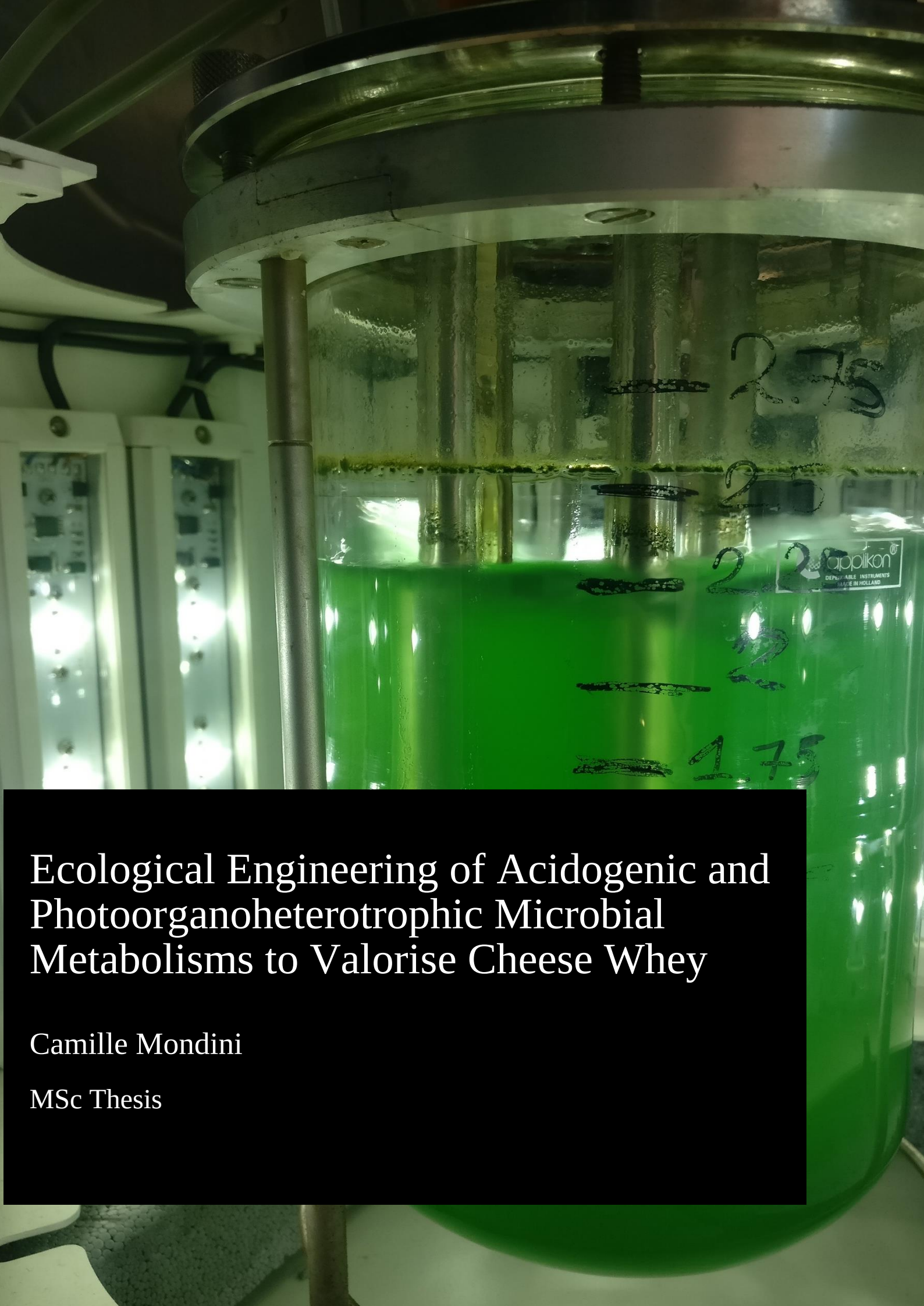

Ecological Engineering of Acidogenic and Photoorganoheterotrophic Microbial Metabolisms to Valorise Cheese Whey

Camille Mondini

MSc Thesis

MSc Thesis

Ecological Engineering of Acidogenic and Photoorganoheterotrophic Microbial Metabolisms to Valorise Cheese Whey

by

Camille Mondini

(Student number: 4751930)

in partial fulfilment of the requirements for obtaining the degree of

Master of Science in Civil Engineering

at Delft University of Technology

to be defended publicly on Friday, December 13, 2019, at 01:15 PM

This thesis was performed at the Weissbrodt Group for Environmental Life Science Engineering,
Environmental Biotechnology Section, Department of Biotechnology, Faculty of Applied Sciences,
van der Maasweg 9, 2629 HZ Delft, Netherlands
www.tudelft.nl/davidweissbrodt

on international collaboration with

Gustavo Mockaitis Group / Interdisciplinary Group of Biotechnology for Agriculture and the Environment,
University of Campinas (Unicamp), Faculty of Agricultural Engineering
Avenida Cândido Rondon, 501, Cidade Universitária, 13083875 Campinas, SP, Brasil
https://www.feagri.unicamp.br/gbma/

Correspondence:
D.G.Weissbrodt@tudelft.nl ; mp8109@gmail.com ; C.Mondini@student.tudelft.nl / mondinicamille@gmail.com

Project duration: April 15, 2019 – December 13, 2019

Thesis direction:	David Weissbrodt, Assistant Professor, TU Delft /TNW; Thesis director and chair of committee Maria Paula Giulianetti de Almeida, PhD candidate, Unicamp, Brazil and visiting PhD candidate, TU Delft; Co-supervisor
Committee members:	Merle de Kreuk, Full Professor, TU Delft /CiTG Ralph Lindeboom, Assistant Professor, TU Delft /CiTG Gustavo Mockaitis, Adjunct Professor, Unicamp, Brazil

Abstract

Green phototrophs such as microalgae and cyanobacteria have been proven to be able to perform photoorganoheterotrophic metabolism. The use of organic carbon can result in higher biomass production and increased concentrations of valuable compounds. Organic waste streams can serve for this purpose and lower the biomass production costs. Cheese whey, a by-product of the dairy industry with a high organic content, can be a suitable organic carbon source.

Previous studies have focused on axenic cultures, determining the species that can perform this metabolic pathway and the best substrates for their growth. However, the use of organic substrates by phototrophs in mixed microbial communities is less understood, as it is the result of multiple metabolic processes. As mixed cultures are economically preferable to pure ones, further research is needed to understand the competition mechanisms taking place in mixed-culture processes and how they can be engineered to promote the selection of phototrophs.

The first part of this work focused on the production and spectrum of volatile fatty acids from the acidogenic fermentation of 40% demineralized cheese whey. The maximum degree of acidification (77±7%) of 40% demineralized cheese whey (DWP40) was obtained when thermal (90°C) pre-treatment of the inoculum was applied and combined with a F/M ratio of 0.5 g COD g VS^{-1}.

The second part aimed to assess the selection for green phototrophs in a photoorganoheterotrophic mixed culture, using organic carbon sources derived from cheese whey, namely DWP40, lactose (as a model constituent of cheese whey), and acetate (as model volatile fatty acid derived from acidogenic fermentation of cheese whey). The cultivations were carried out in shake-flasks prior to implementation in a continuous-flow stirred-tank photobioreactor. DWP40, lactose, and acetate sustained the growth of green phototrophs in the mixed culture. Amongst the organic carbon sources, the use of acetate resulted in the highest biomass growth (170 mg VSS^{-1} L^{-1}) and pigment content (87 µg mg VSS^{-1}). The selection for phototrophic organisms was possible both in batch and continuous mode.

The results obtained showed that the conversion of the lactose inside cheese whey to acetate could improve its uptake by phototrophs. Their selection inside a photoorganoheterotrophic mixed culture can be improved by higher pH and inorganic nutrient concentrations, and lower dissolved oxygen levels.

Keywords: photoorganoheterotrophy - green phototrophs - cheese whey - mixed culture - photobioreactor

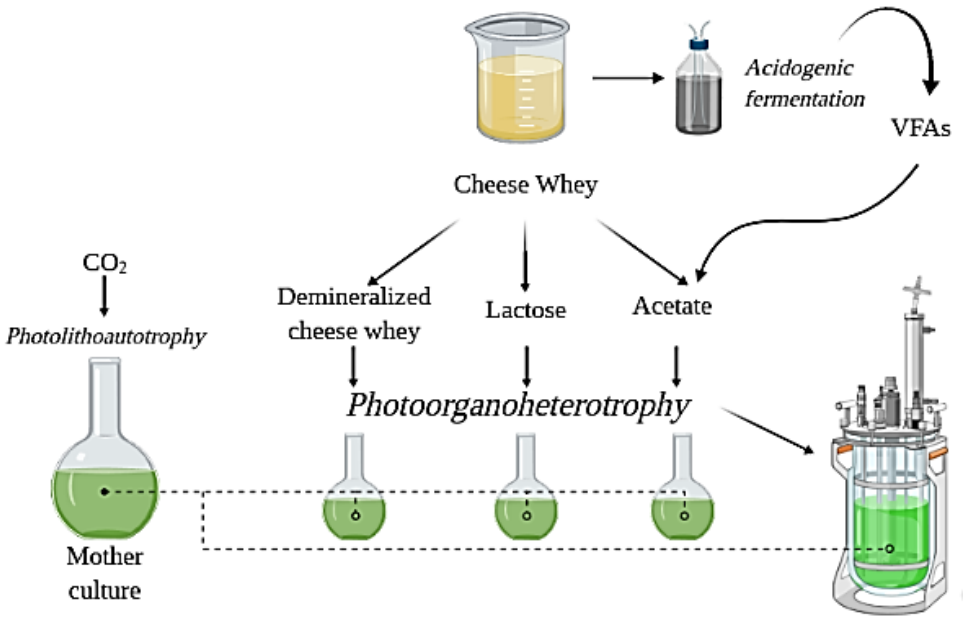

Acknowledgements

The journey leading to the composition of this work has been exciting, challenging, and at times, quite stressful. This work would not have been possible without the help of the wonderful people around me. I want to say thank you to all those that contributed, in one way or another, to the realization of this manuscript.

To Prof. David Weissbrodt for his dedication and enthusiasm for this project. For his meticulosity and precision, which pushes his students to always improve themselves. The long hours spent discussing the science of phototrophs together were always insightful and prolific.

To Prof. Gustavo Mockaitis, for sharing this project with the TU Delft and with me. To Prof. Merle de Kreuk and Prof. Ralph Lindeboom, for enthusiastically jumping on board. Thank you all for the precious feedback during our meetings and your availability.

To Maria Paula Giulianetti de Almeida, for introducing me to the world of phototrophs. Thank you for your passion, your tenacity, your knowledge, and your support. Despite the distance in the later months, you were always very much present and involved in every step. I hope that we will meet again soon.

To the great people working at the BT labs. To Sofie Rox, for her invaluable help inside the lab and her friendship outside of it, which made my time at EBT much simpler and more enjoyable. To Zita van der Krogt, *fairy godmother* of the labs, for helping out with pretty much everything. To Ben Abbas, for sharing his knowledge on molecular biology and for his availability and patience. To Dirk Geerts, Marcel Langeveld, and Rob Kerste for their help with building, assembling, and operating the photobioreactor. To Johan Knoll, for the many TOC analysis and his precious advice.

To the EBT group. So many of you have contributed to this work by sharing your knowledge, giving me feedback, and suggesting your advice or by helping me orient in the lab facilities. Thank you for being such nice and fun people to share the working environment with. A special thanks to my officemates, for all the good times and moral support during the bad ones.

To my friends in Delft. Thank you for bringing sunshine to the Netherlands and for going through this journey with me. You made my time at TU Delft so much better. To my flatmates, for their friendship and support, and for making our house a home. To Adrien, for bearing with me through the highs and the lows and never losing his positivity.

Finally, to the people back home. To my long-time friends in Milano, for staying close to me despite the distance and enabling me to make it to Delft in the first place. And mostly to my family, for always believing that I could achieve this goal and for always giving me the support necessary to actually do it.

Contents

Contents 1
List of Acronyms and Symbols 5
1. General introduction 7
2. State of the knowledge and research question 9
2.1 The potential of phototrophic cultures for bioprocessing and environmental purification 9
2.2 Metabolic pathways underlying growth in phototrophic cultures 10
2.3 Photoheterotrophic cultivations in waste and wastewater treatment: suitable substrates 12
2.4 Cheese whey: a valuable product or a highly polluting waste? 12
2.5 Cheese whey as a substrate for photoheterotrophic growth 15
2.6 Research gaps 15
2.7 Hypothesis and research question 16
3. Product spectrum during the acidogenic fermentation of cheese whey 19
3.1 Materials and Methods 19
3.1.1 Anaerobic sludge inoculum 19
3.1.2 Substrate solution with partially demineralized cheese whey powder 19
3.1.3 Experimental set-up 20
Thermal pre-treatment procedure 20
Thermal pre-treatment test set-up 20
F/M test set-up 20
3.1.4 Analytical and calculation methods 21
Sugars and fermentation products 21
Organic content, nitrogen and pH 21
Biogas composition 22
Analysis of the microbial community composition 22
3.2 Results 23
3.2.1 Partially demineralized cheese whey powder characterization 23
3.2.2 Effect of the thermal pre-treatment of the inoculum on the inhibition of methanogenesis and on the degree of acidification 23
Methanogenesis inhibition in the thermally pre-treated inoculums 23
Improvement of the degree of acidification by the pre-treated inoculums 24
Impact of the inoculum thermal pre-treatment and of the acidogenic fermentation of cheese whey on the microbial community composition 26
3.2.3 Effect of food-to-microorganism (F/M) ratio on the degree of acidification and VFA spectrum 27
Impact of the food-to-biomass (F/M) ratio on sugar consumption and acidification 27
Effect of the F/M ratio on the initial and final alkalinity 28
3.3 Discussion 30

3.3.1 Volatile fatty acids production was improved by the thermal pre-treatment of the inoculum, lower food-to-microorganism ratio and higher alkalinity 30
3.3.2 VFA spectra variations were not only defined by thermal pre-treatment or food-to-microorganism ratio 31
3.3.3 Carbon and COD losses could not be fully explained with the available data 31
4. Growth, selection, and competition of green phototrophs on cheese whey and derived organic compounds 33
4.1 Materials and Methods 33
4.1.1 Experimental set-ups for phototrophic cultures 33
Surface water inoculum 33
Incubator for shake-flask cultures 33
Enrichment mother culture 33
Shake-flask batch cultures for green phototroph selection 34
Continuous-flow photobioreactor 35
4.1.2 Analytical and calculation methods 37
Water quality parameters 37
Organic carbon sources and fermentation products 37
Phototrophic biomass 37
Flow cytometry analysis of cell counting and cell viability 37
Cell viability by methylene blue analysis 38
Analysis of the microbial community composition 38
Pigment extraction 38
4.2 Results 40
4.2.1 Characteristics of the photolithoautotrophic culture grown in shake-flasks: growth parameters, pigment content, and microbial populations 40
Biomass growth and cell viability 40
Influence of the C-content, N-source and gas exchange on the growth rate and biomass concentration 41
Pigment content 42
Individuation of phototrophic cells by phase-contrast microscopy 43
4.2.2 Photoorganoheterotrophic growth on partially demineralized cheese whey as the sole nutrient source 43
4.2.3 Identification of microbial populations from 16S and 18S rRNA gene amplicon sequencing 44
4.2.4 Mixotrophic cultures using acetate, lactose, cheese whey as a carbon source 45
Low carbon concentrations resulted in rapid organic carbon depletion and carbon dioxide utilization 45
Higher organic substrate concentrations allowed for the selection of green phototrophs in mixed cultures 46
4.2.5 C:N:P ratio determined the biomass production and the pigment content 48
4.2.6 Stirred-tank photobioreactor 49

Photobioreactor run under batch mode for photolithoautotrophy for the acclimatisation of green phototrophs 49

Photoorganoheterotrophic growth under continuous reactor regime was possible with an adequate retention time 50

4.3 Discussion 53

4.3.1 Culture enriched on BG-11 media produced a mixed culture of photolithoautotrophs and chemoorganoheterotrophs 53

4.3.2 Photoorganoheterotrophic mixed cultures could be grown using demineralized cheese whey, lactose, or acetate as a carbon source, with the selection of green phototrophs 54

4.3.3 Varying the nitrogen source, carbonate concentration, and dissolved oxygen level lead to differences in the growth of phototrophs 55

4.3.4 Selection mechanisms in the PBR under CSTR regime allowed the growth of green phototrophs 56

4.3.5 Carbon consumption and transformation in the PBR under CSTR regime was likely the result of symbiotic relationships between the metabolisms of different microbial populations 57

4.3.6 Acetate provided a better carbon source than lactose in batch photoorganoheterotrophic cultures, therefore pre-acidification of cheese whey may improve the phototrophic biomass harvesting 58

5. Conclusions 61

6. Recommendations 63

7. References 65

Appendix i

A. Biogas measurements in the acidogenic fermentation experiments i

B. COD consumption and VFA production in the acidogenic fermentation experiments iii

C. Cell counting and cell viability measurements v

D. Biomass calibration line from A_{750} vii

E. Nutrient consumption in the photoorganoheterotrophic cultures viii

F. Carbon dioxide in the off-gas and dissolved oxygen in the Photobioreactor x

List of Acronyms and Symbols

A_x	Absorbance at the *x* nm wavelength
AOA	Phototroph culture using acetate as a carbon source (A), allowing gas exchange (O), and using ammonium as a nitrogen source (A)
AOA_{100}	Phototroph culture using acetate as a carbon source (100-fold concentration, hence the subscript) (A), allowing gas exchange (O), and using ammonium as a nitrogen source (A)
AXA	Phototroph culture using acetate as a carbon source (A), not allowing gas exchange (X), and ammonium as a nitrogen source (A)
AXA_{100}	Phototroph culture using acetate as a carbon source (100-fold concentration, hence the subscript) (A), not allowing gas exchange (X), and using ammonium as a nitrogen source (A)
BG-11	Allen's Blue-Green Algal Medium
BOD	Biological Oxygen Demand
C	Carbon
Car	Carotenoids
C_X	Concentration of *X*
Chl_a	Chlorophyll A
Chl_b	Chlorophyll B
(s)COD	(Soluble) Chemical Oxygen Demand
CSTR	Continuous-flow stirred-tank reactor
CWON	Phototroph culture using demineralized cheese whey as a carbon source (CW), allowing gas exchange (O), and using nitrate as a nitrogen source (N)
$CWXA_{100}$	Phototroph culture using demineralized cheese whey as a carbon source (100-fold concentration, hence the subscript) (CW), not allowing gas exchange (X), and using ammonium as a nitrogen source (A)
DA	Degree of acidification
DMSO	Dimethyl sulfoxide
DO	Dissolved Oxygen
DWP40	40% demineralized cheese whey powder
F/M	Food-to-microorganism
FCM	Flow cytometry
GC	Gas Chromatograph
HPLC	High Performance Liquid Chromatography
LOA	Phototroph culture using lactose as a carbon source (L), allowing gas exchange (O), and using ammonium as a nitrogen source (A)
LOA_{100}	Phototroph culture using lactose as a carbon source (100-fold concentration, hence the subscript) (L), allowing gas exchange (O), and using ammonium as a nitrogen source (A)
LXA	Phototroph culture using lactose as a carbon source (L), not allowing gas exchange (X), and using ammonium as a nitrogen source (A)

LXA_{100}	Phototroph culture using lactose as a carbon source (100-fold concentration, hence the subscript) (L), not allowing gas exchange (X), and using ammonium as a nitrogen source (A)
MB	Methylene Blue
N	Nitrogen
P	Phosphorus
P_X	Production rate of the compound *X*
PBR	Photobioreactor
PHA	Polyhydroxyalkanoate
PI	Propidium Iodide
q_S	Substrate *S* conversion rate
TIC	Total Inorganic Carbon
(s)TOC	(soluble) Total Organic Carbon
T(S)S	Total (Suspended) Solids
V(S)S	Volatile (Suspended) Solids
$Y_{X/S}$	Yield of the product *X* from the substrate *S*

1. General introduction

Sustainable development is one of the main challenges of today's world (UN, 2019). Thus, the United Nations has set 17 sustainable development goals to be achieved for the year 2030. Many of these goals are centred on the protection of natural resources and the environment, while others indirectly defend the environment by including the hidden costs of the exploitation of natural resources in our production and consumption systems.

The pressure to protect natural resources originates in large part to the pollution caused by industrial production. Along with industries, municipal waste has been on the rise in the past decades and its management is an issue of utmost importance. Although legislation attempts to control these activities, much improvement is still needed (Tsakali *et al.*, 2010). This is especially true in developing countries, where limited wealth distribution and political instability play an active role in environmental degradation. To avoid pollution and to provide a solution for waste management, streams that once were considered as disposable are now regarded as resources.

An example of such streams is cheese whey. It is a by-product of the dairy industry originated during the production of cheese. If disposed as waste, it can cause severe pollution of the soil and water bodies due to its high organic content, salinity, and acidity (Tsolcha *et al.*, 2016). With adequate treatment, cheese whey can be transformed into high-end products thanks to its highly nutrient components. However, these treatments are often expensive and inaccessible in remote areas, where significant amounts of cheese whey are produced (Alves *et al.*, 2014).

Simple, low-cost alternatives are therefore required for the upgrading of cheese whey: biological treatments can serve to this purpose. A sustainable and widely applied option is the use of anaerobic digestion for biogas production. However, methane is not the only nor the most valuable product that can be produced by fermentation (Dahiya *et al.*, 2015). Volatile fatty acids (VFAs), which are produced during the acidogenic stage of anaerobic digestion, are a good example. Nevertheless, the excess bacterial biomass produced also constitutes a waste.

Green phototroph cultures are being increasingly studied as their biomass is highly nutritive and can constitute a feed for livestock and even be included in human foods (Odjadjare *et al.*, 2017). These cultures can also be engineered to enhance the content of the metabolites with higher values (Pulz and Gross, 2003). The phototrophic biomass can be further processed for extracting valuable products, most commonly pigments and lipids (Fei *et al.*, 2015; D'Imporzano *et al.*, 2018). Although typically considered autotrophic organisms, green phototrophs have been proved to be able to grow on organic carbon as well (Qiao *et al.*, 2009). This implies the possibility of using phototrophs to treat organic waste streams. The biological treatment of cheese whey by phototrophic biomass would be relatively inexpensive, prevent pollution of natural water bodies and deliver a valuable end-product.

This study focused on the potential of cheese whey-derived organics (demineralized cheese whey, lactose, and acetate) as substrates for the growth of green phototrophs in mixed-culture bioprocesses. Specifically, the state of the knowledge concerning the cultivation of phototrophs, their metabolic pathways, and the role they can play in biologically degrading cheese whey was critically reviewed from the scientific literature in order to underline the research gaps, main research question, working hypothesis, and experimental research objectives.

In short, this work aimed at understanding the selection mechanism for the guild of green phototrophs determined by the type of carbon substrate supplied to the biological system as a mean to drive the ecological engineering of phototrophic mixed cultures for the treatment and valorisation of cheese whey. A comparison between photolithoautotrophic and photoorganoheterotrophic growths on inorganic carbon (*i.e.*, carbon dioxide) and organic substrates derived from demineralized cheese whey was made. In the latter context, combination with acidogenic pre-fermentation of demineralized cheese whey was studied in order to define whether green phototrophs would better grow on the intrinsic organic mixture of demineralized cheese whey, on lactose (*i.e.*, the main organic component of demineralized cheese whey), or on volatile fatty acids from pre-fermented demineralized cheese whey.

First, the investigation method comprised batch experiments in shake-flasks to study *(i)* the product spectrum of the acidogenic fermentation of 40% demineralized cheese whey; *(ii)* the growth and enrichment of green phototrophs on carbonate, acetate, lactose, and demineralized cheese whey, out of a surface water sample. Then, a continuous-flow photobioreactor was designed, built, and operated to test the selection of green photoorganoheterotrophs on acetate, the competition of bacterial and eukaryal populations of this guild, the physiology of the predominant organism, and their potential competition with ordinary heterotrophic organisms in a mixed-culture process.

The significance of the research outputs was put back into the context of the microbial ecology of mixed culture photobiotechnology and of the use of green phototrophic biomass to treat and valorise aqueous organic residues from cheese whey. By understanding the ecology of microbial mixed cultures, it is possible to select the best conditions to optimize microalgal biomass production for further down-streaming.

2. State of the knowledge and research question

2.1 The potential of phototrophic cultures for bioprocessing and environmental purification

Phototrophic organisms are defined by their ability to capture and convert electromagnetic energy into chemical energy, which can be used for cellular maintenance and growth. This process drives the biogeochemical cycles of all existing ecosystems, directly and indirectly (Overmann and Garcia-Pichel, 2013). While terrestrial phototrophs mostly consist of plants, their variety in the aquatic ecosystem is richer: it includes plants, protists, archaea, phytoplankton and bacteria (Singh *et al.*, 2018). Phototrophs can use different parts of the light spectrum; green phototrophic microorganisms are characterized by the absorbance of red and blue light for their photosynthesis (Stomp *et al.*, 2007). Green phototrophs are found in different Domains and can have diverse structures, sizes, and metabolisms. They include eukaryotic algae, Cyanobacteria, green sulphur bacteria *Chlorobiaceae*, and filamentous green non-sulphur bacteria *Chloroflexi*.

Microalgae are amongst the oldest photosynthetic eukaryotes on Earth and the primary producers of aquatic ecosystems (Hu *et al.*, 2018). The phylum Cyanobacteria, despite being prokaryotic, is often included in the term *microalgae* because of the strong similarity amongst the two and is frequently referred to as the *blue-green microalga*. Eukaryotic microalgae and Cyanobacteria are unicellular, microscopic organisms, with a dimension ranging between 2-200 μm, with the ability to proliferate under harsh environmental conditions due to their simple structure (Odjadjare *et al.*, 2017). They operate oxygenic photosynthesis, using water as an electron donor and producing O_2. The light-harvesting pigments consist mainly of chlorophyll and carotenoids (Griffiths *et al.*, 2011). Growth rates of Cyanobacteria and eukaryotic microalgae can range between 0.1 and 10 d^{-1} and vary based on the species and the culture conditions, such as the nutrient composition, light intensity and spectrum, and temperature (Nielsen, 2006).

The cultivation of green phototrophs has been gaining increasing attention because of the many products that can be derived from it (Ting *et al.*, 2017; Hu *et al.*, 2018; Singh *et al.*, 2018). The algal biomass contains several valuable compounds, including lipids, proteins, pigments, and biopolymers (Fei *et al.*, 2015; D'Imporzano *et al.*, 2018). While similar products could also be obtained from terrestrial plants, the growth rates of microalgae are typically 5 to 10 times higher, with doubling times reaching 24 h (Yen *et al.*, 2013). The use of land can be significantly reduced. The same amount of the pigment *lutein* can be extracted from 500 m^2 of microalgal culture or 36 Ha of the terrestrial flower Marigold (Fernández-Sevilla *et al.*, 2010). It was estimated that with hardly 0.1% of the climatically suitable lands in the US (200,000 Ha) destinated to microalgae cultivation, 1.055 EJ of biofuel could be produced (Yen *et al.*, 2013). Unfertile land can be used as well (Chen *et al.*, 2019). Moreover, brackish or seawater can also be used, as several microalgal and cyanobacterial species are found in such environments (Yamagishi *et al.*, 2016). Such water sources cannot be used for terrestrial crops as their high salinity interferes with osmotic forces stunting water uptake by the roots and increases the pH leading to micronutrient deficiency (FAO, 2005).

Low-end and high-end products generated from phototrophic biomass can be used by food, aquaculture, nutraceutical, pharmaceutical, cosmetical and energetical industries (Chen *et al.*, 2019). Compounds such as pigments and proteins are exploited for their colorant, nutritional, antioxidant, anti-inflammatory and hepatoprotective properties, while the production of lipids has been gaining increasing interest for the

generation of biofuel (Mooij *et al.*, 2016; Odjadjare *et al.*,2017; Hu *et al.*, 2018; Chen *et al.*, 2019). Other added-value metabolites include polysaccharides, fatty acids such as eicosapentaenoic acid, docosahexaenoic acid, and arachidonic acid (Grima *et al.*, 2002).

Another significant application of microalgal and cyanobacterial cultures is environmental purification, especially in wastewater treatment. These microorganisms can uptake a high amount of nutrients, such as nitrogen and phosphorus, which are often not entirely removed by traditional treatment plants (Melo *et al.*, 2018). Photolithoautotrophs are advantaged by their ability to use light as a source of energy and CO_2 as a source of carbon when the amount of organic matter is insufficient for heterotrophic growth (Ting *et al.*, 2017). As previously discussed, the biomass they produce does not constitute a waste and can easily be reused.

In water treatment, phototrophic microorganisms have therefore traditionally been studied for the removal of inorganic pollutants (Ting *et al.*, 2017). More recently, their application for organic carbon removal has received growing interest (Qu *et al.*, 2019). While they are mostly known for being photolithoautotrophic microorganisms, some species have been proven to be capable of varying their energy and carbon sources depending on their nutrition regime (Qiao *et al.*, 2009). In the presence of organic carbon, different metabolisms can take place: *(i)* chemoorganoheterotrophy, in which organic matter is used as a source of energy, carbon, and electron donor; *(ii)* photoorganoheterotrophy, in which light is used as a source of energy, but organic matter is used as a carbon source and electron donor. Moreover, *(iii.)* mixotrophy is defined as a combination of photolithoautotrophy and either chemoorganoheterotrophy or photoorganoheterotrophy (Mondal *et al.*, 2016; Salati *et al.*, 2017). Studies have shown that the algal biomass yield is higher in heterotrophic and mixotrophic cultures (Mondal *et al.*, 2016). However, these metabolic pathways are still less known (Zanette *et al.*, 2019).

Further research on the use of organic carbon by phototrophic microorganisms is needed in order to optimise phototrophic biomass production and simultaneously purify organic waste streams. The following sections will explain more into depth the mechanisms of photolithoautotrophic and photoorganoheterotrophic growth and the possible applications of the latter in environmental technology. Specifically, its applicability in pure and mixed cultures will be discussed.

2.2 Metabolic pathways underlying growth in phototrophic cultures

As many phototrophic organisms, microalgae are capable of photosynthesis. In this process, light and carbon dioxide (CO_2), together with a reduced compound (H_2X), produces glucose ($C_6H_{12}O_6$) and an oxidized compound (X_2) through a complex process that can be simplified by the following reaction:

$$\text{Light} + 6CO_2 + 6H_2X \rightarrow C_6H_{12}O_6 + 6X_2 \quad (1)$$

In the case of microalgae, water is used as an electron donor, and as a result of its oxidative breakdown, oxygen (O_2) is produced. This process is therefore called oxygenic photosynthesis. Cyanobacteria are the only prokaryotes that perform this type of oxygenic metabolic reaction, while all other prokaryotic phototrophs do anoxygenic photosynthesis, *e.g.* using hydrogen sulphide (H_2S), organic compounds, or arsenite (As^{+3}) as electron donors (Overmann and Garcia-Pichel, 2013; McCann *et al.*, 2017). The oxygenic photosynthetic reaction becomes:

$$\text{Light} + 6CO_2 + 6H_2O \rightarrow C_6H_{12}O_6 + 6O_2 \quad (2)$$

A second photo-driven anabolic step takes place, in which the produced glucose is turned into biomass. The process can be summarized as follows:

$$\text{N-source} + \text{P-source} + C_6H_{12}O_6 \rightarrow C_{106}H_{263}O_{110}N_{16}P \quad (3)$$

The nitrogen (N) and phosphorus (P) sources can vary based on the microorganism and can include nitrogen gas (N_2), ammonium (NH_4^+), nitrate (NO_3^-), organic nitrogen, and mineral or organic phosphate (PO_4^{3-}). $C_{106}H_{263}O_{110}N_{16}P$ is the theoretical formula of microalgal and cyanobacterial biomass (Redfield, 1934). For bacterial cultures, the biomass formula is $C_1H_{1.8}O_{0.5}N_{0.2}P_{0.03}$ (Heijnen, 1997). The production of biomass also generates or consumes H_2O, CO_2, and hydrogen protons (H^+). For example, using ammonium and phosphate as N-source and P-source, the equation becomes:

$$16NH_4^+ + PO_4^{3-} + 53/3C_6H_{12}O_6 \rightarrow C_{106}H_{263}O_{110}N_{16}P + 13H^+ \qquad (4)$$

In heterotrophy, organic carbon cannot be synthesised as in reaction 1. Carbon must come from an external organic source, which must be provided. If light is not available, energy must be derived from catabolic reactions such as cellular respiration or fermentation.

Certain microalgae and cyanobacteria have been proven to grow chemoorganoheterotrophically in the absence of light (Bouarab *et al.*, 2004; Qiao *et al.*, 2009; Patel *et al.*, 2016; Hu *et al.*, 2018). Even more species can grow photoorganoheterotrophically or mixotrophically on organic carbon when illumination is provided. Researchers have observed that when mixotrophic metabolism occurs, the growth and the yield of the biomass appear to be the sum of the photolithoautotrophic and chemoorganoheterotrophic terms (Laliberté and de la Noüe, 1993; Bouarab *et al.*, 2004), suggesting that mixotrophy is indeed a combination of both pathways. Moreover, mixotrophic growth produces carbon dioxide that can again be used by the algae to grow autotrophically.

In axenic cultures, the distinction between the three possible metabolic routes is clear. In nature or in controlled mixed cultures however, microalgae live together with different forms of life, which can maintain symbiotic relationships (Yao *et al.*, 2018). For instance, aerobic heterotrophic bacteria can degrade organic matter into carbon dioxide, enabling phototrophs to perform photosynthesis. Photosynthesis will, in turn, produce the oxygen needed by aerobic bacteria (Yao *et al.*, 2018). In mixed cultures, the extent to which a photosynthetic microorganism performs mixotrophy or simply uses the metabolised CO_2 is more difficult to determine. As different populations inhabit the culture, the metabolism of one and other cannot easily be distinguished. This ecological symbiosis constitutes an advantage of mixed cultures over pure cultures, as strictly photolithoautotrophic species can indirectly use organic carbon.

However, it is difficult to obtain a balance between the bacterial and algal community that allows the domination of the phototrophic species (Chew *et al.*, 2018). Besides symbiosis, other ecological interactions can occur between algae and bacteria, such as predatorial behaviours in which photolithoautotrophs are predated by chemoheterotrophs, or competition for substrate (Ramanan *et al.*, 2016). Moreover, the addition of organic matter introduces a potential electron donor for anoxygenic photosynthesis and for the growth of obligate photoorganoheterotrophs. Alternative electron donors for photosynthesis are generally not provided in media for the photolithoautotrophic growth of oxygenic photosynthetic microorganisms. Photoheterotrophic cultivation, therefore, not only determines the competition between phototrophs and bacteria but also within the guild of phototrophs itself.

Phototrophs using organic carbon as either an electron donor or a carbon source include purple non-sulphur bacteria (PNSB), filamentous green non-sulphur bacteria (*Chloroflexi*), Acidobacteria, and Heliobacteria. PNSB in mixed cultures can have growth rates of 1.51-1.69 d^{-1} and are typically selected using infrared irradiation (Alloul *et al.*, 2019). *Chloroflexi* are naturally found in hot springs (45°C-70°C), and although they are generally outcompeted by Cyanobacteria at lower temperatures, certain species can still thrive (Garrity *et al.*, 2001). Acidobacteria are found in natural environments, often acidic, but have been hard to isolate and to cultivate under laboratory conditions (Bryant *et al.*, 2011). Heliobacteria are primarily soil resident but have also been found in hot springs preferring high light intensities (Madigan and Ormerod, 1995).

The selection for oxygenic green phototrophs constitutes the main challenge in the application of photoheterotrophic mixed cultures (Chen *et al.*, 2015). To overcome such issues, ecological engineering is required. Strategies to ensure the selection of microalgae and cyanobacteria in photoorganoheterotrophic mixed cultures must be designed. Mixed cultures are generally preferred for large scale cultivation as they

don't require sterilization of the substrate and the equipment (Chen *et al.*, 2015). Economically, algae growth for wastewater treatment is only feasible under non-sterile conditions (Chen *et al.*, 2015).

2.3 Photoheterotrophic cultivations in waste and wastewater treatment: suitable substrates

Some researchers have studied microalgae heterotrophic growth using glucose as a substrate due to its high efficiency for cell growth (Bouarab *et al.*, 2004; Bernát *et al.*, 2008; Sijil *et al.*, 2019). However, the feasibility of large-scale microalgae production is limited by the cost of using such a refined carbon source (Fei *et al.*, 2015). Many other studies have therefore turned to organic waste streams to pursue a low-cost microalgae cultivation substrate.

Municipal wastewater has been used for both inorganic and organic pollutant removal in mixotrophic cultures (Chew *et al.*, 2018). Posadas *et al.* (2013) have reported the improved chemical oxygen demand (COD), nitrogen, and phosphorus removal in an open algal–bacterial biofilm reactor compared to the traditional bacterial one. The green algae *Chlorella* sp. has been successfully grown by Wang *et al.* (2010) on municipal wastewater and sludge centrate (*i.e.*, the liquid phase obtained from sludge dewatering) in axenic cultures. Most studies focus on industrial wastewaters due to their high pollutant content.

Effluents from anaerobic digestion have also been used as substrates. The removal of the organic load is typically between 70-90%, while nitrogen and phosphorus are only removed to a minimal extent (Gonçalves *et al.*, 2017). González-Fernández *et al.* (2011) have compared the microalgal growth on a mixed culture using fresh or anaerobically digested cheese whey, proving the latter to be a more suitable substrate at higher influent strength. Franchino *et al.* (2013) have compared the microalgae cultivation on digested agro-zootechnical waste and obtained good nitrogen and phosphate removal, between 83.7-99.9% and 94.4-97.3% respectively. Another viable carbon source are VFAs, which are produced during the acidogenic phase of anaerobic digestion (Silva *et al.*, 2013). These organic acids are directly converted into acetyl-CoA by acetyl coenzyme-A synthetase and used for the biosynthesis of fatty acids and lipid accumulation (Fei *et al.*, 2015).

Heterotrophic growth on agricultural waste flows has also been investigated. Mondal *et al.* (2016) have compared the growth of two microalgal strains with different carbon sources such as carbon dioxide, sodium acetate, sodium bicarbonate, fructose, cheese whey permeate, and molasses. They have observed a higher biomass production (0.04 g L^{-1} d^{-1}) and lipid conversion (38.6% transesterification productivity) of the microalgae *Chlamydomonas* sp. when using cheese whey permeate. The stimulatory effect of cheese whey has been explained by the presence of nutrients such as phosphorous and calcium. Tsolcha *et al.* (2018) have also indicated second cheese whey (*i.e.*, whey resulting from cottage cheese production) as a preferable carbon source for microalgal growth and lipid production when compared to other agro-industrial wastewater such as poplar sawdust and grass hydrolysates.

Additional studies reported microalgal growth on cheese whey under different forms: anaerobically pre-treated cheese whey (Riaño *et al.*, 2016), aerobically treated second cheese whey (Tsolcha *et al.*, 2016), cheese whey permeate (Mondal *et al.*, 2016), deproteinized cheese whey (Melo *et al.*, 2018), cheese whey powder (Dragone *et al.*, 2011), and demineralized cheese whey (Freyssinet and Nigon, 1980). These results indicate that cheese whey is a potential substrate for mixotrophic microalgae cultivation.

2.4 Cheese whey: a valuable product or a highly polluting waste?

Cheese whey is a by-product of the dairy industry (Tsakali *et al.*, 2010). It appears as a watery, thin liquid of a green-yellowish colour (Prazeres *et al.*, 2012). Cheese whey is formed during the production of cheese when

the casein proteins coagulate and are separated from the milk (Tsakali *et al.*, 2010). For every kg of cheese produced, 10 L of milk are used, resulting in 9 L of cheese whey (Prazeres *et al.*, 2012). Additional waste-streams originating from the dairy industry consist of second cheese whey and dairy wastewater (Tsolcha *et al.*, 2018).

The characteristics of cheese whey can vary significantly due to several factors (Tsakali *et al.*, 2010; Prazeres *et al.*, 2012). It can be acid or sweet and come from several animal sources (bovine, sheep, and others). The characteristics of cheese whey depend on the feed given to the cattle, the cheese process used and the season of production (Tsakali *et al.*, 2010). Cheese whey is typically characterized by elevated organic loads and salinity and low pH. The average characteristics of cheese whey are summarized in Table 1.

Despite being a by-product, cheese whey can be reused for several purposes due to its highly nutritive components (Tsakali *et al.*, 2010; Prazeres *et al.*, 2012). Such components can be repurposed in many fields such as the food industry itself and in pharmaceutical chemical production (Siso, 1996; Smithers, 2008). According to the United States Department of Agriculture (USDA, 2019) of the 152 million tons of whey produced per year worldwide, 89 million are utilized inside the industry for the production of whey powder and other added-value products recovering proteins, lactose and minerals, as shown in Figure 1. The remaining 41% is either used as animal feed, fertilizer or disposed. The use of cheese whey as a fertilizer is not ideal. Its salinity is significant, and its high suspended solid content causes soil fouling (Prazeres *et al.*, 2012). As for disposal, it is evident that cheese whey cannot be discharged into water bodies without previous treatment, as this would cause acidification and eutrophication. Unfortunately, this practice is still widespread in many parts of the world (Prazeres *et al.*, 2012). Ecological engineering strategies are needed to "harness eutrophication" into environmental biotechnology processes to treat and valorise the concentrated aqueous residues of cheese whey.

Table 1: Average characteristics of cheese whey (Tsakali et al., 2010; Prazeres et al., 2012; Tsolcha et al., 2016).

COD ($g\ L^{-1}$)	**BOD ($g\ L^{-1}$)**	**BOD COD^{-1}**	**Lactose ($g\ L^{-1}$)**	**Proteins ($g\ L^{-1}$)**	**Fats ($g\ L^{-1}$)**	**Solids (%)**	**pH**
50-102	27-60	>5	0.18-60	1.4-33.5	0.08-10.85	6.5	3-6

Alternatives for cheese whey treatment must be therefore considered before disposal. Physicochemical treatments can be applied to recover specific components, such as proteins (Prazeres *et al.*, 2012). Biological solutions, however, are usually preferred (Prazeres *et al.*, 2012). These can include or not its valorisation. While aerobic processes reduce the organic and nutrient load of the influent significantly by converting the COD to biomass and CO_2, anaerobic processes can convert the organics in cheese whey to more valuable compounds.

Demineralized cheese whey is often obtained by physical separation processes such as precipitation, filtration or dialysis, and it consists of the whey with partial minerals removed after pasteurization (Think USA Dairy, 2019). It is often conserved as a powder, which is obtained after spray-drying. This is the derived product most similar to raw cheese whey and, given the tendency of cheese whey to acidify, the easiest way to keep its original composition for longer periods (Mockaitis *et al.*, 2006).

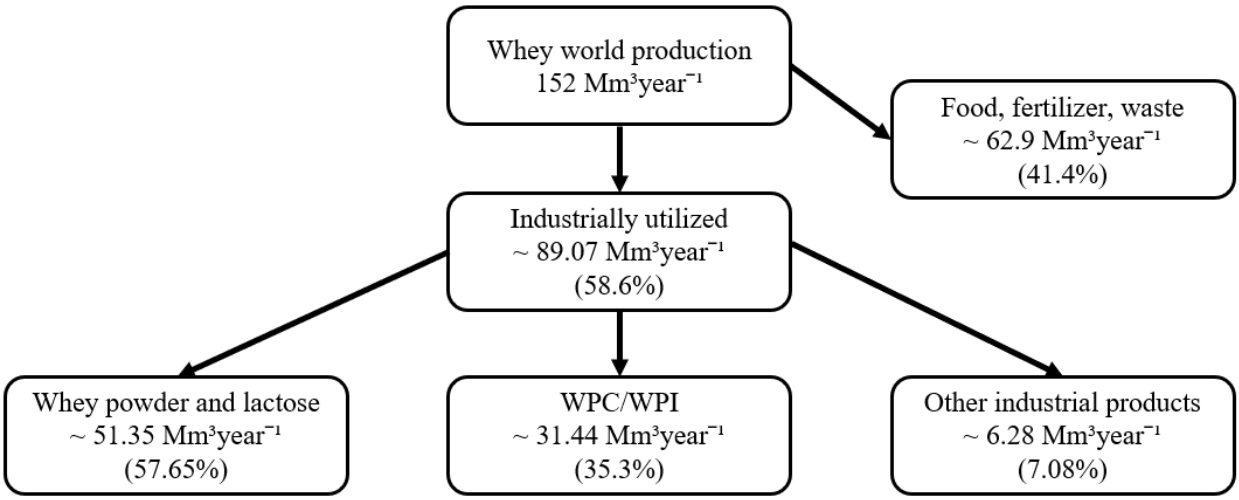

Figure 1: Global cheese whey production and utilization. While 58.6% of the cheese whey produced is utilized industrially, 41.4% is used as food, fertilizer, or disposed. Typical industrial products that can be obtained from cheese whey are whey powder and whey protein concentrate (WPC) or isolate (WPI) (USDA, 2019).

Several studies have focused on the anaerobic digestion of cheese whey. Methane has traditionally been the most common end-product of anaerobic treatments. However, other biological metabolites, such as hydrogen gas or VFAs, actually have a higher value (Liu *et al.*, 2012; Dahiya *et al.*, 2015). Due to its tendency to acidify very rapidly, cheese whey is an excellent substrate for VFA production (Calero *et al.*, 2018). VFAs can also be used as a resource for biodegradable polymer production such as polyhydroxyalkanoates (PHA), biological nutrient removal, or building blocks for starting materials in the chemical industry (Silva *et al.*, 2013). On an industrial scale, VFAs are mostly produced by chemical synthesis from fossil fuels. Biological VFA production is a preferable and more environment-friendly option (Silva *et al.*, 2013).

Although cheese whey is easily converted to VFAs, the production can be controlled and improved by operational parameters. Temperature, pH, and retention time are known for influencing the acidogenesis process (Gouveia *et al.*, 2017; Calero *et al.*, 2018). The food-to-microorganism ratio (F/M) also affects the yield and composition of the VFA (Silva *et al.*, 2013). The optimal F/M value depends on both the inoculum and the substrate used (Shah *et al.*, 2014). To maximise the amount of VFA produced, inhibition of methanogenesis is advisable (Kisaalita *et al.*, 1986; Calero *et al.*, 2018). In continuous processes, sludge retention time is generally used to washout methanogens, while in batch experiments, other techniques such as sludge pre-treatment can be used (Jayakrishnan *et al.*, 2019).

Following on section 2.3, another possibility for cheese whey recovery is the production of algal biomass. On the one hand, microalgae and cyanobacteria cultivation can be used as a polishing step in the biological treatment of cheese whey. For example, anaerobically treated cheese whey still contains inorganic nutrients such as nitrogen and phosphorus, since these are not substantially removed by fermentation (Riaño *et al.*, 2016). Another option is to use raw cheese whey, or to select the treatment of cheese whey in order to optimise the growth of green phototrophs. While raw and pre-treatment cheese whey has already been applied for the purpose of microalgal growth (Melo *et al.*, 2018), the selection of the pre-treatment has not been focused on algal productivity.

The cultivation of microalgae or cyanobacteria using wastewaters with high organic loadings is a less well-known and established process than that of anaerobic digestion, and these solutions are still the most researched on (Tsolcha *et al.*, 2016). However, their use is overall more sustainable than other biological processes as it does not produce residual waste such as sludge (Tsolcha *et al.*, 2016).

2.5 Cheese whey as a substrate for photoheterotrophic growth

The high organic content of cheese whey can be used to grow photoorganoheterotrophic cultures. The main organic product present in cheese whey is lactose (90% of the BOD) (Kisaalita *et al.*, 1986). Lactose is a disaccharide formed by one molecule of glucose and one of galactose. It is hydrolysed by the enzyme β- galactosidase (Zanette *et al.*, 2019). Few studies report the direct assimilation of lactose by microalgae and cyanobacteria, while the consumption of glucose is more common (Zanette *et al.*, 2019).

Cheese whey also contains proteins, which are degraded to amino acids during hydrolysis and then to ammonia during acidogenesis (Dahiya *et al.*, 2015). Ammonia can be used by algae and is usually considered a more efficient nitrogen source than nitrate, as the latter needs to be reduced to nitrite and ammonium before it can be assimilated for amino acids formation in biomass (Gonçalves *et al.*, 2017; Chew *et al.*, 2018). However, the NH_4^+ uptake can cause acidification, as the consumption of the cation requires the production of hydrogen protons, which may negatively influence the microalgal culture (Gonçalves *et al.*, 2017). Proteins also contain phosphorus (Prazeres *et al.*, 2012), which is essential for microalgal growth (Melo *et al.*, 2018).

The high salinity (7–23 mS cm^{-1}) and low pH (3-6) of untreated cheese whey can inhibit the growth of certain microalgal strains but still enable the proliferation of others (Ullrich *et al.*, 1998; Budinoff *et al.*, 2007; Kumar *et al.*, 2014; Ríos *et al.*, 2018). These parameters can be adjusted with physicochemical pre-treatments, such as base addition or ion exchange (Marwaha and Kennedy, 1988).

In 2016, Tsolcha *et al.* showed a mutually beneficial relationship between indigenous cheese whey bacteria and microalgae for the removal of organic and inorganic nutrients, especially when high concentrations were employed.

Cheese whey can be therefore be used as a substrate for microalgal growth, either raw or pre-treated, the latter transforming the organic matter present in the cheese whey. Physical pre-treatment such as spray-drying maintains the COD content and can simplify the study of cheese whey uptake by microorganisms, as it produces a powder that can easily be conserved (Marwaha and Kennedy, 1988). Biological pre-treatments such as aerobic degradation or anaerobic digestion for the production of methane lower the organic load of the waste stream. As a result, the use of microalgae is focused on the removal of phosphorus and nitrogen rather than on organic matter (González-Fernández *et al.*, 2011; Franchino *et al.*, 2014). Conversely, if cheese whey fermentation aimed at VFA production is applied, the COD is transformed rather than consumed. In this case, the organic content remains high and microalgal growth depends on their ability to grow heterotrophically. The possible uptake of lactose, monosaccharides or VFAs and the improved yield is species-related (Jiang, 2009).

2.6 Research gaps

Although several studies have been published on green phototroph cultivation and the valorisation of organic wastes such as cheese whey, there are still some gaps in research that could be solved with environmental biotechnology. Five main aspects are provided here:

1. The study of mixed microalgal and cyanobacterial cultures to treat wastewater has mostly focused on inorganic nutrients and micropollutant removal. However, improved growth and lipid content have been observed in heterotrophic than in autotrophic cultures. Although some studies on organic carbon uptake in wastewater exist, these metabolic pathways are still less known, and further research is necessary to enable the largescale application of such systems

2. Photoorganoheterotrophic metabolisms in axenic microalgal and cyanobacterial cultures have been described for different species on organic carbon sources, including pure compounds such as glucose

and acetate. Waste-derived substrates such as cheese whey by-products, including demineralized cheese whey, whey permeate, and cheese whey wastewater, have been shown to sustain growth as well. However, the use of mixed cultures for large scale applications is economically preferable. In mixed cultures, the consumption of organic carbon is the result of the complex symbiotic and competitive relations that take place between the microorganisms. Mixed cultures require the use of strategies to control the competition between phototrophs and other microorganisms.

3. One of the main problems in upscaling microalgal cultures is their limited competitive advantage compared to aerobic heterotrophs and fermenters, due to their lower growth rates (ca. 1 d^{-1} vs. >10 d^{-1}) (Yu *et al.*, 2013). It is known that different reactor regimes determine different selection mechanisms. Batch regimes select the fastest growing microorganism, while continuous-flow regimes make a selection based on both the growth rate and the affinity for the substrate (Rombouts *et al.*, 2019). The regime choice should, therefore, be a parameter to consider to promote the growth of phototrophs inside the mixed culture.

4. Biological treatments can result in the upgrade of cheese whey with limited costs. Cheese whey has mostly been used as a substrate for the production of biogas in anaerobic digestion processes. However, less attention has been placed on the anaerobic digestion of whey for the generation of alternative fermentative products such as volatile fatty acids and even less on the production of phototrophic biomass. Both end products present higher market value once biomass is further processed into lipids, pigments, or other products.

5. Cheese whey has been proven to be a suitable substrate for the growth of microalgal and cyanobacterial species capable of heterotrophy. However, its treatment with phototrophs has mainly been used as a polishing step after biogas production, aerobic treatment and other pre-treatments. The pre-treatment has not been focused on the growth of the phototroph itself, but rather on the requirements for disposal. Phototrophic cultures have been successfully grown on VFAs, which can be easily produced from cheese whey. However, a VFA-producing pre-treatment of cheese whey for the growth of phototrophic cultures has not yet been applied.

2.7 Hypothesis and research question

From the research gaps defined, the following question emerged:

How does the use of organic carbon sources derived from cheese whey impact the selection for green phototrophs in photoorganoheterotrophically grown mixed microbial cultures?

Based on the literature review and the research gaps found, the following hypothesis was formulated:

The selection for green phototrophs in mixed cultures grown on cheese whey can be improved by pre-treating cheese whey via acidogenic fermentation. Parameters such as pH, the nitrogen source, and the level of dissolved oxygen will influence the selection. Selection mechanisms will vary in a batch and in a chemostat regime.

The three main research objectives were prioritized and addressed experimentally to:

Part 1 [30% of the work]. Product spectrum during acidogenic fermentation of cheese whey:

1. The acidogenic fermentation of 40% demineralized cheese whey was studied. Inoculum from the local municipal wastewater treatment plant digestate was used. The effect of a thermal pre-treatment of the inoculum (90°C) on the inhibition of methanogenesis was determined. The variation in the microbial

community composition as a result of the thermal pre-treatment, before and after the fermentation, was analysed. The effect of different F/M ratios on the degree of acidification and the spectrum of volatile fatty acids produced was determined.
The following questions were answered:

1. *What is the degree of acidification that can be achieved with anaerobic digestion of cheese whey?*
2. *Can sludge pre-treatment and different F/M ratios play a role in improving the VFA production*?

Part 2 [70% of the work]. Growth, selection, and competition of green phototrophs on cheese whey and derived organic compounds:

1. The growth of green phototrophs on inorganic carbon, demineralized cheese whey powder, lactose and acetate was studied. To this end, an inoculum extracted from a local surface water source was photolithoautotrophically enriched. The influence of mineral nutrients (nitrogen, phosphorus, and trace elements) was determined. The microbial populations selected in these cultures were compared. The possible metabolic pathways occurring inside the cultures were identified. The maximum growth rate and total biomass concentration of the cultures were determined.
   The following questions were answered:
   1. *Under which conditions can demineralized cheese whey sustain the growth of phototrophic microorganisms, in terms of carbon, nitrogen, and phosphorus concentrations?*
   2. *How does the population of a phototrophic mixed culture vary when transitioning from photolithoautotrophy to photochemoheterotrophy?*
   3. *Are demineralized cheese whey, lactose and acetate suitable carbon sources for the selection and growth of photoorganoheterotrophs?*
   4. *Which carbon source results in the highest phototrophic biomass production?*
   5. *How is the growth of phototrophs in mixed cultures influenced by the concentration of the organic carbon source, the type of nitrogen source, the dissolved oxygen level?*

2. A photoorganoheterotrophic culture was grown in a continuous-flow photobioreactor (*i.e.*, chemostat regime), using acetate as a carbon source, to determine the different selection mechanisms for green phototrophs taking place in a batch operation mode and a chemostat operation mode. Determine the composition of the population, the biomass production, the pigment content, and the influence of the retention time.
   The following question was answered:
   1. *How will the equilibrium between the microbial species inside the mixed culture change from a batch to a chemostat?*

3. Product spectrum during the acidogenic fermentation of cheese whey

3.1 Materials and Methods

3.1.1 Anaerobic sludge inoculum

Digestate from a local wastewater treatment plant (RWZI Harnaschpolder, Peuldreef 4, 2635 BX Den Hoorn, The Netherlands) was collected. The total (TS) and volatile solids (VS) contents were determined, as shown in Table 2. The biomass was stored at 5°C until inoculation.

Table 2: Total, volatile, and inorganic solids of the anaerobic sludge. Concentrations are given together with the percentage over the total solids (TS).

	Total solids (g L^{-1})	**Volatiles solids (g L^{-1})**	**Inorganic solids (g L^{-1})**
Digestate sludge	38 ± 2	27 ± 1 (71±3% of TS)	11 ± 0.4 (29±1% of TS)

3.1.2 Substrate solution with partially demineralized cheese whey powder

Partially demineralized (40%) cheese whey powder (DWP40) was used as the organic substrate for fermentation. A powder was used instead of raw cheese whey to simplify its storage and conservation in the laboratory facilities. The powder was provided by Senel & Co., B.V. (The Netherlands). The characteristics of the powder provided by the producer (Senel & Co.) are shown in Table 3.

The DWP40 was dissolved in water at the concentration of 4 g L^{-1}, as in Torres (1992). The obtained solution was then characterized to determine solids, soluble COD (sCOD), nitrogen, phosphorus, sugar content and pH.

Table 3: Characteristics of the cheese whey powder provided by Senel & Co., B.V.

Demineralization	**Milk fat**	**Protein**	**Moisture**	**Ash content**	**Lactose**
40%	1.2% max	11%	4.5% max	5.5%	75%

An additional micronutrient solution (2.016 g L^{-1} $FeCl_3 \cdot 6H_2O$, 2 g L^{-1} $CoCl_2 \cdot 6H_2O$, 0.504 g L^{-1} $MnCl_2 \cdot 4H_2O$, 0.032 g L^{-1} $CuCl_2 \cdot 2\ H_2O$, 0.051 g L^{-1} $ZnCl_2$, 0.053 g L^{-1} H_3BO_3, 0.094 g L^{-1} $(NH_4)_6Mo_7O_2 \cdot 4\ H_2O$, 0.103 g L^{-1} Na_2SeO_3, 0.006 g L^{-1} $NiCl_2 \cdot 6\ H_2O$, 1.006 g L^{-1} EDTA, 0.082 g L^{-1} Na_2WO_4) was dosed (0.3 mL per g COD in the substrate) in order to optimize the growth of microorganisms as described by de Kreuk *et al.* (2012).

3.1.3 Experimental set-up

Fermentation of DWP40 for VFA production was performed by contacting the anaerobic sludge inoculum with the 4 g L^{-1} cheese whey solution.

The experiments were carried out in batch mode, using 1-L closed bottles (Duran, Schott) with a working volume of 750 mL, kept inside an incubator (Certomat® BS 1, Sartorius Stedim Biotech, Germany). The bottles were continuously mixed at 145 rpm and at 35°C.

Two different sets of acidogenesis experiments were made. In the first set, a thermal pre-treatment of the inoculum was tested to inhibit methanogenesis, and it was compared to the untreated inoculum. In the second set, different food-to-mass (F/M) ratios were used. The fermentation lasted between 10 days for the former and 14 days for the latter. The set-ups of the two experiments are shown in Figure 2.

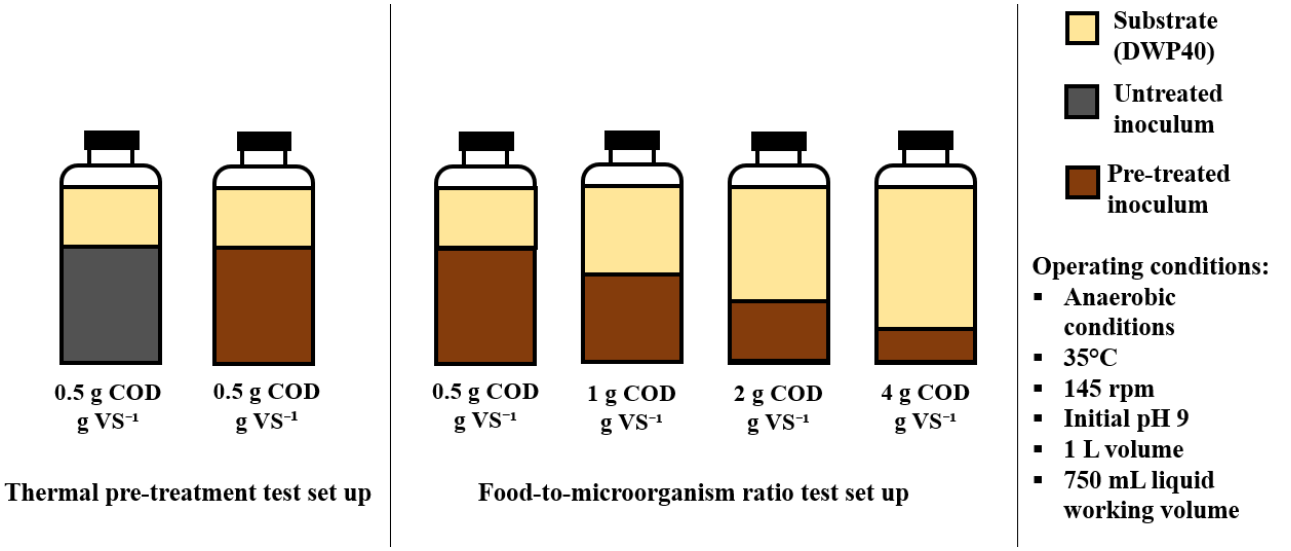

Figure 2: The experimental set-ups are presented. All set-ups were performed in anaerobic conditions at 35°C, with a 145-rpm mixing. The pH was initially set to 9. A liquid working volume of 750 mL was used in 1-L bottles. The substrate used was partially demineralized cheese whey powder (DWP40). The thermal pre-treatment test was performed in triplicates. The food-to-microorganism ratio test was performed in duplicates.

Thermal pre-treatment procedure

The methodology for the pre-treatment was described by Mockaitis *et al.* (2020). Sludge was heated in a water bath (90°C) and continuously mixed for 20 minutes. Heat was then halted in an ice bath until the sludge reached ambient temperature (23°).

Thermal pre-treatment test set-up

To test the efficiency of the pre-treatment procedure, six batches were inoculated with triplicates of treated and untreated sludge. Each batch contained 6.6 g VS L^{-1} (from the inoculum), 3.37 g COD L^{-1} (from the substrate) and a F/M ratio of 0.51 g COD g VS^{-1}. The pH was initially set to 9. The experiment lasted ten days, after which VFA production stopped. Samples for DNA extraction were taken at the beginning and the end of the experiment.

F/M test set-up

Four different F/M ratios (0.5 g COD g VS^{-1}, 1 g COD g VS^{-1}, 2 g COD g VS^{-1}, 4 g COD g VS^{-1}) were used. Experiments were conducted in duplicates. The characteristics of each F/M batch are shown in Table 4. Thermally pre-treated sludge was used to inoculate all batches. pH was initially set to 9, as described in Figure 2.

Table 4: VS and COD content in the batch experiments with F/M 0.5, 1, 2 and 4. The VS referrers to the inoculum and COD to the substrate.

	F/M 0.5	F/M 1	F/M 2	F/M 4
VS (gL^{-1})	6.3	3.3	1.8	1.0
COD (gL^{-1})	3.2	3.6	3.9	4.0

The experiment lasted for 14 days.

3.1.4 Analytical and calculation methods

Liquid and gas samples were taken daily for pH, gas content and VFAs monitoring, while sCOD and sugars were measured every second day. Soluble total organic carbon (TOC), total inorganic carbon (TIC), total nitrogen (TN), solid content and alkalinity were measured on the first and last day of each experiment.

Sugars and fermentation products

The main organic substrates of the DWP40 are sugars: the disaccharide lactose is naturally present and can hydrolyse into glucose and galactose. Sugars (lactose, glucose, galactose) were either measured with the HPLC analyser or following the colorimetric Dubois method (Dubois *et al.*, 1956).

For the colorimetric determination of sugars concentration, 500 µL of phenol (5% w/w solution) and 2.5 mL of sulphuric acid (97%) were added to 500 µL of diluted sample in 20 mL soda glass test tubes (150x16x0.6- 0.7 mm). The glass tubes were covered with aluminium foil and kept for 15 minutes in a dark environment. The samples were then vortexed for 30 seconds, and after 10 more minutes, the absorbance at 490 nm of each sample was measured. With the use of a calibration curve ($C_{sugar}(mgL^{-1})=OD_{490}*106.83$, $R^2=0.9936$, $OD_{490}=\{0:1.6\}$, $C_{sugar}=\{0\ mgL^{-1}; 160mgL^{-1}\}$) the absorbance was then converted to mgL^{-1} of sugar (glucose was used for the calibration curve).

Fermentation products (FPs) were measured using an HPLC analyser. The analyser consisted of a BioRad HPX-87H (300 x 7.8 mm) with a BioRad Cation-H refill cartridge (30 x 4.6 mm) guard column (BioRad, USA); a 717 plus Autosampler; a 2489 UV/Vis Detector and 2414 Refractive Index Detector (Waters Corporation, USA). The mobile phase was 1.5 mM phosphoric acid diluted in Milli-Q water. The degree of acidification (DA) was calculated using equation 1:

$$DA = \frac{VFA_{Max}}{COD_{Initial} - VFA_{Initial}} \quad (1)$$

Organic content, nitrogen and pH

sCOD was measured using Hach Lange (USA) kits (LCK-014, LCK-114). The soluble fraction of TOC and TIC were measured with a TOC analyser (TOC-L CSH, Shimadzu, Japan) and TN with a TN analyser (TNM-L, Shimadzu, Japan). pH was measured with probes (C6010, Consort, Belgium). Solid contents were measured by heating either filtered (TSS and VSS, using glass fibre filters (type A/E, 47 mm, 1 µm, PALL Corporation, USA) and rinsing with demineralized water) or unfiltered (TS, VS) biomass first at 105°C for 24 h to analyse the total solids and then at 550°C for 2.5 hours to determine the ash content. VS were calculated as the difference between the TS and the ashes. Total alkalinity was measured with Tritino Plus (Metrohm, Switzerland) with 0.1 M HCl.

As COD and TOC of the suspended fraction could not be measured, they were approximated considering the average between the values for lactose (0.42 g C g VS^{-1} and 1.2 g COD g VS^{-1}) and biomass ($C_1H_{1.8}O_{0.5}N_{0.2}P_{0.03}$,0.49 g C g VS^{-1} and 1.47 g COD g VS^{-1}), equal to 0.46 g C g VS^{-1} and 1.36 g COD g VS^{-1}.

Biogas composition

For the fermentation experiments, the gas composition was measured by taking 10 mL of gas sample from the headspace of the bottles and analysing it with a gas chromatograph (GC) (Agilenttech 7890 A, Agilent Technologies Inc., USA). The GC contains an HP-PLOT Moleseive GC column (Agilent 19095P-MS6, Agilent Technologies Inc., USA) of 60 m x 0.53 mm x 200 µm and a thermal conductivity detector (TCD). The carrier gas used is helium (14.8 psi, 23 $mLmin^{-1}$), and the operating temperature is 200 ºC. The relative content of CO_2, CH_4, H_2, N_2 and O_2 was measured.

The biogas content was calculated as the sum of the volume fractions of carbon dioxide, methane, and hydrogen gas measured over the total volume of the gas measured. The calculation is shown in eq. 2:

$$Biogas\ (\%) = \frac{CO_2(\%) + CH_4(\%) + H_2(\%)}{CO_2(\%) + CH_4(\%) + H_2(\%) + O_2(\%) + N_2(\%)} \quad (2)$$

Analysis of the microbial community composition

16S rRNA gene amplicon sequencing was carried out to identify the bacterial and archaeal species present in the underlying microbial communities and their relative abundances. The DNeasy® UltraClean® Microbial Kit (QIAGEN, Germany) was used to extract the genomic DNA of biomass samples. Samples were collected on the first and on the last day of the thermal pre-treatment test, from one from each batch containing the untreated and from the treated sludge. The concentration and quality of DNA extracts were measured by a fluorometer (Invitrogen Qubit 4, Thermo Fisher Scientific, USA). Samples were stored at -20°C. Volumes of 200 µL of DNA extracts at a concentration ranging between 13.9 and 95 ng/µL were sent to Novogene Co., Ltd. (China) for amplicon sequencing. 16S rRNA amplicon gene sequencing was performed, to identify bacterial and archaeal cells. The primer set used was 341F/806R, which is suitable for the identification of both bacterial fermenters and archaeal methanogens. Additional information on the primer set is shown in Table 5.

Table 5: Primers selected with the targeted region and sequences.

Primer	Region	Primer sequences 5'-3'
341F	V3-V4	CCTAYGGGRBGCASCAG
806R	V3-V4	GGACTACNNGGGTATCTAAT

At Novogene, DNA concentration and purity were evaluated on 1% agarose gels. According to the concentration, DNA was diluted to 1ng/µL using sterile water. All PCR reactions were performed in 30µL reactions with 15µL of Phusion® High-Fidelity PCR Master Mix (New England Biolabs), 0.2µM of forward and reverse primers, and about 10 ng template DNA. Thermal cycling consisted in the initial denaturation at 98 for 1 min, followed by 30 cycles of denaturation at 98℃ for 10 s, annealing at 50℃ for 30 s, and elongation at 72℃ for 60 s, and then at 72℃ for 5 min. PCR products were quantified and qualified, then mixed in equidensity ratios. The mixed PCR products were purified with a GeneJET Gel Extraction Kit (Thermo Scientific). Sequencing libraries were created using NEBNext Ultra™ DNA Library Prep Kit for Illumina ®. The library quality was evaluated with a Qubit ® 2.0 Fluorometer (Thermo Scientific) and Agilent Bioanalyzer 2100 system. The library was then sequenced on an Illumina platform and 250 bp paired-end reads were generated.

3.2 Results

3.2.1 Partially demineralized cheese whey powder characterization

The solution used as substrate was prepared from the dissolution of partially demineralized cheese whey powder (DWP40) as described in section 3.1.2. The obtained solution had the characteristics shown in Table 6.

Table 6: Characteristics of the cheese whey solution obtained from the dissolution of 4 g of demineralized cheese whey powder into 1 L of demineralized water.

TS	VS	TSS	sCOD	Sugars	TOC	TN	$N\text{-}NH_4^+$	$P\text{-}PO_4^{3-}$
3.94 g L^{-1}	3.71 g L^{-1}	0.07 g L^{-1}	4.14 g L^{-1}	3.2 g L^{-1}	1.5 g C L^{-1}	25 mg N L^{-1}	1.11 mg N L^{-1}	22.01 mg P L^{-1}

3.2.2 Effect of the thermal pre-treatment of the inoculum on the inhibition of methanogenesis and on the degree of acidification

Methanogenesis inhibition in the thermally pre-treated inoculums

GC measurement of the gas present in the fermentation bottles revealed the presence of N_2, CO_2, O_2, CH_4 and H_2. The biogas fraction (determined as the sum of CO_2, CH_4 and H_2, see eq.2) over the total gas showed an exponential increase in the first 20-27 h, increasing from 0% to 27% in the control and from 0% to 19% in the batches containing thermally pre-treated inoculums. The biogas remained stable during the first week (around 15% in the pre-treated batches and 11% in the control batches) and decreased after the first week, reaching approximately 5%.

The control batches run with untreated inoculum produced methane during the initial and the final phase of the experiment, while no methane was detected in the biogas produced by the batches run with untreated inoculum.

In the control batches, CH_4 production was limited to the first 24 hours, except for one replicate that increased again after the fourth day. H_2 was measured between the 18^{th} and the 48^{th} hour in low concentrations (0.03-0.56% v/v) in both the control and pre-treated batches. The composition of the biogas in the control batches is given in Figure 3. In the treated batches, the biogas composition remained almost unvaried over time.

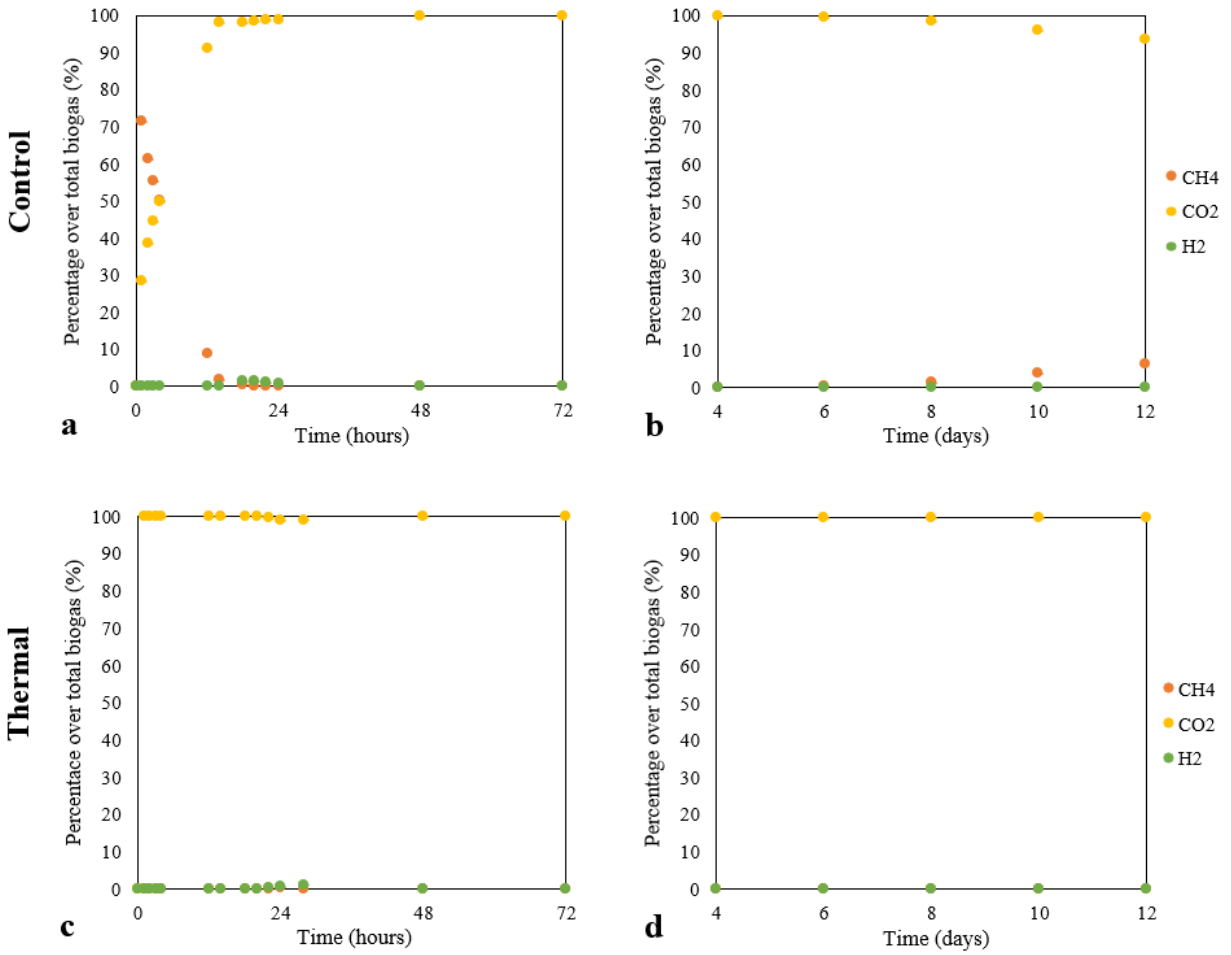

Figure 3: Biogas composition (CO_2, CH_4 and H_2) in the control (a,b) and in the thermal (c,d) batches. Figures «a» and «c» show the biogas composition during the first 24 hours, while Figures «b» and «d» illustrate composition variations between day 4 and day 12. The graphs show that while methane was produced in the batches containing untreated inoculums, the thermal pre-treatment of the sludge resulted in the inhibition of methanogenesis. H_2 was produced in both cases between 18 and 28 h.

Improvement of the degree of acidification by the pre-treated inoculums

Substrate consumption was measured with the colorimetric Dubois method via the total concentration of sugars (initially at ca. 2.6 g_{sugar} L^{-1}, ca. 3 g COD L^{-1}), which decreased by over 90% in the first 4 days. The concentration later stabilized around 50 mg_{sugar} L^{-1} and 65 mg_{sugar} L^{-1} in the control and in the pre-treated batches, respectively. The consumption of additional nutrients was not measured.

Acidification was exponential during the first 24 h, reaching a volatile fatty acid (VFA) concentration of 0.8 and 1.9 g COD L^{-1} at a rate of 2.3 and 1.9 d^{-1} in the control and pre-treated batches respectively. The VFA stabilized during the first week of the experiment around 3.1 g COD L^{-1} in the pre-treated batches and around 1 g COD L^{-1} in the control. The pH stabilized around 7 in the control batches and around 6 in the pre-treated batches. After the first week, the VFAs decreased to 2.9 g COD L^{-1} and 0.7 g COD L^{-1} in the pre-treated batches and in the control. The acidification of the substrate is shown in Figure 4.

The concentration of VFAs reached after the fast-growing phase was approximately two times higher in the thermally pre-treated batches than in the control (0.8 vs. 1.9 g COD L^{-1}).

The absolute maximum concentration of VFAs was reached around the third day in the control batches (1.4 g COD L^{-1}) and around the sixth day in the pre-treated batches (3.3 g COD L^{-1}). The degree of acidification (DA,

see eq.1) was 40 ± 12% in the control batches and 85 ± 11% in the pre-treated batches. VFA consumption occurred in all control replicates and in two of the pre-treated replicates.

The VFA composition varied between the control and the pre-treated batches. The major fermentation products (FPs) in the control were acetate (ca. 60%), propionate (ca. 24%) and hexanoic acid (ca. 9%). In the thermally pre-treated batches, the main FPs were acetate (ca. 34%), hexanoic acid (ca. 30%), butyrate (ca. 16%) and valerate (ca. 15%). These percentages refer to the maximum amount of VFA produced. Their amounts are shown in Figure 4. Hexanoic acid was present at the start of the experiment (ca. 128 mg COD L^{-1} in the C batches and ca. 81 mg COD L^{-1} in the T batches) and was first consumed then produced after the first 24 hours. Formate was produced during the first 24 hours but was not measured from day 3 onwards.

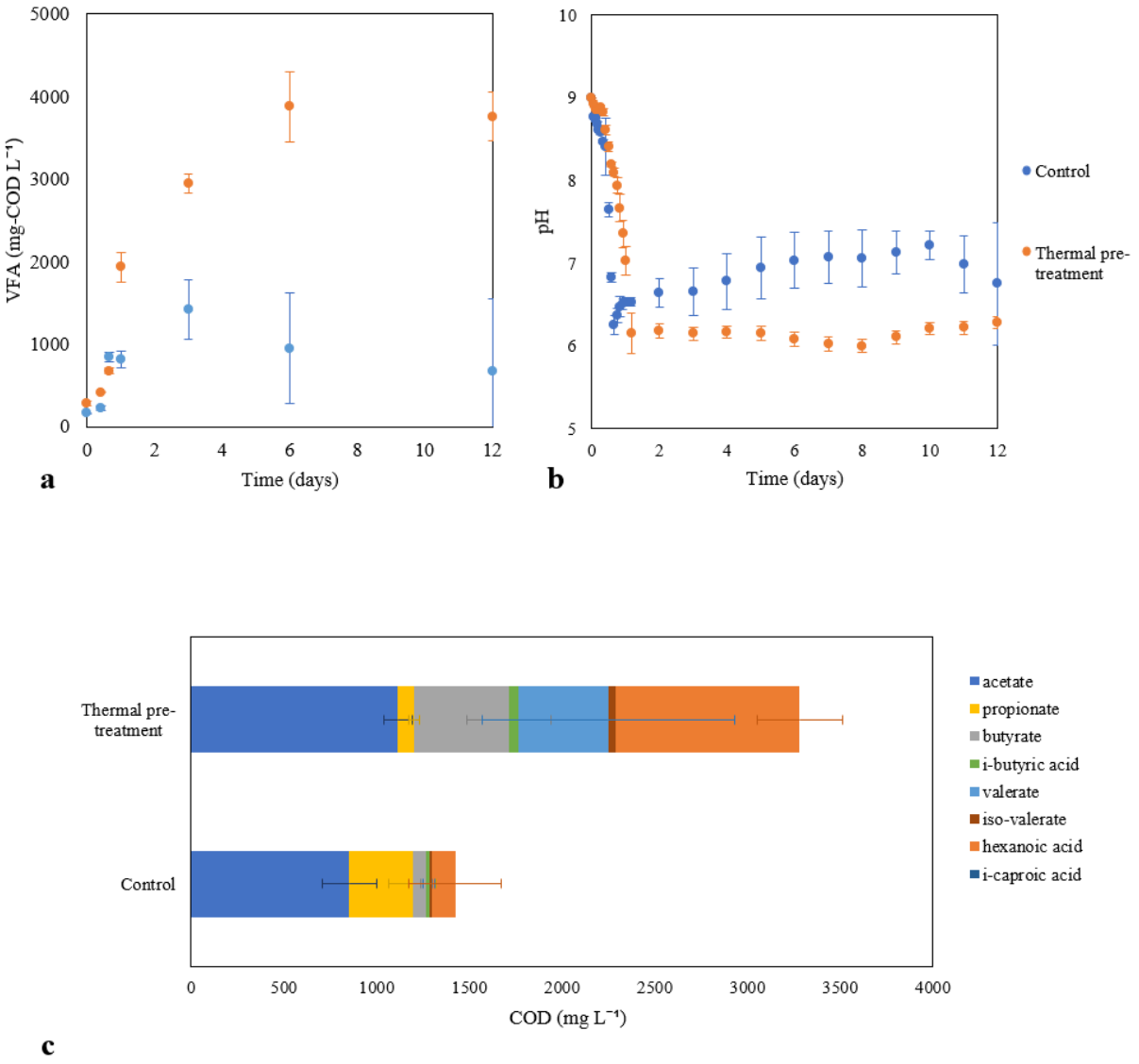

Figure 4: ***a-b.*** *Volatile fatty acids production and pH variation in the control and thermally pre-treated batches. The production of VFAs was higher in the batches containing thermally pre-treated inoculums. The high VFA concentration caused the pH to decrease to 6. VFAs were consumed in the control, causing the VFA concentration to decrease and the pH to increase.* ***c.*** *VFA composition in the control and in the thermally pre-treated batches at the peak of VFA production. VFA concentration was over 2 times higher in the thermal batches (3.3 g COD L^{-1}) than in the control batches (1.4 g COD L^{-1}). The main VFAs in the thermal were acetate, butyrate, valerate, and hexanoic acid. In the control, the main VFAs were acetate and propionate.*

Losses in soluble COD (sCOD) occurred in all batches. In the control batches, the loss was more rapid in the first six days (40 ± 10 % loss) and increased up to 72 ± 11 % at the end of the experiment (sCOD went from

3.7 to 1 g L^{-1}). In the pre-treated batches, the loss was more gradual and reached 23 ± 2 % (sCOD went from 4.2 to 2.4 g L^{-1}).

Volatile solids were measured at the beginning and the end of the experiment. In the control, VS decreased from 6.71 to 5.45 g L^{-1}. In the pre-treated batches, VS decreased from 4.92 to 4.74 g L^{-1}. Considering a carbon content of 0.46 g C g VS^{-1}, this results in a difference of 0.57 and 0.08 g C L^{-1} in the control and the pre-treated batches respectively. This amount of carbon had therefore left the solid-liquid phase in the form of gas resulting in 36 and 5 mmol (907 and 131 mL at 35°C) of CO_2 and or CH_4. A COD content of 1.36 g COD g VS^{-1} results in a difference between the initial and final values of 1.7 and 0.2 g COD L^{-1} for the control and pre-treated batches, equivalent to 509 and 74 mL of methane or 2 L and 294 mL of hydrogen gas.

Alkalinity in all batches was initially 1.53 ± 0.10 g $CaCO_3$ L^{-1}. At the end of the experiment, the alkalinity in the control batches was 2.10 ± 0.08 g $CaCO_3$ L^{-1} (one replicate had a lower value, 0.41 g $CaCO_3$ L^{-1}, which was not included in the average). In the pre-treated batches, the alkalinity decreased to 1.45 ± 0.07 g $CaCO_3$ L^{-1}.

Impact of the inoculum thermal pre-treatment and of the acidogenic fermentation of cheese whey on the microbial community composition

Figure 5 displays the shift in bacterial and archaeal community composition along the acidogenic batch experiments as measured by V3-V4 16S rRNA gene amplicon sequencing. It shows the abundance of genera having a percentage higher than 2%, at the beginning and the end of the experiment, for the control batches and the batches run with thermally pre-treated sludge.

In the inoculum, the most abundant bacterial population was affiliated with the unclassified transient genus Blvii28, wastewater-sludge group (ca. 5% in the control and ca. 9% in the treated sludge). The most abundant archaeal genus was *Methanosaeta* (ca. 3%). Other genera included *Sedimentibacter* (ca. 3%), *Longilinea* (ca. 2-5%), *Candidatus Microthrix* (ca. 2-5%), and *Pseudomonas* (ca. 2-3%). Sulphur oxidizing genus *Sulfurovum* sp. was found as well.

By the end of the experiment, there was a shift in the microbial communities. In the control batches, the most abundant genera were *Comamonas* (ca. 13%), *Escherichia* and *Shigella* (ca. 10%), and *Pseudomonas* (ca. 5%). In the pre-treated batches, the largest fractions consisted of *Desulfitobacterium* sp. (ca. 6%), "*Candidatus* Microthrix sp." (ca. 5%), and *Bacillus* sp. (ca. 5%). *Comamonas* sp. and *Pseudomonas* sp. made up for 4% of the microbial community each. The most abundant archaea was again *Methanosaeta* sp. (ca. 2%).

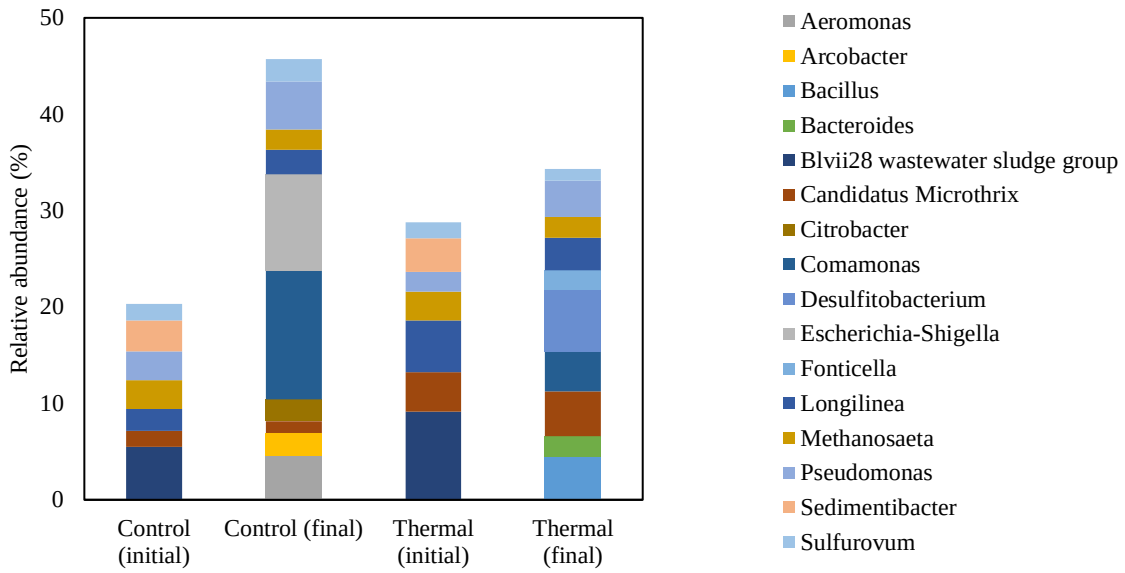

Figure 5: Microbial community compositions of the control and thermally pre-treated inoculum batches. Community profile given by 16S rRNA gene amplicon sequencing targeting both bacteria and archaea with 341F/806R primers, targeting the V3-V4 region. The genera with a relative abundance higher than 2% of the total sequencing read counts are displayed. The remaining fraction is 77% in the control (initial), 69% in the thermal (initial), 53% in the control (final), and 63% in the thermal (final).

3.2.3 Effect of food-to-microorganism (F/M) ratio on the degree of acidification and VFA spectrum

Impact of the food-to-biomass (F/M) ratio on sugar consumption and acidification

The organic substrate concentration measured as total sugar content decreased by over 95% in the first 3 days in all set-ups, from 2.5-3.1 g_{sugars} L^{-1} to 40-96 mg_{sugars} L^{-1}. The final concentration was lower than 90 mg_{sugars} L^{-1}.

Acidification of the substrate occurred rapidly in the first 48 h (1056 mg COD L^{-1} d^{-1}, 789 mg COD L^{-1} d^{-1}, 486 mg COD L^{-1} d^{-1}, 390 mg COD L^{-1} d^{-1}, in the F/M-0.5, F/M-1, F/M-2, and F/M-4[1] batches, respectively) and continued at a lower rate during the first week of the experiment. pH stabilized around 6.4 in the F/M-0.5 batches, although in one of the duplicates the pH started to increase from day 5 onwards. Similar behaviour occurred in the F/M-1 and F/M-2 batches. Before one of the duplicates started to deacidify, pH was stabilized at 5.3 and 5.1 in F/M-1 and F/M-2, respectively. In F/M-4, pH stabilized and remained at 4.5. Figure 6 shows the variation of VFA production with the F/M ratio applied.

The maximum VFA concentration was reached between the third and the sixth day. VFA consumption occurred in most replicates after the first week. The maximum degree of acidification is shown in Table 7.

Table 7: Variation of the degree of acidification obtained with the F/M ratio imposed.

	F/M-0.5	**F/M-1**	**F/M-2**	**F/M-4**
DA	77 ± 7%	60 ± 4%	43 ± 3%	35 ± 3%

The composition of the VFAs produced varied with the F/M ratio. Moreover, the composition varied with time in each batch and quite significantly between replicates. At the maximum degree of acidification, the major fermentation products were acetate (0.6-1.5 g COD L^{-1}), butyrate (0.07-0.8 g COD L^{-1}), and hexanoic acid (0.1-0.65 g COD L^{-1}). The amount in each F/M batch is shown in Figure 7. Butyrate production occurred until

[1] F/M-0.5, F/M-1, F/M-2, and F/M-4 refer to the batches having a food-to-microorganism ratio of 0.5, 1, 2, and 4 g COD g VSS^{-1} respectively.

day 3, while its consumption was later observed. Based on when the maximum DA occurred (*i.e.*, before or after the third day), butyrate was found or had already been consumed. This explains its large variation in the F/M duplicates. If maximum DA was reached on day 3, its concentration was high; if maximum DA was reached later, butyrate had been consumed. Formate was produced during the first 24 h, but it was not detected from day 3 onwards, except in F/M-2.

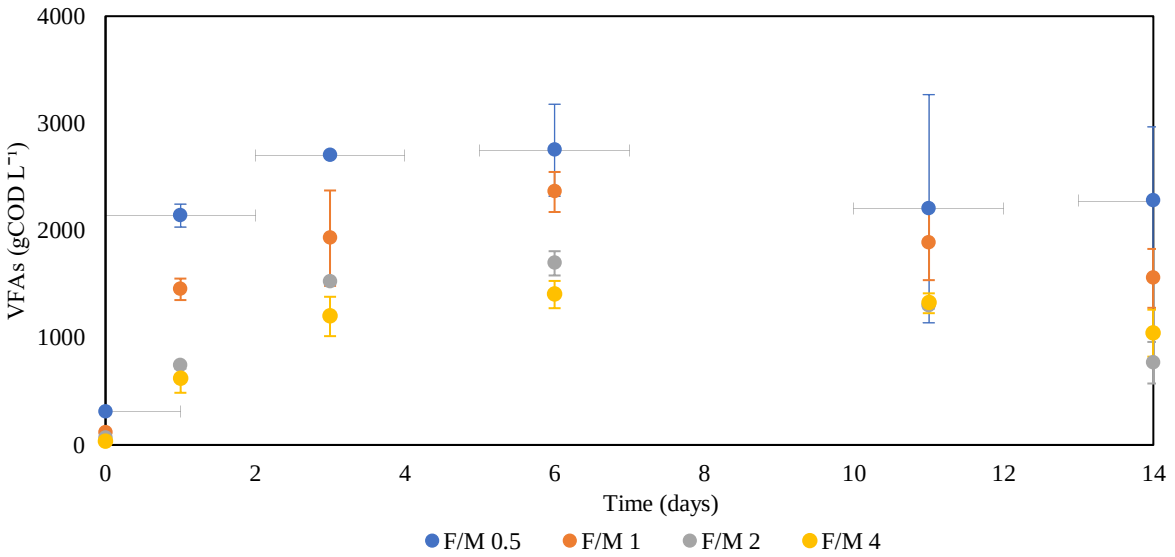

Figure 6: Volatile fatty acids production and pH variation in the different F/M ratio batches. The increase in F/M ratio determined a decrease in VFA production. The VFA content stabilised between the 3rd and the 6th day and subsequently decreased.

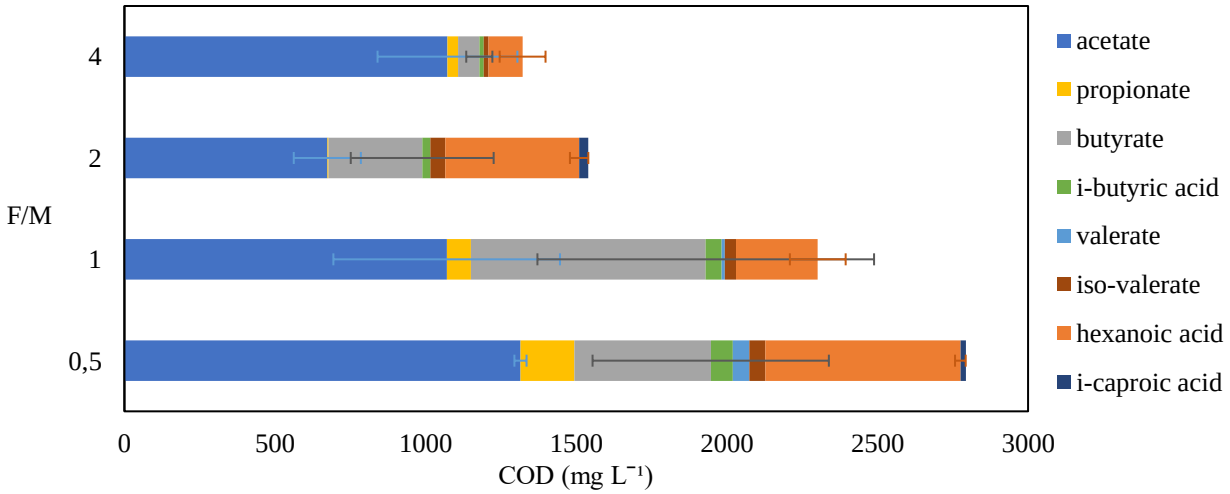

Figure 7: VFA composition in the different F/M batches at the peak of VFA production. The main products were acetate, butyrate, and hexanoic acid. Acetate made up for 80% of the VFA in F/M-4. For the other F/M ratios, it made up for 40-50% of the total products.

Effect of the F/M ratio on the initial and final alkalinity

Alkalinity variations are described in Table 8. Different F/M ratio let to a significant variation in initial alkalinity. This resulted from the low alkalinity of the DWP40 solution. The initial alkalinity decreased by 58%, 73%, and 82% compared to the F/M-0.5 condition in the F/M-1, 2, and 4, respectively. Alkalinity determines the pH at equilibrium and influences the VFA formation. Therefore, the DAs obtained are not only a function of the F/M but also of alkalinity, as shown in Figure 8.

In all batches, an initial sCOD loss occurred in the first 3 days (ca. 28% in F/M 0.5, ca. 34% in F/M 1, ca. 43% in F/M 2, ca. 40% in F/M 4). Additional sCOD losses varied between each replicate. When sCOD did not decrease much further, the maximum DA was reached between day 6 and 11. When an additional loss occurred (up to 70%), the maximum DA took place between day 3 and day 6.

For the F/M experiment, gas measurements showed no methane nor hydrogen production. Oxygen was detected in concentrations between 2.2-8.9% (v/v), even though nitrogen was sparged at the beginning of the experiment.

Volatile solids were measured at the beginning and at the end of the experiment. VS decreased from 8.20 to 5.74 g L^{-1}, from 4.12 to 3.53 g L^{-1}, from 3.78 to 2.11 g L^{-1}, and from 4.02 to 1.52 g L^{-1}, for F/M ratios of 0.5, 1, 2, and 4 g COD g VS^{-1}, respectively. This results in a difference of approximately 1.1, 0.3, 0.8, and 1.1 g C L^{-1}. This amount of carbon had therefore left the solid-liquid phase in the form of gas resulting in 93, 22, 63, and 94 mmol (1.75, 0.42, 1.19, and 1.78 L at 35°C) of CO_2 and or CH_4. The same approximation for the total COD results in a difference between the initial and final values of approximately 3.36, 0.8, 2.28, and 3.41 g COD L^{-1} for the control and pre-treated batches, equivalent to 995, 237, 674, and 1000 mL of methane gas.

Table 8: Alkalinity variation amongst the different F/M ratios imposed and over time.

Alkalinity	**F/M 0.5**	**F/M 1**	**F/M 2**	**F/M 4**
Initial (g $CaCO_3$ L^{-1})	1.66 ± 0.10	0.7 ± 0.04	0.44 ± 0.01	0.30 ± 0.00
Final (g $CaCO_3$ L^{-1})	1.80 ± 0.07	0.87 ± 0.06	0.57 ± 0.03	0.18 ± 0.06

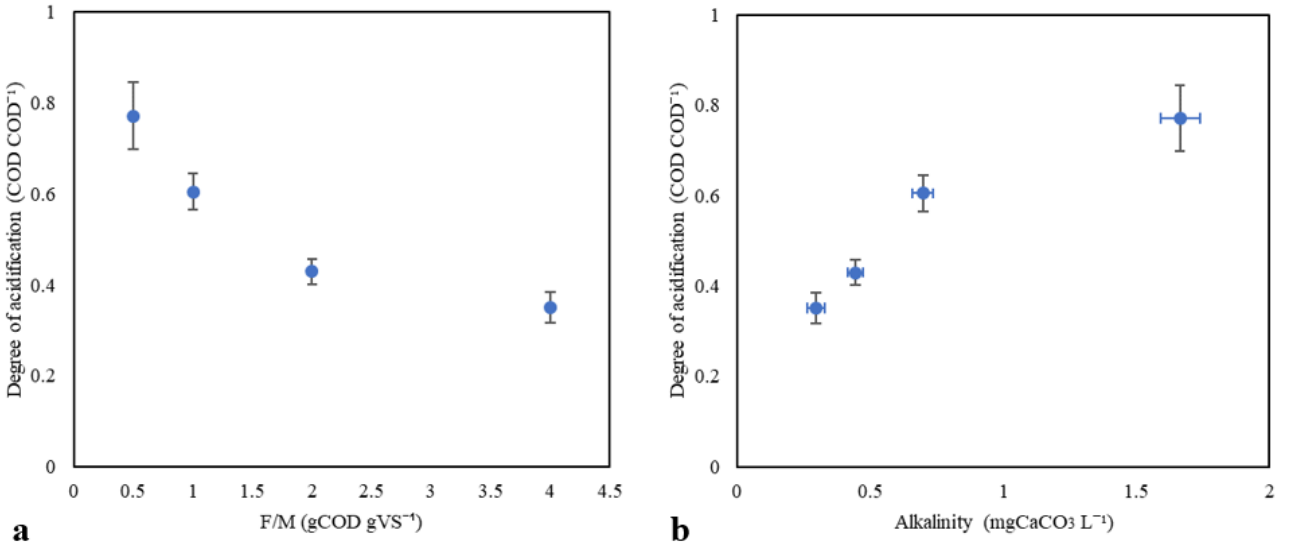

Figure 8: Influence of F/M ratio (a) and alkalinity (b) on the degree of acidification. F/M was imposed and caused a variation in the degree of acidification obtained. Alkalinity varied as a result of the F/M imposed; the degree of acidification was also influenced by the variation in alkalinity.

3.3 Discussion

3.3.1 Volatile fatty acids production was improved by the thermal pre-treatment of the inoculum, lower food-to-microorganism ratio and higher alkalinity

The experiments conducted on acidogenic fermentation highlighted the differences in VFA production from 40% demineralized cheese whey determined by the thermal pre-treatment of the inoculum and the food-to-microorganism ratio.

Thermally pre-treating the sludge at 90°C inhibited methanogenic activity and impacted the degree of acidification reached, which increased from 40% in the control to 85% in the pre-treated batches. The lower accumulation of VFAs can be explained with the production of methane that occurred in the control batches, which derives from VFA consumption when acetotrophic methanogenesis occurs (van Lier *et al.*, 2008). No methane was detected in the batches containing thermally pre-treated inoculums. Similar results have been found by Mockaitis *et al.* (2020) and Xia *et al.* (2015), who have described the improvement of hydrogen production by inhibiting hydrogen consumers such as methanogenic archaea. In batch cultures, where no operational parameters are controlled, this can offer an advantage for VFA production and accumulation by rapidly eliminating the methanogens.

The F/M ratio also had a strong impact on the degree of acidification obtained. The maximum degree of acidification (77%) was obtained with a F/M ratio of 0.5 g COD g VS^{-1}, and it decreased for higher F/M ratios (the lowest DA was 35%). Therefore, high demineralized cheese whey loadings caused inhibition of the acidogenesis process. Conversely, low substrate concentrations were sufficient to sustain the acidogenic microbial activity and provide a high degree of acidification. Lower F/M ratios have resulted favourable for VFA production from cheese whey: Silva *et al.* (2013) have observed decreasing degree of acidification with higher F/M ratios (from 50% to less than 29% using 2 and 10 g COD g VSS^{-1}).

However, the F/M ratio was not the only parameter influencing the acidogenic fermentation. Because of the low alkalinity of the substrate, the main fraction of the alkalinity was provided by the inoculum. Since no extra alkalinity was added, F/M ratios also determined the alkalinity of the systems, decreasing from 1.66 to 0.3 g $CaCO_3$ L^{-1}. Alkalinity is a crucial parameter in anaerobic digestion in order to control the production of fermentative metabolites. In other studies, high alkalinity has been found to favour VFA production (Silva *et al.*, 2013; Dahiya *et al.*, 2015).

In this study, it is difficult to separate the effect of the F/M and alkalinity as the increase of the former caused the decrease of the latter. These two factors played together in the determination of the degree of acidification obtained in different conditions. Lower F/M ratio allowed a faster VFA production, which, however, did not cause an excessive pH decrease due to the alkalinity provided by the higher inoculum fraction. The pH reached at equilibrium was higher (6.5) than for lower F/M ratios (4.5-5.3), despite the higher accumulation of VFAs.

Untreated inoculums were not used in the F/M experiment since, based on the results of the previous test, it was expected that the degree of acidification reached would have been lower than for the treated inoculums. However, batches with lower alkalinity (higher F/M) might present a less significant difference between the degree of acidification for both treated and untreated inoculum. Acidification of the media inhibits methanogenesis (van Lier *et al.*, 2008), hence the acidic pH (4.5-5.3) would have contributed to halting methane production in the untreated inoculums as well.

3.3.2 VFA spectra variations were not only defined by thermal pre-treatment or food-to-microorganism ratio

The acidogenic fermentation of demineralized cheese whey resulted in the production of several volatile fatty acids, mainly acetate, butyrate, propionate and hexanoic acid. The quantity and relative abundance of these VFAs varied with the experimental conditions applied.

In the first experiment, untreated inoculums resulted in higher fractions of acetic acid (60% vs. 34% in terms of COD). This can be explained by the lower pH (6 vs. 6.7) reached in the pre-treated batches. A lower pH is known to direct a higher presence of longer-chain VFAs (Liu *et al.*, 2012) since under these more acidic conditions there are more reducing equivalents available to be incorporated into the fatty acid chains (Silva *et al.*, 2013).

When F/M ratio was varied, different VFA spectra were found. However, the correlation between the VFAs found and the F/M ratio and alkalinity is not clear. Higher pH did not correspond to a higher acetate fraction, as observed in the first experiment and other studies. On the contrary, the lowest pH (4.5) corresponded to the highest acetate fraction (80% in g COD). Moreover, the VFA spectra are difficult to compare because the variation was significant between duplicates, as shown by the error bar in Figure 7. Compounds such as butyrate were consumed after their production in only one of the duplicates, resulting in a concentration with a relative error between 62 and 87%.

The VFA composition may have been affected by factors other than F/M, pH or alkalinity. Although the pressure was released to 1 atm while taking samples, pressure build-up was not measured. Pressure can exert a significant effect on the thermodynamics of the anaerobic conversions and selection of different metabolic pathways, resulting in different metabolic products (Fynn and Syafila, 1990). Further investigation is advisable to understand the VFA production and consumption mechanisms better. This will be crucial for driving the spectrum of fermentation products to desired compounds.

Overall, a higher concentration of VFA with even carboxylic chains (85-96% of the total VFAs in terms of COD) was produced by the thermally pre-treated inoculums. VFAs with even carboxylic chains can be used for polyhydroxybutyrate (PHB) production (Silva *et al.*, 2013; Calero *et al.*, 2017). For microalgae and cyanobacteria growth, mostly acetate, the simplest even carboxylic chain VFA, has successfully been used as an organic carbon source. Fei *et al.* (2015) have used a mixture of VFAs (acetate, propionate, and butyrate) to grow the microalga *Chlorella protothecoides* and observed that the more complex VFAs were mostly consumed once acetate had been depleted.

3.3.3 Carbon and COD losses could not be fully explained with the available data

Soluble COD and TOC measurements showed a decrease in all experiments. These were related to *(i)* biomass growth and, therefore, suspended COD and TOC increase. To biogas production *(ii)*, with CO_2 and CH_4 resulting in TOC losses, and CH_4 and H_2 resulting in COD losses. To organic matter oxidation *(iii)*, with CO_2 production causing TOC and COD losses. These streams were estimated based on the sCOD, sTOC, VS and gas chromatography measurements.

The untreated inoculum was the only batch that presented methane production in the gas samples. In this case, a part of the COD and carbon losses estimated (1.7 g COD L^{-1} and 0.57 g C L^{-1}) is a result of the production of biogas. However, it is surprising that no methane nor hydrogen gas was detected after the first 24, while VFAs and sCOD continued to be depleted. On the other hand, an increase in aerobic or facultative aerobic populations (*Comamonas*, *Aeromonas* and *Arcobacter* (Hilton *et al.*, 2001) along with the acidogenic genera

(*Bacillus*, *Bacteroides*, *Escherichia*, and *Pseudomonas* (Anderson *et al.et al.*, 2003; Shah *et al.*, 2014)) were observed. The increase in aerobic species could indicate partial oxidation of the organic matter.

In the first experiment, the treated inoculum presented a lower estimated COD and carbon losses (0.2 g COD L^{-1} and 0.08 g C L^{-1}). This could be related to the H_2 production measured or organic matter oxidation, as aerobic populations were also found in the biomass samples taken at the end of the experiment. However, in the food-to-microorganism ratio experiment more substantial COD and carbon losses (0.8-3.41 g COD L^{-1} and 0.3-1.1 g C L^{-1}) were observed, despite gas chromatography did not detect any methane nor hydrogen gas production. These numbers suggested an error in the gas measurements or a substantial overestimation of the COD and carbon losses. It is evident than VFAs were somehow depleted after the first week in all experiments. The sCOD measurements (often close to the total amount of VFAs) suggested that they were transformed either into suspended or gaseous products. The presence of aerobic populations and, consequently, organic matter oxidation is still to be determined by 16S rRNA gene amplicon sequencing.

For future research, it is suggested to perform quantitative gas measurements and total TOC and COD measurements. This was not possible for the set-ups and equipment used in the current study.

4. Growth, selection, and competition of green phototrophs on cheese whey and derived organic compounds

4.1 Materials and Methods

4.1.1 Experimental set-ups for phototrophic cultures

Surface water inoculum

Sample from a local canal (location: 51.9892190, 4.3809350 – Delft, The Netherlands) was collected and used as inoculum for the production of the microalgal mother culture.

Incubator for shake-flask cultures

Phototrophic cultures were grown in shake-flasks inside an incubator (shaker KS-15, hood TS-15, Edmund Bühler GmbH, Germany) at 145 rpm mixing at 35°C. A led lamp (10 W, 700 LM, 300K, 230V-50 Hz, GAMMA, The Netherlands) was placed inside the incubator, providing a continuous illumination of 80 μmol photons m^{-2} s^{-1}.

Enrichment mother culture

An enrichment of green phototrophs was cultivated from the surface water inoculum. This mother mixed culture was grown photolithoautotrophically in flask cultures (500-mL Duran™ flasks). The inoculum was first acclimatized for 15 days on Allen's Blue-Green algal medium (BG-11) (Allen and Stanier, 1968), containing inorganic nutrients, as shown in Table 9. The medium was autoclaved at 121°C.

Table 9: The composition of the inorganic medium for photolithoautotrophic algal growth (Allen and Stanier, 1968).

BG-11 medium composition	
Na_2MG EDTA	1.000 mgL^{-1}
Ferric ammonium citrate	6.000 mg L^{-1}
Citric acid · $1H_2O$	6.000 mg L^{-1}
$CaCl_2$ · $2H_2O$	36.00 mg L^{-1}
$MgSO_4$ · $7H_2O$	75.00 mg L^{-1}
K_2HPO_4	30.50 mg L^{-1}
H_3BO_3	2.860 mg L^{-1}
$MnCl_2$ · $4H_2O$	1.810 mg L^{-1}
$ZnSO_4$ · $7H_2O$	0.222 mg L^{-1}
$CuSO_4$ · $5H_2O$	0.079 mg L^{-1}
$COCl_2$ · $6H_2O$	0.050 mg L^{-1}
$NaMoO_4$ · $2H_2O$	0.391 mg L^{-1}
Na_2CO_3	0.020 g L^{-1}
$NaNO_3$	1.500 g L^{-1}

The growth of green phototrophs was monitored for fifteen days by absorbance measurement at 750 nm using a spectrophotometer (DR3900, Hach Lange, USA).

Shake-flask batch cultures for green phototroph selection

Selection for phototrophic microorganisms was tested in mixed cultures grown on a medium composed of either inorganic (*i.e.*, carbonate) or organic carbon sources (*i.e.*, acetate, lactose, and DWP40). The media were amended with nutrients and trace elements, as described in Table 9, except for when DWP40 was used as the sole source of nutrients (DWP40 contains C, N, and P, as shown in Table 6). The photolithoautotrophic mother enrichment culture was used as an inoculum. The cultivations were tested in systems with and without gas exchange with the atmosphere (*i.e.*, open and closed flasks, respectively). In open systems, flat-bottom Duran™ flasks of 250-500 mL were used and equipped with cotton stoppers that let air diffuse in the flask. In closed systems, bottles of 100 mL were sealed with rubber stoppers and aluminium crimp caps, and sparged with nitrogen. Dissolved oxygen was stripped out from the cultivation medium to ensure initial anaerobic conditions and determine the effect of dissolved oxygen concentrations on the mixed microbial culture.

Photolithoautotrophic growth

Autotrophic cultures were first grown on standard BG-11 using flasks of 250-500 mL that allowed gas exchange. Cultures were grown over 30 days. Samples were taken for absorbance measurements (750 nm), nutrient consumption, pH measurements, chlorophyll extraction, DNA sequencing, phase-contrast microscopy, cell counting and cell viability.

Additional experiments were performed. The dissolution of carbonate was improved by heating the medium up to 90°C. Using the medium with improved CO_3^{2-} dissolution, $NaNO_3$ was replaced by an equal amount (17.6 mmol-N L^{-1}) of NH_4Cl in a culture with gas exchange and in one without. VSS, nutrients (C, N, P) and pH variation were measured. Microscope images were taken.

Photoorganoheterotrophic growth using cheese whey as the sole nutrient source

Photoorganoheterotrophic cultures were grown solely on cheese whey in open flasks of 500 mL. The medium used for these experiments consisted of a solution of dissolved DWP40 in demineralized water, at a concentration of 4, 2, and 1 g L^{-1} (ca. 4, 2, and 1 g COD L^{-1}), respectively. Samples were taken for absorbance measurements (750 nm) and amplicon sequencing.

Photoorganoheterotrophic growth using acetate, lactose and cheese whey

The first set of photoorganoheterotrophic cultures was conducted on sodium acetate and cheese whey – using open flasks of 250 mL. The cultivation medium was a modified BG-11 solution, in which the sodium carbonate was replaced with an equivalent number of C-moles (0.189 mM) in the form of acetate or DWP40. The TOC content of DWP40 was used to determine the carbon content of the powder (see Table 6). Samples were taken for absorbance measurements (750 nm), pH measurements, chlorophyll extraction, phase-contrast microscopy, cell viability and cell counting. Amplicon sequencing was performed on the culture grown on cheese whey.

In the second set, open and sealed flask cultures were compared using sodium acetate, lactose and DWP40 as carbon sources. The carbon concentration was 0.189 mmol C L^{-1} in a first experiment and 18.9 mmol C L^{-1} in a second experiment. Additional nutrients were provided by a BG-11 medium in which $NaNO_3$ was replaced by an equal amount (17.6 mmol-NL^{-1}) of NH_4Cl. This change was made since cheese whey mostly contains nitrogen in the form of proteins, which are first degraded to ammonium. Samples were taken for absorbance measurements (750 nm), nutrient consumption, pH measurements, and phase-contrast microscopy.

The experiments performed are summarized in Table 10. Experiment codes are given for future reference.

Table 10: Summary of the experiments performed, showing their reference code and their main characteristics. The experimental code is given by the carbon source (A: acetate; CW: 40% demineralized cheese whey; L: lactose), the gas exchange (O: open flask; X: sealed flask), the nitrogen source (N: nitrate; A: ammonium), while the "100" subscript indicates a 100-fold carbon concentration.

Experiment code	Carbon source	Carbon concentration	Gas exchange	Nitrogen source	Measurements
AON	Acetate	0.189 mmol C L^{-1}	Allowed	Nitrate	VSS, cell counting and viability, pH, chlorophyll extraction, amplicon sequencing (CWON only), phase-contrast microscopy
CWON	Demineralized cheese whey	0.189 mmol C L^{-1}	Allowed	Nitrate	
LOA	Lactose	0.189 mmol C L^{-1}	Allowed	Ammonia	VSS, nutrient consumption (N, P), pH, phase-contrast microscopy
LXA	Lactose	0.189 mmol C L^{-1}	Not allowed	Ammonia	
AOA	Acetate	0.189 mmol C L^{-1}	Allowed	Ammonia	
AXA	Acetate	0.189 mmol C L^{-1}	Not allowed	Ammonia	
LOA_{100}	Lactose	18.9 mmol C L^{-1}	Allowed	Ammonia	VSS, nutrient consumption (C, N, P), pH, chlorophyll extraction, phase-contrast microscopy
LXA_{100}	Lactose	18.9 mmol C L^{-1}	Not allowed	Ammonia	
AOA_{100}	Acetate	18.9 mmol C L^{-1}	Allowed	Ammonia	
AXA_{100}	Acetate	18.9 mmol C L^{-1}	Not allowed	Ammonia	
$CWXA_{100}$	Demineralized cheese whey	18.9 mmol C L^{-1}	Not allowed	Ammonia	

C:N:P variation in photoorganoheterotrophic cultures

The effect of an increasingly higher addition of C-moles in the form of DWP40 and acetate to the BG-11 medium was studied in 48-well plate experiments. The carbon concentration ranged from 0.221, 0.947, 2.524, 6.31, 12.621 to 25.241 mmol C L^{-1}, with a resulting C:N:P of 1:101:1, 5:101:1, 14:101:1, 36:101:1, 72:101:1, 144:101:1. The experiment lasted 10 days. Absorbance was measured over the visible light spectrum using a microplate reader (Synergy™ HTX, BioTek, USA).

Continuous-flow photobioreactor

A 3.5-L photobioreactor (PBR) operated at a working liquid volume of 2 L was used to grow phototrophs under photolithoautotrophic followed by photoorganoheterotrophic conditions. The lighting was provided by a 75-W light jacket (PhotoBioSim, Designinnova, India) emitting photosynthetically-active radiation between 400-700 nm (with peaks at 470 and 660 nm). The emitted light intensity was 96 µmol photons m^{-2} s^{-1}. An external structure consisting of polyisocyanurate (PIR) boards was constructed to avoid the interference of external light sources. A specially made anchor paddle provided mixing (120 rpm) and removed the biofilm formed on the reactor walls. The temperature was kept at 35°C, and argon (50 mL min^{-1}) was used as the off-gas carrier. The gas flow was regulated by a mass flow controller (0154 Microprocessor Flow Control & Read Out Unit, Brooks Instruments, USA), and the CO_2 and O_2 content in the off-gas were measured with an online gas analyser (NGA 2000, Rosemount, USA).

pH and dissolved oxygen (DO) were measured continuously in all set-ups using sensors (Applisens, Appliko, United States). The scheme and pictures of the reactor set-up are shown in Figure 9.

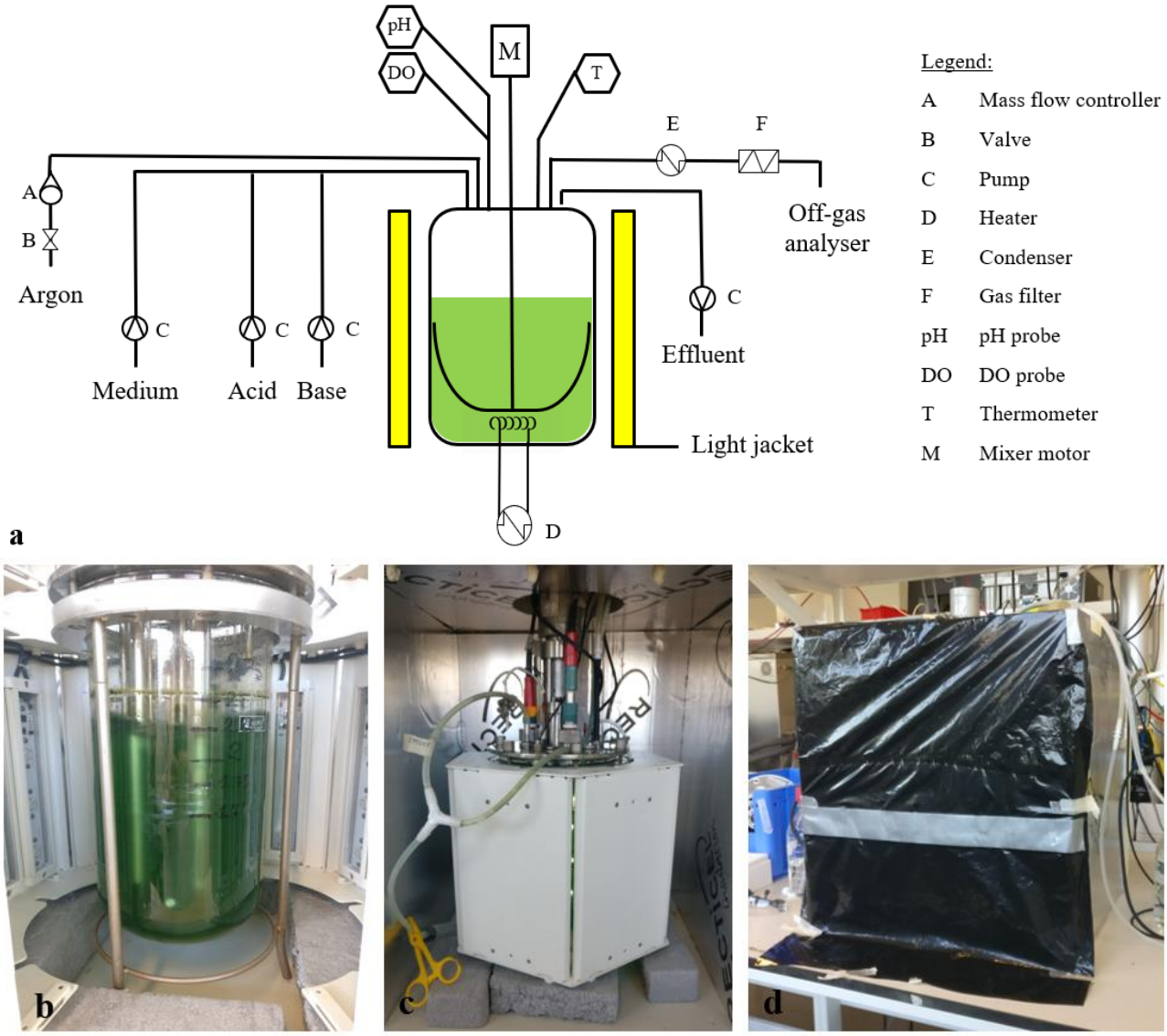

Figure 9: ***a.*** *Scheme of the photobioreactor built and used for this study. Illumination was provided by a light jacket surrounding the vertical walls of the reactor. Mixing was provided by a home-made anchor paddle. In all set-ups, the temperature was kept at 35°C and argon was injected in the reactor. The incoming gas flow was controlled by a mass flow controller, while the off-gas was cooled by a condenser and passed through a cotton filter before being sent to the off-gas analyser. DO, temperature and pH were continuously measured in all set-ups. For the chemostat regime, influent and effluent flows were regulated by pumps. Acid and base were dosed in order to maintain the pH at 7.* ***b.*** *Picture of the reactor and the interior of the light jacket.* ***c****. Picture of the exterior of the light jacket and the interior of the PIR-boards structure.* ***d.*** *Picture of the exterior of the PIR-boards structure; access to the reactor was possible by an opening in the front, covered by a black plastic sheet.*

Initial operation as a photolithoautotrophic batch

The PBR was first run in batch mode to activate the inoculum (taken from the mother culture) for autotrophic growth. The BG-11 medium was used to this end. The batch experiment lasted for 12 days. Carbonate dissolution in the cultivation medium was improved in an additional experiment by heating the medium up to 90°C. This experiment lasted for 7 days. Biomass growth and nutrient consumption were monitored.

Photoorganoheterotrophic chemostat

The PBR was run as a continuous-flow stirred tank reactor (CSTR) using acetate as a carbon source (18.9 mmol C L^{-1}). Additional nutrients were provided as described in BG-11 medium composition, except for nitrogen, which was supplied in equal moles of nitrogen but using NH_4Cl instead. The dilution rate was initially set to 0.24 d^{-1} and later decreased to 0.17 d^{-1}. pH was kept at 7.00 ±0.15 by acid and base addition (HCl 0.1 mol L^{-1}, NaOH 0.1 mol L^{-1}).

CO_2 and O_2 in the off-gas were measured continuously. Biomass growth was monitored daily until a steady-state was reached. Nutrient consumption was measured at steady-state.

4.1.2 Analytical and calculation methods

Water quality parameters

DO and pH were measured with probes (C6010, Consort, Belgium and 9300, Jenway, United Kingdom, respectively). Nitrate, nitrite, ammonium and phosphate content were either measured by Hach Lange kits (LCK-304, LCK-339) or with a discrete analyser (Gallery™ Discrete Analyzer, Thermo Fisher Scientific, USA). Absorbance was measured by a spectrophotometer (DR3900, Hach Lange, USA).

COD, TOC, TIC, TN and solid content were measured as described in section 3.1.4.

Organic carbon sources and fermentation products

Lactose, glucose, galactose, acetate and FPs were measured using an HPLC analyser as described in section 3.1.4.

Phototrophic biomass

Biomass growth was monitored by measuring the absorbance at 750 nm (A_{750}) of the culture using a spectrophotometer (DR3900, Hach Lange, USA). To convert the absorbance to grams of biomass per litre, a calibration curve was created using eq. 3:

$$C_{biomass}\,(g\ VSS\ L^{-1}) = m * A_{750} + q \quad (3)$$

VSS measurements were performed as described in section 3.1.4.

Maximum growth rates, yields, production rates, biomass specific rates of substrate conversion were calculated as described by equation 4, 5, 6, and 7, respectively:

$$\mu_{max}(d^{-1}) = \frac{\ln\left(C_{biomass,2}\right) - \ln\left(C_{biomass,t1}\right)}{t_2 - t_1} \quad (4)$$

$$Y_{VSS/C}(mgVSS\ mgC^{-1}) = \frac{C_{biomass,2} - C_{biomass,1}}{C_{Carbon,2} - C_{Carbon,1}} \quad (5)$$

$$P_{VSS}(mgVSS\ d^{-1}) = \frac{C_{biomass}}{Q} \quad (6)$$

$$q_S(mg_{acetate}mgVSS^{-1}\ d^{-1}) = \frac{C_{acetate,2} - C_{acetate,1}}{P_{VSS}} \quad (7)$$

In batch systems, only the yield was calculated. In this case, subscript 1 and subscript 2 refer to the beginning of the experiment and to the end of the exponential growth phase, respectively. In the chemostat, subscript 1 and subscript 2 refer to the inflow and outflow concentration, respectively.

Flow cytometry analysis of cell counting and cell viability

Cell counting and cell viability were measured by flow cytometry using a BD Accuri™ C6 cytometer (BD Biosciences, Belgium). The cytometer is equipped with a 50 mW laser emitting at a fixed wavelength of 488 nm and operated at a flow rate of 66 µL min^{-1}. Fl1 (533 ± 30 nm Band Pass Filter) was used for forward scatter light and Fl3 (> 670 nm Band Pass Filter) for side scatter light. Gating strategy and data collection were performed as described by Prest *et al.* (2013).

To determine the total number of cells, samples were diluted and stained (5 µL of dye and 45 µL of diluted sample) with a SYBR green dye (10000 x conc. stock solution (Invitrogen, USA), working solution of 10 µL

into 1 mL of 10 mmol L^{-1} Tris buffer pH 8). SYBR green was used in combination with propidium iodide (PI) dye (30 mmol L^{-1} in DMSO stock solution (Invitrogen, USA)) to determine the cell viability. Cells were stained with a solution made of 10 µL SYBR Green I stock solution and 20 µL of propidium iodide stock solution in 1 mL of 10 mmol L^{-1} Tris buffer pH 8.

Cell viability by methylene blue analysis

Methylene blue (MB) uptake was used to evaluate cell viability, following the methodology proposed by Bicas *et al.* (2015). Two samples of 3 – 5 mL were taken from the culture, and one of the two was heated at 99°C using a water bath for 5 min. After cooling down, the samples were centrifuged for 3 min at 4000 g min^{-1}. The supernatant was discarded, and the pellet was resuspended into 4 mL of MB solution (85 µM of MB in phosphate buffer solution 0.1 M, pH 7.4); the solution was vortexed. After two minutes, the samples were centrifuged again for 3 minutes at 4000 g min^{-1}. The absorbance of the supernatant at 664 nm was then measured and compared with the A_{664} of the MB solution. The uptake of MB was measured with eq. 8:

$$MB_{uptake} = 14.86 * 4 * \left(A_{664}^{solution} - A_{664}^{sample}\right) \quad (8)$$

as in Bicas *et al.* (2015). The cell viability was measured by considering the ratio between the MB uptake in the raw sample and the boiled sample.

Analysis of the microbial community composition

The microbial communities were studied using a phase-contrast microscope (Axioplan 2 imaging, ZEISS, Germany).

Amplicon sequencing was carried out to determine the species present in the microbial communities. Both V3-V4 16S and V4 18S rRNA gene amplicon sequencing were performed to identify prokaryotic and eukaryotic cells, respectively. The primer sets used are defined in Table 11. DNA extraction and sequencing were carried out as described in section 3.1.4. Operational taxonomic units were also analysed using the SINA (v.1.2.11) aligner based on the global SILVA alignment for rRNA genes.

Table 11: Primers selected with the targeted region and sequences.

Amplicon sequencing	Primer	Region	Primer sequences 5'-3'
16S rRNA gene	341F	V3-V4	CCTAYGGGRBGCASCAG
	806R		GGACTACNNGGGTATCTAAT
18S rRNA gene	528F	V4	GCGGTAATTCCAGCTCCAA
	706R		AATCCRAGAATTTCACCTCT

Pigment extraction

Pigments were extracted from the biomass using a DMSO and acetone (80%) solution (1:1 v/v), adapted from Shoaf and Lium (1976). Pellets extracted from 1 mL of biomass by centrifugation (13300 g min^{-1}, 3 min) were resuspended using 1 mL of the DMSO/acetone solution and kept at 4°C in dark conditions. After 24 h, the mixture was centrifuged (13300 g min^{-1}, 3 min), and the absorbance spectrum of the supernatant was measured using the DMSO/acetone solution as a blank.

Pigment contents were calculated as a function of the absorbance, as described by Wellburn (1994). The content of chlorophyll *a*, chlorophyll *b* and total carotenoids in an 80% acetone solution are calculated with eq. 9, 10, and 11, respectively. While the same compounds in a DMSO solution are calculated with eq. 12, 13, and 14:

$$Chl_a = 12.21 * A_{663} - 2.81 * A_{646} \quad (9)$$

$$Chl_b = 20.13 * A_{646} - 5.03 * A_{663} \quad (10)$$

$$Car = (1000 * A_{470} - 3.27 * Chl_a - 104 * Chl_b)/198 \quad (11)$$

$$Chl_a = 12.19 * A_{665} - 3.45 * A_{649} \quad (12)$$

$$Chl_b = 21.99 * A_{649} - 4.53 * A_{665} \ (13)$$

$$Car = (1000 * A_{480} - 2.14 * Chl_a - 70.16 * Chl_b)/220 \ (14)$$

The pigment content was estimated by calculating the average between the results for pure DMSO and pure acetone (80%) solutions. This approximation was justified by the fact that the difference between the equations is generally considered negligible (Arnon *et al.*, 1948; Speziale *et al.*, 1984).

4.2 Results

4.2.1 Characteristics of the photolithoautotrophic culture grown in shake-flasks: growth parameters, pigment content, and microbial populations

Biomass growth and cell viability

Photolithoautotrophic cultures grew on BG-11 over more than 30 days. pH increased from 7 to over 11 during this period. Carbon was continuously available since gas exchange with the outside air was possible, which, together with the high pH, enabled CO_2 dissolution. No limitation of nitrogen or phosphorus occurred. However, the amount of nutrients readily available was reduced by the formation of carbonate precipitates, which was identified by the increased turbidity of the medium.

The VSS content was determined from absorbance measurements at 750 nm (A_{750}) using eq. 3. The calibration line (m=0.332; q=0.0003; R^2=0.9915) was valid for the interval A_{750}={0:1.8} and $C_{biomass}$(g VSS L^{-1})={0:0.63}. The maximum growth rate μ_{max} (0.97 d^{-1}, R^2 = 0.9957) was calculated during the exponential phase using eq.4. The VSS concentration increased to over 650 mg VSS L^{-1} during the duration of the experiment.

According to the flow cytometry (FCM) measurements conducted after staining the cells with SYBR Green dye, the number of cells increased from $1.75*10^5$ to $249.5*10^5$ counts in the first two days. The number of cells continued to grow at a lower rate ($15.3*10^5$ counts d^{-1}) afterwards. The population size slightly decreased on the 23rd and 25th day but was again higher on the 31st. This final trend, when compared to the VSS increase, would suggest an inaccuracy in the measurement, with an underestimation on the 25th day and an overestimation on the 31st. The evolution of VSS (derived from the absorbance measurements) and FCM cell count throughout the experiment are given in Figure 10.

Methylene blue was used to determine cell viability. This measurement showed a percentage of viable cells close 100% during the first 10 days, which later decreased down to 17% on the last day of measurements. FCM also determined cell viability, although the only reliable measurements were obtained on the 25th and 31st day, possibly due to degradation of the PI-SYBR green dye in the working solution previously used. The degradation of the dye was visible from the unusual position of cell counts in the Fl1 vs. Fl3 plots, which were not in the same perimeter as when the SYBR green dye alone was used. This was no longer observed when a new PI-SYBR dye was used (day 25 and 31). The percentage of living cells was higher than the percentage calculated by methylene blue adsorption, as seen in Figure 10.

Cell viability and cell counting showed a high percentage of viable cells during the first 7 to 10 days. The percentage of viable cells decreased after the 10th day. This was less perceptible by the absorbance measurement, which can be related to both cell enlargement and debris formation.

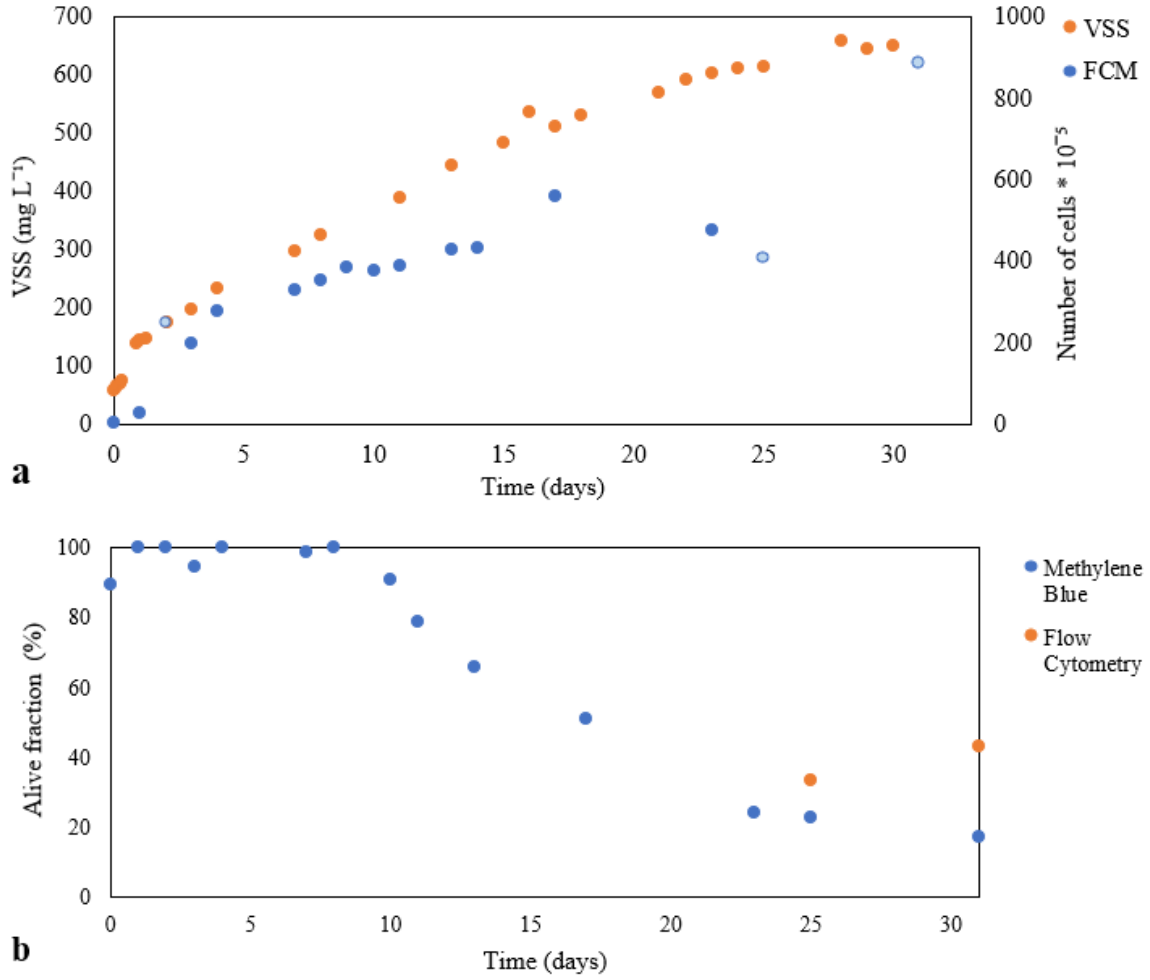

Figure 10: ***a.*** *VSS and cell number increase over 30 days in photolithoautotrophically grown cultures. FCM measurements in light blue are considered outliers. Incorrect FCM measurements can occur when the dilution of the sample is insufficient or excessive.* ***b.*** *Cell viability as measured by methylene blue adsorption and flow cytometry (the latter was reliable only for the last two measurements). The alive fraction was close to 100% during the first week and later decreased. Flow cytometry indicated a higher fraction than methylene blue on the 25th and 31st day of the experiment.*

Influence of the C-content, N-source and gas exchange on the growth rate and biomass concentration

Technical adaptations were made step-wise to optimize the cultures. Variations in the media influenced the growth of the photolithoautotrophic community, as shown in Table 12.

Table 12: Variations in μ_{max} and pH evolution occurred when the mineral media was modified. Next to the pH value is indicated (in brackets) the number of days necessary to reach such value.

	Undissolved Carbonate, Nitrate, gas exchange	**Dissolved Carbonate, Nitrate, gas exchange**	**Dissolved Carbonate, Ammonia, gas exchange**	**Dissolved Carbonate, Ammonia, no gas exchange**
μ_{max} (d^{-1})	0.97	0.47	0.40	0.12
Final pH and period	10 (15 d)	10 (1 d)	5.2 (3 d)	7.7 (6 d)
Biomass increase (mg VSS L^{-1})	600	200	90	15

White precipitates observed in previous cultures were supposed to originate from the incomplete dissolution of carbonates; the preparation of the medium was therefore optimized by stirring and heating the solution to 90°C to reach complete dissolution. When the carbonate minerals were fully dissolved in the solution, the maximum growth decreased to 0.47 d^{-1} (R^2 = 0.9939) and the VSS concentration after 10 days reached over

250 mg L^{-1}. Given the significant difference in biomass production (600 mg VSS L^{-1} with precipitate formation and 200 mg VSS L^{-1} without), it is possible that the formation of precipitates led to increased turbidity inside the culture, and therefore to an overestimation of the biomass by the absorbance measurements. The complete dissolution of the precipitates caused a faster increase in pH (from 7 to 10 in one day).

The nitrogen source was switched from nitrate to ammonium (i) since ammonium is more present in the bulk of acidogenic fermenters than nitrate, and (ii) to avoid the supply of terminal electron acceptors (action more valid to prevent competition with denitrifiers in subsequent photoorganoheterotrophic mixed cultures). When the nitrogen source was changed from nitrate to ammonium, the growth rate further decreased to 0.40 d^{-1} (R^2 = 0.9939). The VSS concentration started to decrease after the 3rd day, reaching a maximum concentration of 125 mg VSS L^{-1}. The limitation in growth was due to the acidification, which resulted in pH values below 5.5, and restricted the dissolution of CO_2 inside the solution, making carbon a limiting factor. Low pH can also be detrimental to certain algal species.

The results above were obtained with systems that let air and CO_2 diffuse in the bottles. Comparison tests were performed with sealed bottles. In the culture without gas exchange, the exponential phase was slower and limited by the impossibility of external CO_2 dissolution. The maximum biomass concentration was 52 mg VSS L^{-1}, a 42% increase of the initial biomass, very limited compared to cultures with gas exchange.

Pigment content

The presence of phototrophic microorganisms was easily detectable due to the green coloration of the cultures. Moreover, the presence of pigments was identified in the absorbance spectra of the cultures: peaks were found at 440, 630 and 680 nm, corresponding to chlorophyll A and B. Both the coloration and the absorbance spectrum of the cultures are shown in Figure 11.

Pellet resuspension into the DMSO/acetone solution allowed to extract the pigments from the biomass. The absorbance of the extracted pigments and the culture are shown in Figure 11. After the extraction, the peaks are more visible since the absorbance of the biomass is no longer measured. The peaks are subject to a slight shift towards the left due to the different solvent used (water vs. DMSO/acetone). The extraction of the pigments allowed their quantification based on the absorbance at the peaks, as described in the *Materials and Methods*.

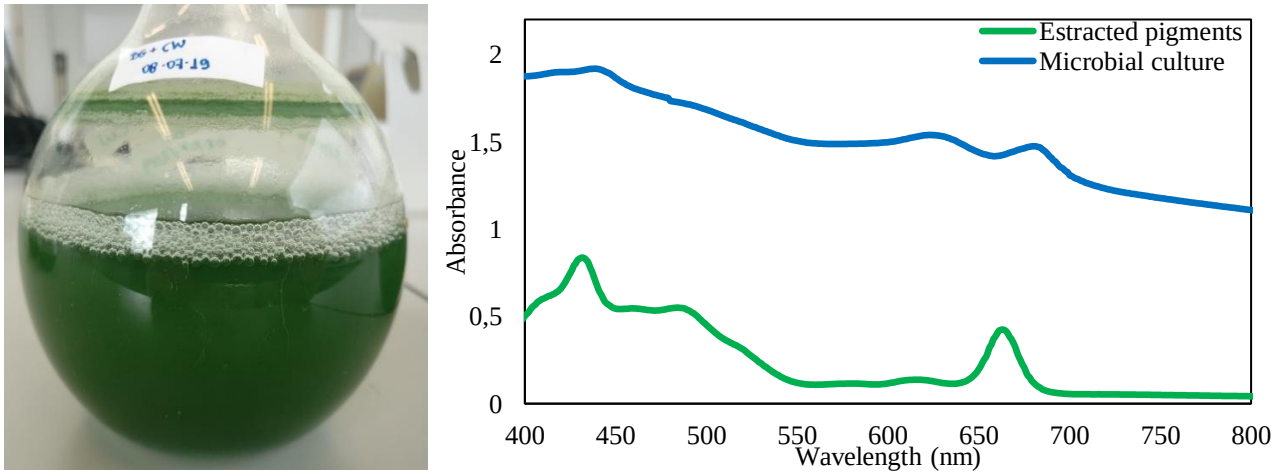

Figure 11: L: Picture of one of the cultures after several days of cultivation. R: Absorbance spectra of the microbial culture and of the pigments extracted with the DMSO/acetone solvent, as measured after thirteen days. Peaks are visible at 440, 630, and 680 nm in the culture, while they are shifted in the DMSO/acetone solution.

The pigment content increased along with the biomass concentration. After the exponential growth phase, the concentration of pigments inside the culture (µg L^{-1}) increased linearly until the end of the measurements (16 days). Biomass specific pigment content also increased, as shown in Table 13.

Table 13: The production rate of the pigments was constant after 5 days of measurements. The amount of pigments per VSS increased over time: the maximum value shown on the table refers to the last day of measurement.

	Chlorophyll A	Chlorophyll B	Total Carotenoids
Production rate (µg L^{-1} d^{-1})	212	143	103
Biomass specific content (day 5) (µg mg VSS^{-1})	10.3	1.2	4.3
Max biomass specific content (day 16) (µg mg VSS^{-1})	14.7	4.8	6.2

Individuation of phototrophic cells by phase-contrast microscopy

Phase-contrast microscopy observations revealed the presence of different types of microorganisms. However, there was a clear abundance of green round-shaped cells (3-4 µm diameter), present as aggregates or isolated cells. The colour of the cells was visible through the ocular, although not recorded by the black-and-white camera. Larger organisms were found as well, but not as frequently. Smaller bacteria were always observable in the background. Variations in the inorganic substrate did not show any clear difference in the microscope observation of the cultures. Microscope images are shown in Figure 12. Pictures were taken with 25x (g), 63x (b; c; f) or 100x (a; d; e) magnification lenses.

Identification of the microbial genera via 16S and 18S rRNA gene amplicon sequencing is discussed in section 4.2.3.

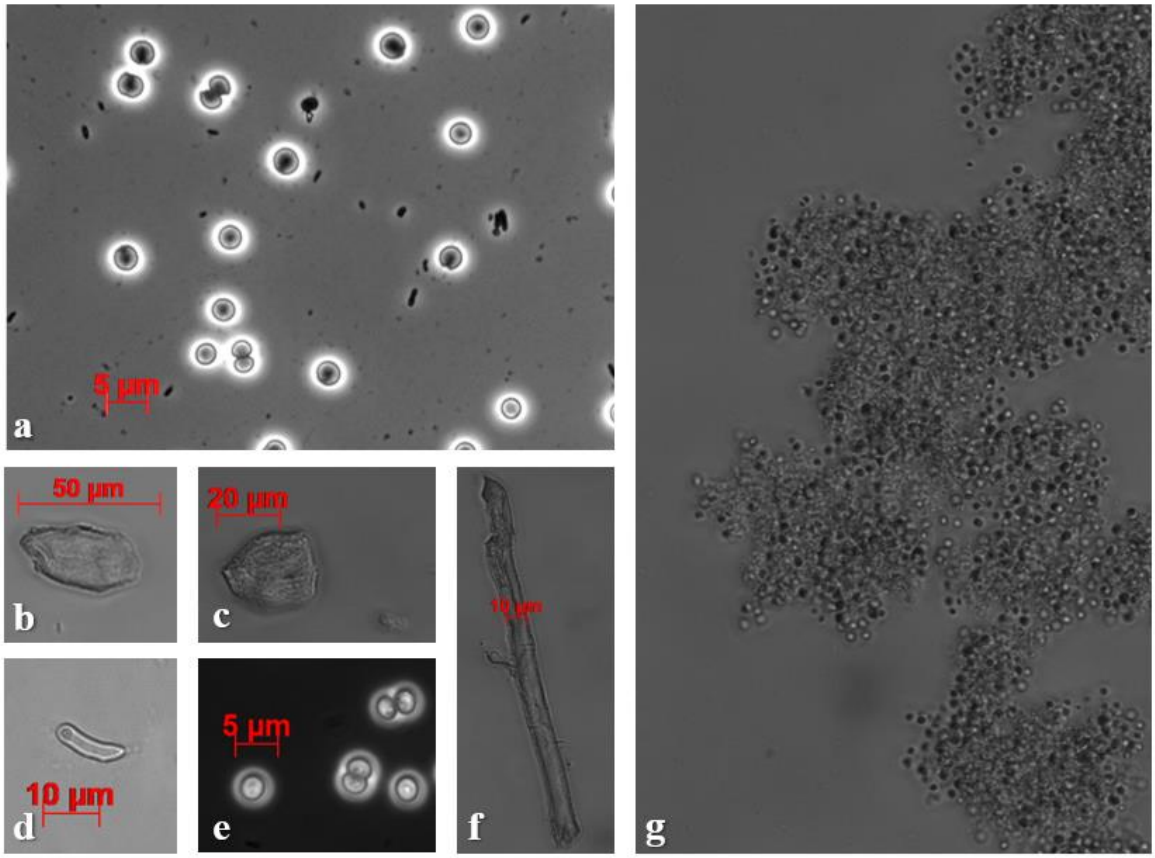

Figure 12: Figures «a» to «g» show the microorganisms found in the photolithoautotrophic cultures. The most abundant and visible cells are round-shaped of 3-4 µm diameter (Figures «a», «e», «g»); they form aggregates (Figure «g»). Larger microorganisms were found (Figure «b», «c», «d», «f»). Smaller bacteria can be observed in the background (Figure «a»).

4.2.2 Photoorganoheterotrophic growth on partially demineralized cheese whey as the sole nutrient source

Cultivation using partially demineralized cheese whey as the sole nutrient source did not successfully produce green phototrophic biomass. The C:N:P ratio of the cheese whey solution is too unbalanced (222:3:1 in moles,

see section 3.2.1), with not enough nitrogen and phosphorus to allow phototrophic growth. The fact that it is readily acidifiable causes an extreme decrease in pH.

The growth was halted after two to three days at a biomass concentration of 140-190 mg L^{-1}(initial concentration of 50 mg L^{-1}). The pH dropped to 3-4. In the cultures fed with 2 g L^{-1} and 4 g L^{-1} (approx. 2 and 4 g COD L^{-1}) of DWP40, the biomass turned white, and no peaks were visible in the absorbance spectra. The culture fed with 1 g L^{-1} of cheese whey gained a yellow coloration and showed peaks at 440 and 680 nm. In addition, biomass agglomeration was visible in the flask.

4.2.3 Identification of microbial populations from 16S and 18S rRNA gene amplicon sequencing

V3-V4 16S and V4 18S rRNA gene amplicon sequencing were performed on selected samples (photolithoautotrophic cultures, photoorganoheterotrophic cultures grown on DWP40). The results indicated the presence of numerous different populations.

Cultures grown on BG-11 or modified BG-11 (experiment CWON, see Table 10) showed similar compositions.

According to 16S rRNA gene amplicon sequencing, Cyanobacteria (mostly *Cyanobium PCC-6307* sp., *Synechocystis PCC-6803* sp.) made up for 10-20% of the bacterial community of these photolithoautotrophic and photoorganoheterotrophic cultures. The versatile phototrophic purple non-sulphur bacterium *Rhodobacter* was found in the initial biomass but was less abundant in the enriched cultures. No other phototrophic genera had a relative abundance >2%. Other abundant bacterial species included aerobic chemoorganotrophic genera, such as *Cupravidus*. Between 20-40% of the bacterial community was composed of populations with relative abundances <2%.

According to the 18S rRNA gene amplicon sequencing, the eukaryotic community of these photolithoautotrophic and photoorganoheterotrophic cultures was less diverse, with an elevated relative abundance of the algae *Desmodesmus* (10-30%), *Scenedesmus* (3-20%) and members of the Chlorophyceae and Trebouxiophyceae classes (*Micractinium pusillum* sp. (1-5%), *Chlorella sorokiniana* sp. (30-40% in the enriched cultures)). The 18S dataset also displayed the presence of amoeba of the genus *Vermamoeba* at a relative abundance between 30-40%.

The photoorganoheterotrophic cultures grown on sole DWP40 (1 g L^{-1}, 2 g L^{-1}, 4 g L^{-1}) showed a higher diversity, which increased with the cheese whey concentration. Cyanobacteria were less abundant, while 63-65% of bacterial genera had a relative abundance <2%. The 18S analysis indicated a higher presence of fungi (*e.g. Cladosporium*), retaria (*e.g. Cladococcus*), amoeba (*e.g. Vermamoeba*) and also Vertebrata. The high content of *Sorodiplophrys* (genus of the Labyrinthulomycetes Class**)** in the culture grown on 1 g L^{-1} of cheese whey explains its yellow coloration, as this microorganism is characteristically golden yellow (Tice *et al.*, 2016).

The relative abundances of the dominant genera are shown in Figure 13.

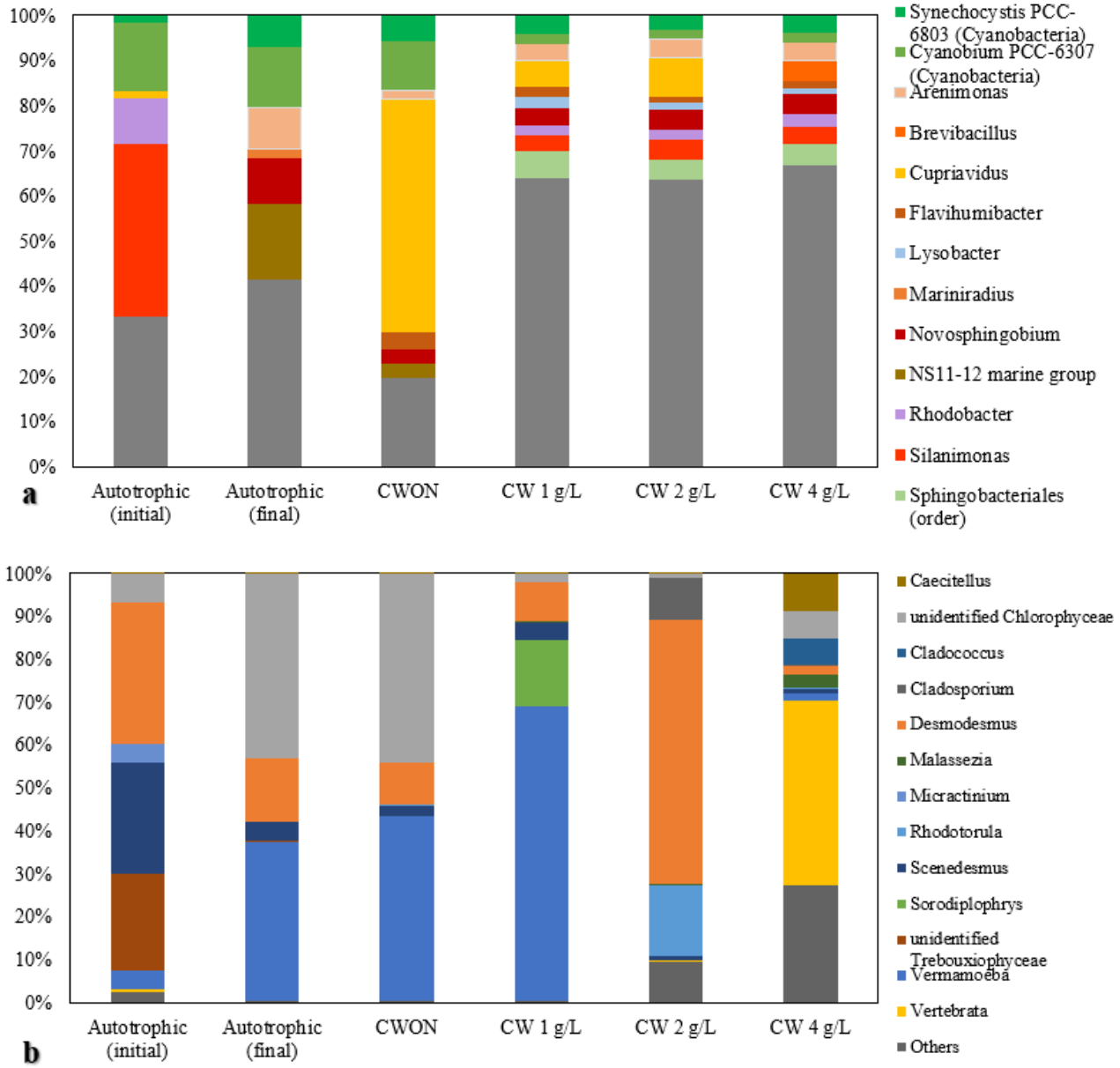

Figure 13: Composition of the bacterial and eukaryotic genera making up the microbial communities. Figure «a» shows the results from V3-V4 region 16S rRNA gene sequencing, while Figure «b» shows the results from V4 region 18S rRNA gene sequencing. Only the most abundant genera are shown (>2%), the others are included in the «Others» category. Autotrophic (initial) and (final) refer to the mother culture photolithoautotrophically grown. CWON refers to the culture grown photoorganoheterotrophically grown on DWP40 (0.18 mol C L^{-1}) and BG-11 medium. CW 1, 2, 3, and 4 g/L refers to the cultures using DWP40 as the sole nutrient source.

4.2.4 Mixotrophic cultures using acetate, lactose, cheese whey as a carbon source

Low carbon concentrations resulted in rapid organic carbon depletion and carbon dioxide utilization

Photoorganoheterotrophic cultures grown on acetate and cheese whey with a concentration of 0.189 mmol C L^{-1} and $NaNO_3$ as a N-source (AON, CWON) showed a behaviour equivalent to that of photolithoautotrophically grown cultures for all parameters (VSS, cell counting, cell viability, pigments and pH variation, microbial community). Because of the low organic carbon concentration that resulted from the direct use and adaptation of BG-11 medium – this traditional medium is primarily designed with a high concentration of nitrogen to enable long-term cultivation of photolithoautotrophic biomass by transfer of CO_2

from air – and the basic pH, the cultures mostly used inorganic carbon as a C-source (*i.e.*, CO_2 from the atmosphere), after rapidly consuming the organic carbon available.

Variations occurred with an equivalent carbon content when using ammonia as a nitrogen source, which was tested in both open cultures and sealed bottles. In cultures with gas exchange (*i.e.*, open cultures), exponential growth was similar under photoorganoheterotrophic (0.46 and 0.44 d^{-1} growth rate with acetate (AOA) and lactose (LOA), respectively) and photolithoautotrophic conditions (0.4 d^{-1} growth rate). However, a faster pH decrease was measured in mixotrophic cultures, which corresponded to a halt in biomass growth. The pH decrease limited the amount of inorganic carbon available for the cultures. This is due to lowering CO_2 dissolution from the atmosphere. The total amount of inorganic carbon present in dissolved water is a function of the pH and is higher at alkaline conditions. The maximum biomass concentration reached was 123 mg VSS L^{-1} for the photolithoautotrophic culture, 100 mg VSS L^{-1} in AOA and 93 mg VSS L^{-1} in LOA. In sealed bottles, no growth was measured in the culture growing on lactose. DWP40 was not tested in these conditions. Growth on acetate showed a lower μ_{max} (0.055 d^{-1}) and maximum biomass concentration (46 mg VSS L^{-1}, 17% increase) than photolithoautotrophic cultures. The low carbon concentration strongly limited growth.

Higher organic substrate concentrations allowed for the selection of green phototrophs in mixed cultures

With a 100-fold addition of carbon, more significant variations in biomass production were observed between the cultures LOA_{100}, LXA_{100}, AOA_{100}, AXA_{100} and $CWXA_{100}$[2]. Biomass growth and pigment content increased in anaerobic cultures, and when acetate was used as a substrate. The main results are summarized in Table 14.

Table 14: Main characteristics of the cultures grown on ammonia and 18.9 mM-C in open (O) and sealed (X) bottles. «+» and «-» signs indicate an increase and a decrease in pH, respectively. "n.a." refers to cultures in which the pigment content was not evaluated.

Experiment	μ_{max} (d^{-1})	Yield (mg VSS mg-C^{-1})	C_{max} (mg VSS L^{-1})	Carbon consumption (%)	pH	Chl_A (µg mg VSS^{-1})	Chl_B (µg mg VSS^{-1})	Carotenoids (µg mg VSS^{-1})
LOA_{100}	0.29	0.34	121	92	-	n.a.	n.a.	n.a.
LXA_{100}	0.14	0.65	111	28	-	11.1	9.3	3.3
AOA_{100}	0.71	0.77	189	96	+	n.a.	n.a.	n.a.
AXA_{100}	0.25	1.15	170	52	+	20.3	13.8	5.3
$CWXA_{100}$	0.56	0.82	140	46	-	8.6	9.5	2.3

LOA_{100} showed a slower exponential growth phase but a higher final concentration than LOA. Both pH evolved similarly. AOA_{100} had a higher μ_{max} and final concentration than AOA and its pH increased to 9. In anaerobic cultures, growth was significantly higher and faster. LXA_{100} pH decreased to 4.5 and increased to 8.5 in AXA_{100}. $CWXA_{100}$ had the highest μ_{max} of all anaerobic cultures but did not grow as much as acetate cultures. pH decreased (from 7 to 4.6) similarly to the lactose cultures. The improved growth using DWP40 rather than lactose can be explained by the additional amount of inorganic nutrients (N, P) provided by the powder (see Table 6). From the absorbance spectra of the cultures, it was possible to observe a higher pigment content in the anaerobic cultures. Pigment extraction from these cultures indicated that the highest amount of pigments per biomass was found in AXA_{100}.

In cultures with gas exchange (*i.e.*, open bottles), dissolved oxygen was available from transfer from the atmosphere according to Henri's law of gas. Without gas exchange (*i.e.*, sealed bottles), the only available oxygen was produced by water oxidation in photosynthesis, or unintentionally introduced during sampling. The growth of aerobic heterotrophic bacteria was therefore advantaged in open cultures, resulting in increased biomass concentration and growth rate, but the limited presence of phototrophs, as shown by the reduced amplitude of pigment-related peaks at 440, 630 and 680 nm. Absorbance spectra are shown in Figure 14.

Carbon was rapidly and almost entirely consumed in the AOA_{100} culture. In all other cultures, carbon was not a limiting factor. Nitrogen and phosphorus concentrations remained higher than 200 mg $N\text{-}NH_4^+$ L^{-1} (80% of the initial concentration) and 2 mg $P\text{-}PO_4^{3-}$ L^{-1} (40% of the initial concentration) respectively, in all cultures,

[2] These cultures were grown on organic carbon (18.9 mmol C L^{-1}), using either lactose (L), acetate (A), or DWP40 (CW), in open (O) or sealed (X) bottles, using ammonium as a N-source.

and were therefore not limiting. The decrease in the growth rate in LOA_{100}, LXA_{100} and $CWXA_{100}$ were concomitant with pH evolution. Consequently, it is possible that acidic pH inhibited growth. The biomass growth inside the cultures is shown together with the evolution of the limiting parameter in Figure 15. No limiting parameter was identified for AXA_{100}. Micronutrients, whose consumption was not measured, might have caused the growth limitation in the AXA_{100}, and possibly LOA_{100}, LXA_{100} and $CWXA_{100}$ cultures.

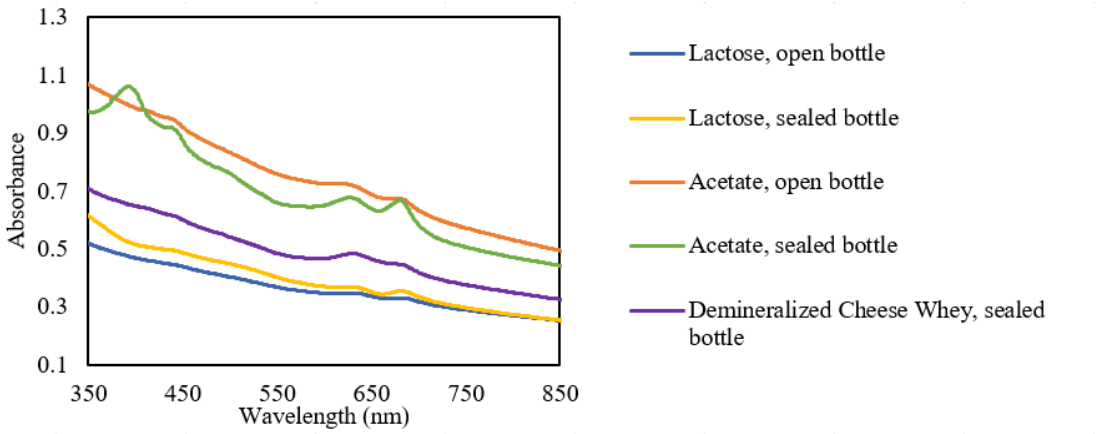

Figure 14: Absorbance spectra of AOA_{100}, AXA_{100}, LOA_{100}, LXA_{100} and $CWXA_{100}$ cultures. The peaks related to the presence of pigments are more visible in sealed bottles. The biomass content (A_{750}) is similar or higher in open bottles.

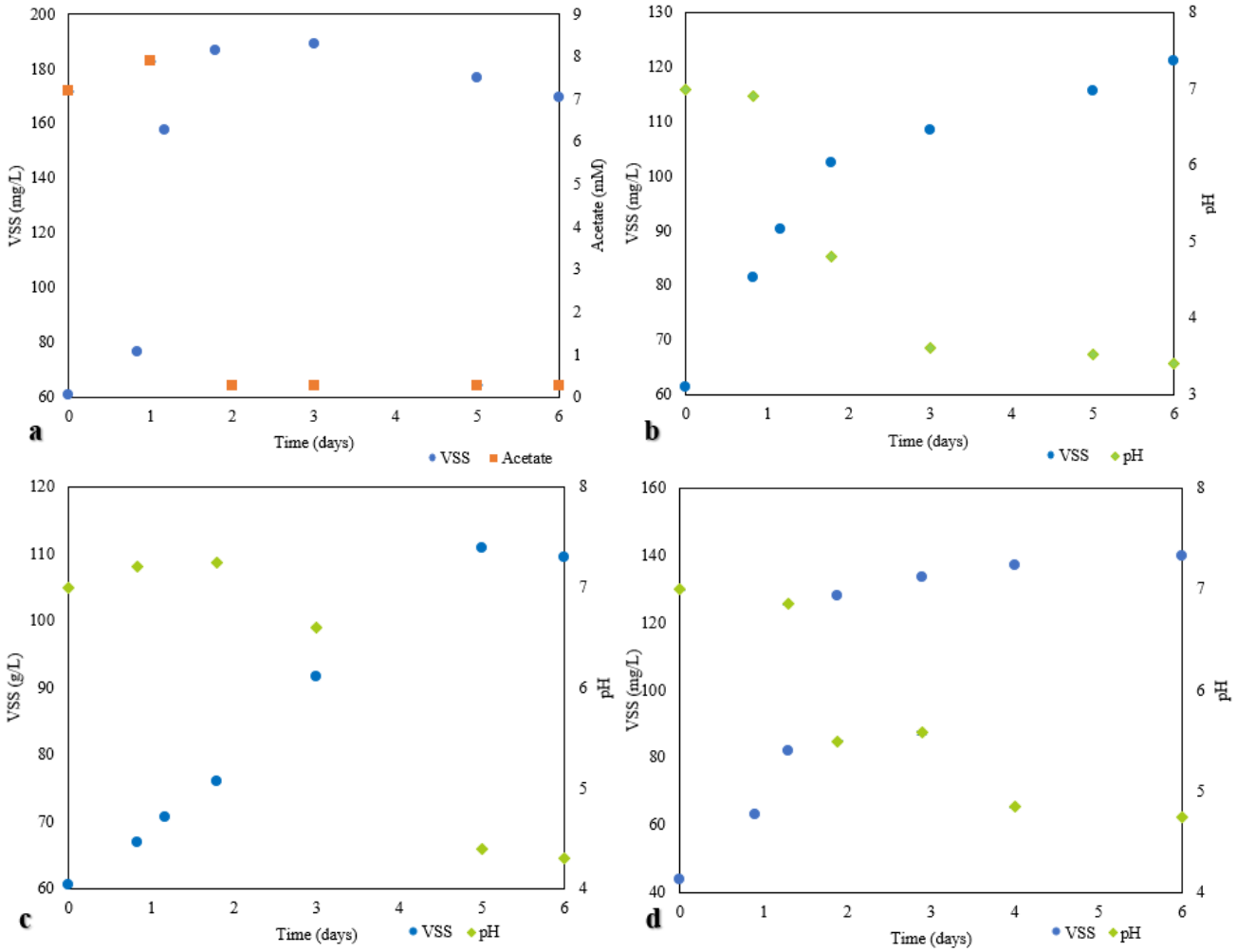

Figure 15: VSS and substrate or pH variations are shown over time. Figure «a», «b», «c», and «d» represent culture AOA_{100}, LOA_{100}, LXA_{100}, and $CWXA_{100}$, respectively. Culture AOA_{100} was limited by the carbon source. LOA_{100}, LXA_{100}, and $CWXA_{100}$ may have been limited by the acidification of the media since the microbial growth decreased after the pH dropped below 4-5.

Microscope observations of the microbial communities were similar to those described in section 4.2.1, as shown in Figure 16.

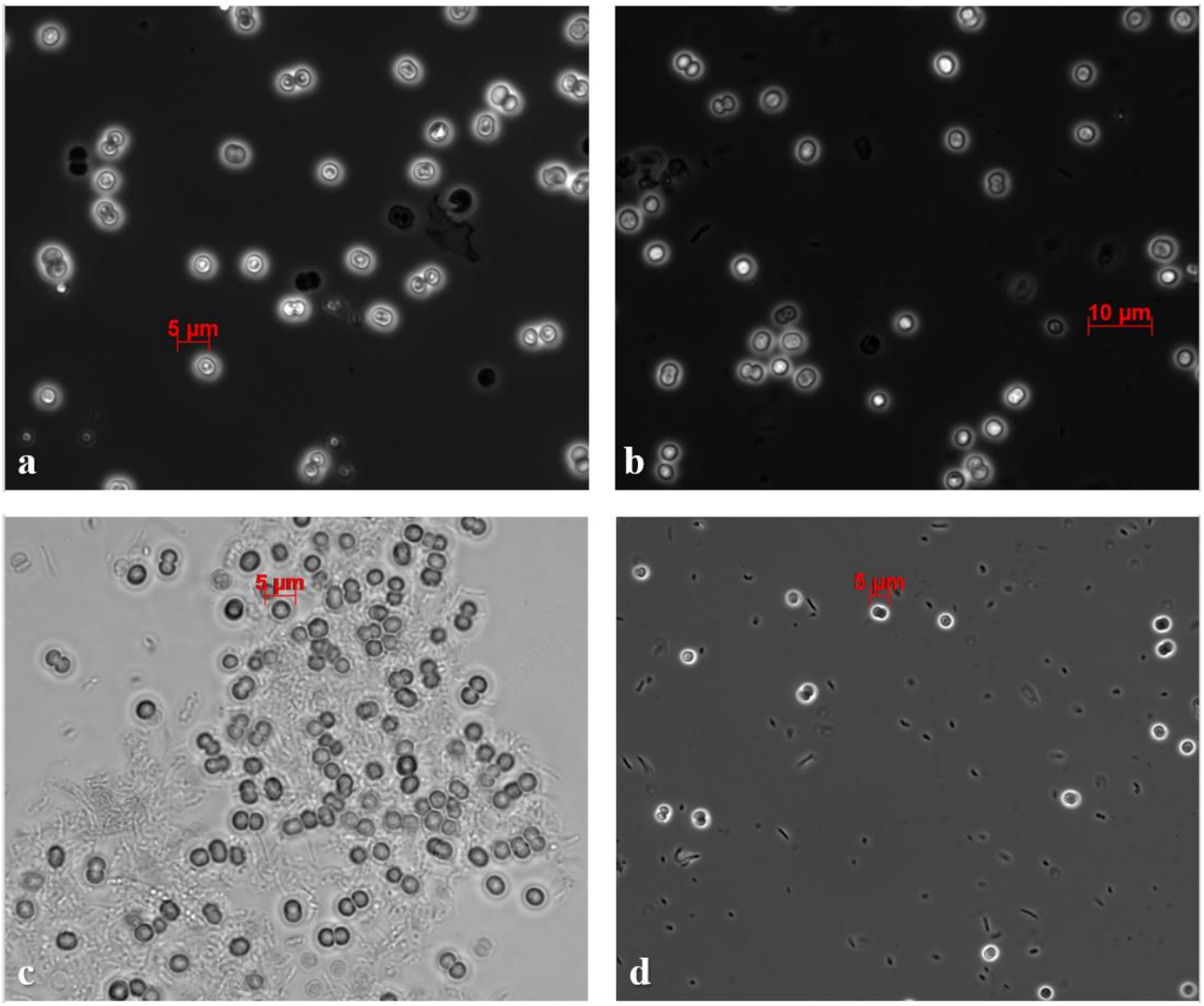

Figure 16: Microscope images from the photo-mixotrophically grown cultures. Figures «a», «b», «c», and «d» show AXA, LOA, AXA_{100} and LXA_{100} cultures, respectively. Small phototrophic cells (3-4 µm diameter) were identified as well as smaller bacterial cells.

4.2.5 C:N:P ratio determined the biomass production and the pigment content

Biomass growth, with the presence of pigments, occurred for all carbon concentrations (ranging from 0.221 to 25.241 mmol C L^{-1}). The results are summarized in Table 15, where A_{750} is used as a proxy for biomass and A_{680} for pigment content (Chlorophyll A). Biomass growth reached a maximum when 2.524 mM of carbon were dosed (C:N:P 36:101:1). The absorbance spectra showed the same peaks (440, 630, 680 nm) present in the photolithoautotrophic cultures (Figure 11). The amplitude of the peaks, similarly to the biomass growth, reached a maximum for a C:N:P ratio of 36:101:1. The variation of the spectra with C:N:P (in terms of moles) is shown in Figure 17.

Based on the composition of algal and cyanobacterial biomass $C_{106}H_{263}O_{110}N_{16}P$ (Redfield, 1934), only the 144:101:1 C:N:P ratio should be limiting, due to a deficit of phosphorus. Nitrogen is never limiting as BG-11 medium supplies over 6 times the N:P ratio required for biomass growth. However, the maximum amount of biomass growth and pigment concentration are reached with a lower amount of carbon. It is possible that, since the system was not closed, gas exchange was possible, and CO_2 could dissolve in the system (pH increased from 6.3±0.1 to 9.6±0.1). Therefore, the total carbon available for the cultures was a combination of carbonate

and organic carbon, thus potentially sustaining photomixotrophic growth. This causes an underestimation of the C:N:P ratio of the cultivation medium and may imply that a mixture of organic and inorganic carbon sources provided a better environment for phototrophs' growth. In this condition, phototrophic microorganisms are advantaged. As a result, at higher carbon concentrations a larger difference is observed in the amount of pigments (A_{680} ca. 2.37 in the best case, 1.75 in second-best case) than in the amount of biomass (A_{750} ca. 1.2 in the best case, 1.1 in the second-best case) with varying C:N:P.

Table 15: Variation of the maximum biomass growth (A_{750}) and the chlorophyll A content (A_{680}) with the carbon content (and therefore with the C:N ratio).

Carbon supply (mmol L^{-1})	C:N:P ratio (mol:mol:mol)	Cheese whey		Acetate	
		Biomass (A_{750})	Chlorophyll (A_{680})	Biomass (A_{750})	Chlorophyll (A_{680})
0.22	1:101:1	0.29	0.37	0.83	0.92
0.95	5:101:1	0.54	0.95	0.90	1.25
2.52	14:101:1	0.76	1.59	0.95	1.62
6.31	36:101:1	1.2	2.33	1.13	2.37
12.62	72:101:1	1.05	1.48	1.11	1.60
25.24	144:101:1	1.11	1.59	0.97	1.75

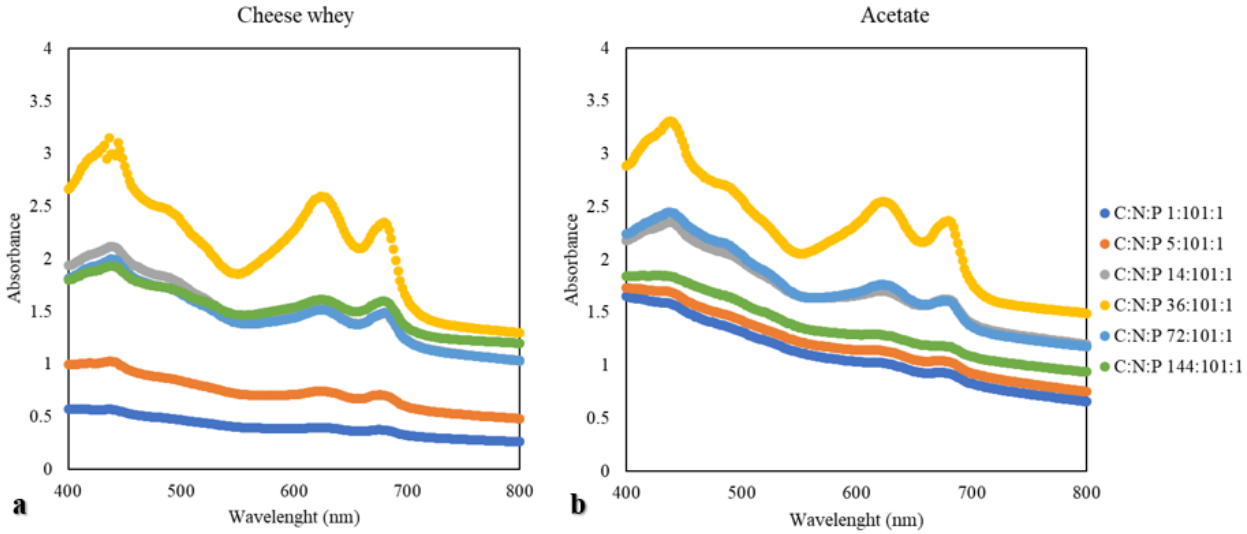

Figure 17: Variation of the absorbance spectra of cultures grown on cheese whey («a») and acetate («b») as a function of the C:N ratio. At a C:N:P ratio of 36:101:1, the biomass and pigment concentration was maximum for both substrates. The spectra are taken at the maximum biomass and pigment content for each culture.

4.2.6 Stirred-tank photobioreactor

Photobioreactor run under batch mode for photolithoautotrophy for the acclimatisation of green phototrophs

The stirred-tank photobioreactor (PBR) was first operated in batch mode to test for the activation and growth of photolithoautotrophic cultures prior to any switch to chemostat experiments with an organic source.

The photolithoautotrophic growth (0.99 d^{-1}) was similar to the one obtained in the flasks during the first six days, but it appeared to be limited afterwards, as shown in Figure 18. pH increased from 6.4 to 7.4.

The limitation in the PBR is likely due to the consumption of carbon and the impossibility to dissolve CO_2 from the outside, as the reactor was sealed, and the gas flow consisted of 100% argon. When carbonate minerals were fully dissolved, the growth decreased significantly, with a biomass increase of approximately 20 mg VSS L^{-1} over seven days, as compared to 300 mg VSS L^{-1} when carbonate precipitates were present

in the primary medium. In the case of fully dissolved carbonates, the pH was initially 8.6 and slightly decreased to 8.5. This behaviour was similar to the one described for the flask cultures.

Nitrogen and phosphorus measurements (over 130 mg $N\text{-}NO_3^-$ L^{-1} and over 5 mg $P\text{-}PO_4^{3-}$ L^{-1}) indicated that these nutrients were not limiting in both cases.

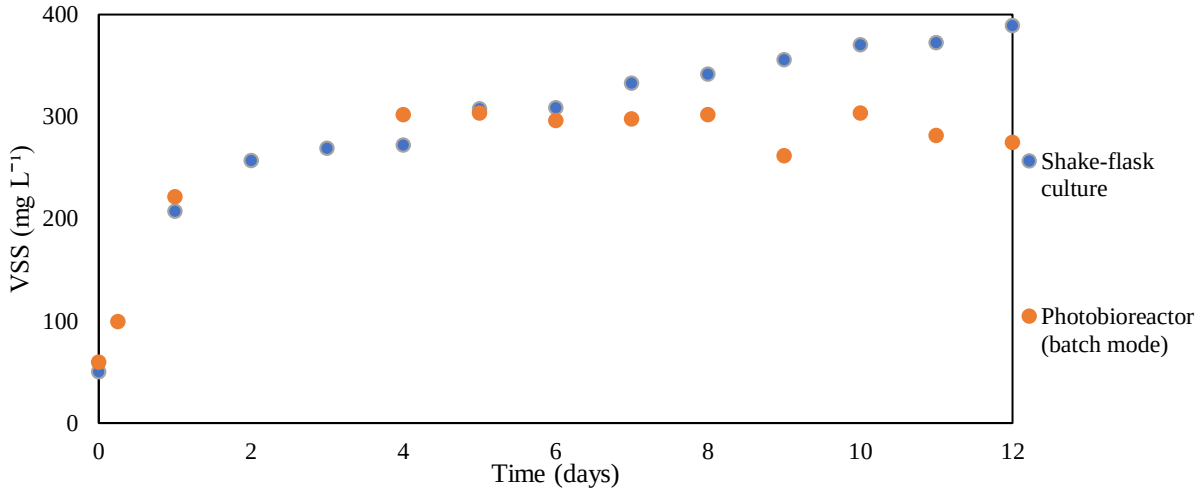

Figure 18: Biomass growth in the photobioreactor (run in batch mode) and in a shake-flask culture. Growth in the photobioreactor was limited after six days. This is due to the impossibility of carbon dioxide dissolution from the outside air.

Photoorganoheterotrophic growth under continuous reactor regime was possible with an adequate retention time

Mixed culture growth on acetate in a continuous-flow stirred-tank reactor (CSTR) mode at a dilution rate of 0.24 d^{-1} resulted in a total biomass production of 41 mg VSS d^{-1}. This dilution rate was initially selected from the maximum growth rate of 0.46 d^{-1} observed in the AOA culture (acetate 0.18 mmol C L^{-1}, open flask, ammonium). The main growth parameters of the culture are shown in Table 16. The culture included a limited number of phototrophic cells. This could be seen in both the absorbance spectra of the culture and of the extracted pigments, which showed little to no peaks at the wavelengths corresponding to chlorophyll *a* (630 nm), chlorophyll *b* (680), and carotenoids (around 440 nm). As shown in Figure 19a, besides the increased bacterial biomass and the already described round-shaped phototrophs, different cells, egg-shaped, ciliated, 20-30 µm long, were found. These cells might be ciliates, which can be predators of microalgae and cyanobacteria. The CSTR PBR was therefore not successful in selecting and harvesting phototrophic biomass with the dilution rate (0.24 d^{-1}) applied.

A different dilution rate (0.17 d^{-1}) was selected based on the maximum growth rate of 0.25 d^{-1} observed in the AXA_{100} culture (acetate 18.9 mmol C L^{-1}, sealed flask, ammonium). No difference in the composition of the medium was made. With the decreased dilution rate, significant improvements were observed. The growth of phototrophic organisms was noticeable by the coloration of the culture and by the absorbance spectra, which presented peaks at 440, 630, and 680 nm, as shown in Figure 20. Moreover, the overall biomass concentration increased from 86 to 125 mg VSS L^{-1}. Biomass evolution over time is given in Figure 21. The dissolved oxygen in the culture increased from close to 0% to 2%. The carbon dioxide in the off-gas decreased from ca. 0.085% to 0.058%, and the transition was oscillatory (Figure 22). The presence of ciliates and smaller bacteria was still visible in the culture, but the number of phototrophic cells became more significant (Figure 19b).

These results imply that with adequate retention time, phototrophic microorganisms were not outcompeted in a chemostat regime.

From CO_2, sCOD, TOC, and VSS measurements, it was not possible to close the carbon and COD balances. The influent concentration was in both cases ca. 571 g COD L^{-1} and 203 mg C L^{-1}. With the higher dilution rate (0. 24 d^{-1}), this resulted in a incoming flow of 274 g COD d^{-1} and 98 mg C d^{-1}, while the measured outflows were 94 mg COD d^{-1} (given by the biomass (65%) and the sCOD (35%)) and 69 mg C d^{-1} (given by the biomass

(30%), the sTOC (21%), and the carbon dioxide (49%)). Therefore, 67% of the COD and 30% of the carbon were not traced. With the lower dilution rate (0. 17 d^{-1}), this resulted in a incoming flow of 206 g COD d^{-1} and 73 mg C d^{-1}, while the measured outflows were 96 mg COD d^{-1} (given by the biomass (69%) and the sCOD (31%)) and 48 mg C d^{-1} (given by the biomass (47%), the sTOC (8%), and the carbon dioxide (45%)). In this case, 53% of the COD and 34% of the carbon were not traced.

*Table 16: G*rowth parameters of the mixed culture grown on acetate (18.9 mmol C L^{-1}), using ammonium as a N-source, in CSTR mode for two different dilution rates.

Dilution rate (d^{-1})	**Yield (mg VSS mg C^{-1})**	**Carbon removal (%)**	**C_{VSS} (mg VSS L^{-1})**	**P_{VSS} (mg VSS d^{-1})**	**P_{CO2} (mL-CO_2 d^{-1})**	**q_s ($mg_{acetate}$ mg VSS^{-1} d^{-1})**
0.24	0.45	93	86	41	62.6	1.30
0.17	0.66	95	125	45	39.6	1.38

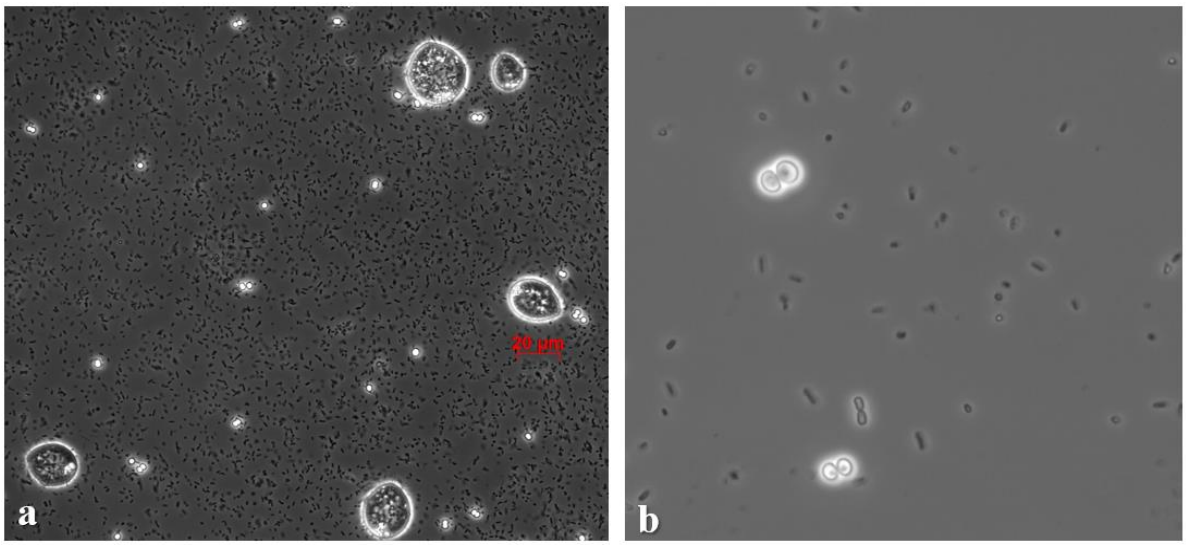

Figure 19: Microscope images of the photo-mixotrophic culture cultivated on acetate in the CSTR PBR. Figure «a» was taken from the cultivation with a dilution rate of 0.24 d^{-1}. Figure «b» was taken from the cultivation with a dilution rate of 0.17 d^{-1}. Both present the small, round-shaped, phototrophic cells found in the previous cultures. Figure «a» also shows larger, ciliated cells (20-30 µm long) and a higher abundance of smaller bacterial cells.

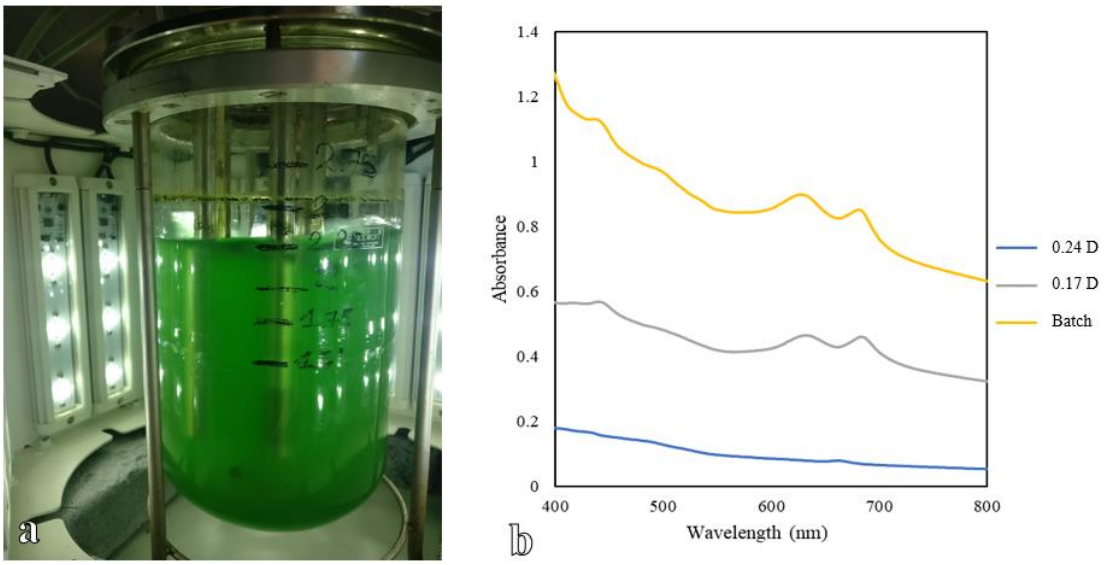

Figure 20: L: CSTR PBR with a dilution rate of 0.17 d^{-1}. The bright green colour is given by the phototrophs present in the culture. R: Absorbance spectra of the microalgal cultivation on acetate in a CSTR (0.17-0.24 d^{-1} dilution rate) and in a batch ($AXAL_{100}$). The higher dilution rate caused the flushing out of phototrophic biomass, while at a lower dilution rate absorbance peaks can be identified at the same wavelengths as in the batch culture ($AXAL_{100}$).

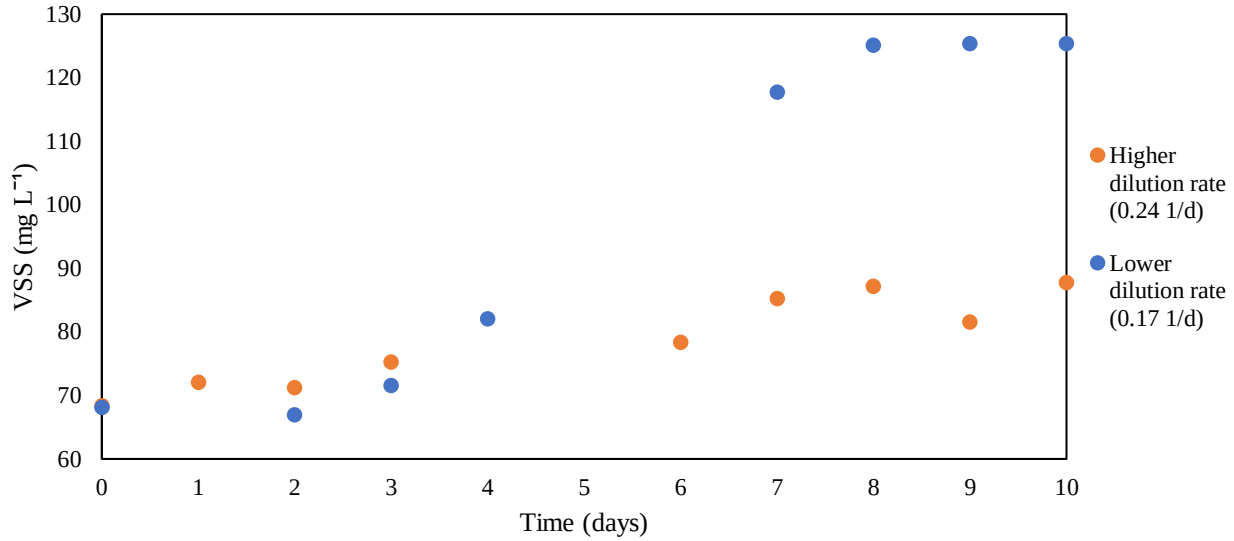

Figure 21: Biomass growth at different dilution rates (0.24 d^{-1} and 0.17 d^{-1}). The 0.17 d^{-1} allowed for a higher biomass growth inside the reactor. The dilution rate applied was the only parameter that varied between the two experiments.

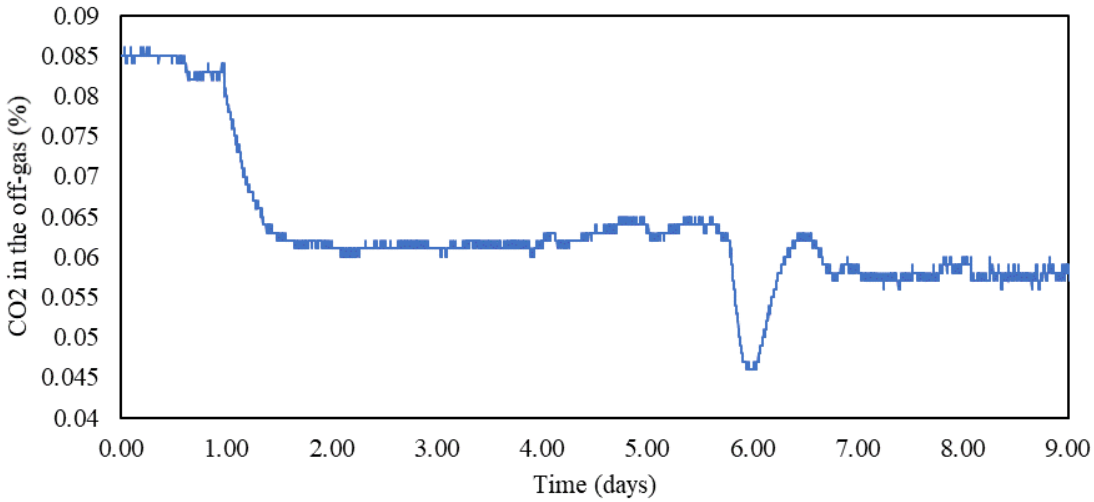

Figure 22: CO_2 fraction (%) in the off-gas in the transition from the 0.24 d^{-1} (day 0 to 1) and 0.17 d^{-1} (day 1 to 9) dilution rates. A first decrease is given by the lower organic loading rate fed to the reactor. Subsequently, a new and lower equilibrium is reached between the production and the consumption of carbon dioxide.

4.3 Discussion

4.3.1 Culture enriched on BG-11 media produced a mixed culture of photolithoautotrophs and chemoorganoheterotrophs

The culture resulting from the enrichment on mineral BG-11 was formed by a high diversity of populations characterized by different metabolisms.

The enrichment aimed to grow phototrophic organisms, which were found in the culture in the form of both eukaryotes and prokaryotes. The most abundant were oxygenic photolithoautotrophs (the microalgae *Micractinium pusillum* sp. and *Chlorella sorokiniana* sp.; the cyanobacteria *Cyanobium PCC-6307* sp. and *Synechocystis PCC-6803* sp.) which coexisted together with aerobic chemoorganoheterotrophs (*Cupriavidus*, *Novosphingobium*, *Arenimonas*). Their relationship can be mutually beneficial, as these oxygenic phototrophs produce O_2 and generate organic carbon by biomass growth and decay. In return, heterotrophs will consume O_2 and produce CO_2.

As shown in Table 17, the green phototrophs found in the cultures can grow in a range of light intensity and temperature (20-2400 μmol photons m^{-2} s^{-1}, 20-35°C) that includes the ones selected for this experiment (80-93 μmol photons m^{-2} s^{-1}, 35°C). The maximum growth rate values found in this study (0.4-0.97 d^{-1}) were inside the range found in literature (0.1-5.52 d^{-1}). Large variations in growth rate can be explained by differences in cultivation conditions such as light intensity and cycles, temperature, CO_2 addition, nutrient solution, and by the fact that this study refers to a mixed culture. The lower growth rates of *Desmodesmus* (0.069-0.21 d^{-1}) and *Scenedesmus* (0.267 d^{-1}) found in literature (Girard *et al.*, 2014; Ríos *et al.*, 2016; Sijil *et al.*, 2019) could imply that these genera were outcompeted inside the mixed culture. In fact, their recognizable colony-forming spiny cells (Trainor *et al.*, 1990) were never identified during phase-contrast microscopy. However, they were found by the 18S rRNA gene amplicon sequencing. Amplicon sequencing could identify populations that were no longer active in the biological system.

In the absence of oxygen addition, oxygenic phototrophs were still able to grow. This was shown in the cultures without gas exchange and in the photolithoautotrophic PBR. This implies that in the conditions applied, the oxygen produced by photosynthesis was enough to sustain the growth of phototrophs and coexisting aerobic heterotrophs. Although illumination was provided, external oxygen could have been necessary for cellular respiration of aerobic phototrophs in zones where light intensity was reduced. This might change if alternation between light and dark cycles is applied, as in the absence of light phototrophs can only perform cellular respiration to sustain their metabolism.

Both nitrate and ammonia could be used by the culture as nitrogen sources, resulting in similar growth rates (0.47 and 0.4 d^{-1}, respectively). Changes in the culture composition were neither noticeable by phase-contrast microscopy, nor from the absorbance spectrum of the culture. Similar peaks and therefore similar pigments could be identified. However, further investigation of the microbial composition via 16S and 18S rRNA gene sequencing is necessary to determine the exact effect of the N-source. DNA extracts from these cultures were submitted for amplicon sequencing (results pending).

Table 17: Growth parameters (μ_{max}, C_{max}, K_s) of the main phototrophic organisms found in the cultures. The parameters vary based on the conditions applied (temperature, light) and the carbon source used. Data on the affinity constant for organic carbon sources are scarce.

Genus	T (°C)	Light intensity (µmol photons m^{-2} s^{-1})	C-source	μ_{max} (d^{-1})	C_{max} (mg L^{-1})	K_S (mg L^{-1})	Source
Chlorella	25	100	Inorganic carbon	0.63	680	-	Li *et al.* (2014)
			Glucose (2 g L^{-1})	3.2	1660	-	
	30	100	Acetate (2 g L^{-1})	2.4	-	76	Kumar *et al.* (2014)
	25	100	Acetate (0.425 g L^{-1})	5.52	-	65.59	Ghosh *et al.* (2017)
Micractinium	35	150-160	Inorganic	0.38	-	-	Bouarab *et al.* (2004)
			Glucose (10 mM)	0.94	-	-	
			Acetate (10mM)	0.58	-	5.5 µM	
	21	80	Anaerobically treated cheese whey effluent	0.35	-	-	Blier *et al.* (1995)
	35	182	Inorganic carbon	0.58	-	-	Peeters & Eilers (1978)
Scenedesmus	22.5	100	Inorganic carbon	0.267			Girard *et al.* (2014)
			Cheese whey permeate	1.083	-	-	
Desmodesmus	30	79	Inorganic carbon	0.21	-	-	Ríos *et al.* (2016)
			Glucose (10 g L^{-1})	0.28	-	-	
	25	30	Inorganic carbon	0.069	227	-	Sijlil *et al.* (2019)
			Glucose (50 mM)	0.138	857	-	
			Acetate (50 mM)	0.1	467	-	
Cyanobium	30	41.6	Inorganic carbon	0.25	-	-	Henrard *et al.* (2014)
	23	60-80	Inorganic carbon	1.16	-	-	Yamagishi *et al.* (2016)
	20	40	Inorganic carbon	0.25	-	-	Budinoff *et al.* (2007)
Synechocystis	-	-	Inorganic carbon	1.7 -2.5	-	-	Yu *et al.* (2013)
	30	202-1701	Inorganic carbon	1.4	350-630		Kim *et al.* (2010)
	30	46.25	Inorganic carbon	0.1388	1180		Patel *et al.* (2016)
	30	1600	Inorganic carbon	0.72-2.16	-	-	Martinez *et al.* (2012)
		400-2400		2.16	-	-	
	30	140	Inorganic carbon	1.32	-	-	Dauta *et al.* (1990)
	30	20	Inorganic carbon	0.2-0.9	-	-	Lopo *et al.* (2012)
			Glucose (5-7 mM)	1	-	-	
	30	200	Inorganic carbon	0.3	-	-	Wang *et al.* (2002)
			Glucose (3.2 g L^{-1})	-	-	-	

4.3.2 Photoorganoheterotrophic mixed cultures could be grown using demineralized cheese whey, lactose, or acetate as a carbon source, with the selection of green phototrophs

The use of organic carbon sources allowed the growth of phototrophs in mixed cultures. This may suggest that photolithoautotrophic microorganisms selected by the enrichment made on mineral BG-11 medium were able to thrive in the presence of lactose, demineralized cheese whey and acetate as carbon sources. As shown in Table 17, previous studies have determined that some of the phototrophic genera present in the photolithoautotrophic cultures (*Chlorella*, *Micractinium*, *Scenedesmus*, *Desmodesmus*, *Synechocystis*) can grow mixotrophically on glucose or acetate. Some studies also showed that they could grow on biologically treated cheese whey (Blier *et al.*, 1995; Girard *et al.*, 2014). However, these studies were performed in axenic cultures and did not assess the competitivity of such species in mixed cultures.

It is also possible that different photoorganoheterotrophic organisms were selected in the photoorganoheterotrophic cultures, although this shift was not noticeable from the absorbance spectra or phase-contrast microscopy. In the photolithoautotrophic culture, mainly oxygenic phototrophs were found. This is because anoxygenic phototrophs require an electron donor other than H_2O, such as H_2, H_2S, arsenite, or organic compounds (Overmann and Garcia-Pichel, 2013; McCann *et al.*, 2017), which were not present in the mineral medium used. The addition of the organic carbon source may have selected for organic compound-using anoxygenic photosynthetic organisms or non-photosynthetic obligate photoorganoheterotrophs.

Chloroflexi, Heliobacteria, and Acidobacteria are typically found in different environments, mostly at higher temperatures, in soil sediments, or in acidic environments as discussed in see section 2.2. PNSB could have flourished with the presence of acetate in the closed-bottle cultures – not in the open ones as they are strictly anaerobic (Imhoff, 1995). However, PNSB make use of infrared light (Suwan *et al.*, 2014), which is generally not strongly provided by led lamps such as the commercial ones used for the shake-flask cultures. However, the emitting light spectrum of the led lamp was neither provided by the supplier nor measured. 16S and 18S rRNA gene amplicon sequencing will be necessary to determine the variety of phototrophic populations.

The experiments also showed that in cultures with O_2 dissolution from the outside air (60% dissolved oxygen), phototrophs suffered from a stronger competition with aerobic heterotrophs; while the total biomass production was higher, the content of phototrophs (identified by the phase-contrast microscopy and wavelength scan) was lower. This competition was lower under microaerobic conditions when the only oxygen available was produced by the microbial photosynthesis. Therefore, it is advisable to reduce the level of dissolved oxygen in mixed culture by stripping the photosynthetically produced oxygen as a strategy to avoid competition.

4.3.3 Varying the nitrogen source, carbonate concentration, and dissolved oxygen level lead to differences in the growth of phototrophs

The BG-11 medium, which is a standard medium for the cultivation of cyanobacteria and microalgae, is highly abundant in phosphorus and even more in nitrogen. The C:N:P ratio supplied by the media is 0.189:101:1, which is significantly imbalanced when considering the theoretical composition of algal biomass $C_{106}H_{263}O_{110}N_{16}P$ (Redfield, 1934). The excess of nitrogen and phosphorus in this medium is actually used to simply grow photolithoautotrophs in shake flasks by capturing CO_2 from the atmosphere without the need for external carbon supply.

Limitations in carbon can be compensated when CO_2 is either bubbled through the culture or can dissolve inside the solution from the outside air, which happens when the pH is above 7. Conditions that lead to pH increase enable further capture of CO_2 from the atmosphere. In this study, the medium quickly became limited in carbon when gaseous CO_2 could not enter the system. This occurred when cultures were sparged with CO_2 free gas and maintained in closed systems. It also occurred when a different N-source than nitrate, such as ammonium, was used. Without NO_3^- consumption, alkalinisation of the system was limited. When using NH_4^+ as N-source, acidification occurred. This was caused by the production of hydrogen ions when ammonium was used for the anabolic production of biomass (see reaction 4). This aspect should be taken into consideration when the transition from nitrate to ammonium is considered. When digesting organic matter like cheese whey, ammonium is primarily produced. The amount of ammonium depends on the extent of the deproteination of cheese whey prior to fermentation. In this study, the nitrate content of the demineralized cheese whey powder was ca. 6 mg TKN g VS^{-1} and less than 1 mg $N\text{-}NH_4^+$ g VS^{-1}.

The BG-11 medium is also imbalanced in N:P ratio. Geider and La Roche (2001) revisited the conventional Redfield ratio determining the elemental composition of algal biomass, arguing that the N:P content of algal and cyanobacterial cells is extremely plastic, meaning that it varies based on the nutrient availability. Different N:P ratios will determine the type of compounds present in the biomass. The abundance of nitrogen determines an increase in proteins, nucleic acids and also chlorophyll. Phosphate increase will produce higher amounts of

phospholipids. The BG-11 can, therefore, guarantee growth, but the resulting biomass will have the characteristics typical of a P-limited condition. It is important to evaluate if the medium is adequate for the targeted biomass composition. Augmentation in phosphate of the BG-11 has also been suggested by Kim *et al.* (2010).

In some cultures, biomass growth was not limited by either carbon, nitrogen or phosphorus. Micronutrient deficiencies may have played a role. Further studies should, therefore, analyse the micronutrient requirements and uptake more closely.

Overall, C:N:P ratios of 0.189:101:1 could only sustain growth only when additional CO_2 could dissolve in the system, while 106:101:1 provided grow even without gas exchange. The experiment with varying C:N:P ratios in microplate cultures suggested that lower C:N and C:P ratios could improve phototrophic growth, as the maximum biomass and pigment content was reached for C:N:P of 36:101:1. The same phenomenon was observed when demineralized cheese whey, having a higher phosphorus content (12 instead of 5 mg $P\text{-}PO_4^{3-}$ L^{-1}), which provided higher and faster growth than lactose at the same carbon concentration. Further investigations should be performed to determine the most appropriate C:N:P ratio, based not only on biomass yield but also on the targeted end product.

4.3.4 Selection mechanisms in the PBR under CSTR regime allowed the growth of green phototrophs

The composition of the nutrient solution used for photoorganoheterotrophic growth on acetate used in the CSTR PBR was equivalent to the one used in the AXA_{100} experiment (acetate concentration of 18.9 mmol C L^{-1}, sealed bottles, ammonium as N-source). The same green round-shaped cells (3-4 μm) were found. Their concentration varied with the dilution rate applied. However, different microorganisms were selected as well, such as larger cells (20-30 μm) possibly belonging to the Ciliata class.

The differences in the selection mechanisms are due to the difference in substrate concentration and variation in batch and chemostat cultivation. In a batch, the substrate concentration is first high and then decreases. In a chemostat at equilibrium, the concentration is constant and equal to that of the effluent. Therefore, in a batch regime the microorganisms are selected based on their maximum growth rate, and in a chemostat the affinity constant with the substrate is relevant as well (Rombouts *et al.*, 2019). Unfortunately, studies on the affinity constant of phototrophs for organic substrates are limited (Table 17). The presence of oxygenic phototrophs may induce the proliferation of aerobic heterotrophs, as discussed in section 4.3.2 and 4.3.3. Such aerobic heterotrophic organisms can have elevated growth rates and lower affinity constants. *E. coli* can have K_s for acetate of 13 mg L^{-1} (Anane *et al.*, 2017); the ASM3 (Activated Sludge Model 3) default value is 2.0 mg COD L^{-1} or 1.75 $mg_{acetate}$ L^{-1} (Hoque *et al.*, 2009). Despite these, green phototrophs were not outcompeted.

The abundance of phototrophs was impacted by the dilution rate applied. At a higher dilution rate, the number of green phototrophs decreased visibly, and smaller bacterial cells increased. According to the maximum growth rate estimated for the AXA_{100} experiment (0.25 d^{-1}), the 0.24 d^{-1} dilution rate was too close to the maximum growth rate and caused the washout of microalgae. This did not occur at a higher residence time. When a lower dilution rate was imposed (0.17 d^{-1}), phototrophs could efficiently compete with other microorganisms. Microbial population selection in the chemostat depended on both the maximum growth and the affinity constant for the liming substrate. Thus, either the affinity constant of photoorganoheterotrophs for the organic substrate was low enough, or a successful symbiotic relationship with other heterotrophic microorganisms occurred (as discussed in section 4.3.5). For large scale applications, the chemostat regime should be compared with other configurations, such as sequenced batch reactors, to determine which is the most suitable for selecting phototrophs. In this study, the chemostat regime was selected before starting the experimental work, as it was expected that phototrophs would be outcompeted by fast-growing fermenters in

batch regimes when grown on sugars such as lactose. However, this was not observed in the batch experiment performed.

Other than the different theoretical selection mechanisms taking place in batch and chemostat regimes, some operational conditions were also slightly different in the PBR. In the reactor, the pH was maintained at 7, while in the flasks, it spontaneously increased from 7 to alkaline conditions. Alkalinisation of the system may have helped in selecting microalgal organisms; studies have suggested that maintaining alkaline pH values (8-11) can prevent the growth of invading microorganisms in microalgal and cyanobacterial cultures (Touloupakis *et al.*, 2016). The neutral pH could explain the presence of the larger ciliated cells found inside the PBR, which were not present in the batch cultures.

Moreover, while in the flasks the gases produced by the microbial metabolism (CO_2, O_2) were kept inside the system, the PBR was continuously sparged with argon gas. Despite the low gas flow, removing the carbon dioxide produced may have limited the metabolism of the phototrophic species. On the other hand, it is also possible that a higher gas flow could limit the dissolved oxygen inside the reactor, inhibiting the growth of aerobic heterotrophs.

Despite having a similar intensity (80-93 μmol photons m^{-2} s^{-1}), the light source used was different in the two cultivation systems. The light used in the PBR was specifically designed for phototrophic cultures, emitting in the range of 400-700 nm (with peaks at 470 and 660 nm), while the light used in the shaker was a commercial led lamp. This difference may have had an impact on the growth, for instance, if intensities varied with the wavelength. Different phototrophic microorganisms absorb at different wavelengths (Stomp *et al.*, 2007). Light intensity inside the culture itself was also reduced as a result of the increased volume over surface ratio in the PBR compared to the flasks.

4.3.5 Carbon consumption and transformation in the PBR under CSTR regime was likely the result of symbiotic relationships between the metabolisms of different microbial populations

Acetate was almost entirely consumed in the PBR. This consumption resulted in biomass and biogas production.

From the CO_2 measurements, it is possible to observe that when phototrophs were abundant in the reactor (dilution rate of 0.17 d^{-1}), the amount of carbon dioxide oscillated before steady state was reached. This can be due to the production of CO_2 by aerobic respiration and its consumption by photosynthesis. As previously discussed, this is either the results of the metabolism performed by two different classes of microorganisms, ordinary heterotrophic organisms (OHOs) and photolithoautotrophs (PLATs), or possibly by photolithoautotrophs performing either chemoorganoheterotrophic (COHT) or photoorganoheterotrophic (POHT) metabolism. Moreover, it can be the result of the mixotrophic metabolism performed by one single microorganism. The consumption and production of compounds by these metabolisms are summarized in Table 18.

The consumption and production of substrates and metabolites in the system can be described as a two-tanks in series reactor with partial recirculation of the effluent. First, the acetate fed by the influent is heterotrophically consumed by the microorganisms, using the oxygen provided by the recirculation (CHOT) or light (POHT). Then, the carbon dioxide produced during this first metabolic phase is used for photosynthesis, which results in the production of oxygen. As a result, the microbial biomass is produced. This could explain the oscillatory measurements of CO_2 before the equilibrium was reached. The mechanism is shown qualitatively in Figure 23.

Table 18: Consumption and production of substrates and metabolites by different metabolic pathways. Ordinary heterotrophic organisms (OHOs) are presented as one metabolism, while for traditionally photolithoautotrophic organisms the three possible metabolisms are presented (chemoorganoheterotrophy (COHT), photolithoautotrophy (PLAT), photoorganoheterotrophy (POHT)).

	Catabolism				**Anabolism**					
	$CH3COO^-$	H^+	O_2	CO_2	CO_2	O_2	$C_6H_{12}O_6$	CH_3COO^-	H^+	$CH_{1.8}O_{0.5}N_{0.2}$
OHOs	-	-	-	+	+			-	-	+
COHT	-	-	-	+	+			-	-	+
PLAT		light			-	+	+ -		+	+
POHT		light			+			-	-	+

For both dilution rates, carbon and COD balances did not close. This may be due to an error in the estimation of the carbon and COD content of the solid or in the gas phase. In the solid phase, underestimations can be due to storage compounds in the microbial cells. In the gas phase, they can be related to the production of compounds such as hydrogen gas or methane, which were not measured by the off-gas analyser. GC analysis of off-gas samples could not detect hydrogen nor methane gas either. The latter would suggest the presence of methanogens, which have on average growth rates lower than 0.17 d^{-1} (0. 12 d^{-1} according to van Lier *et al.* (2018), although certain species can grow faster, *e.g.*, the acetoclastic methanogen *Methanosarcina barkeri* has a growth rate of 0.34 d^{-1} (Krzycki *et al.*,1982)).

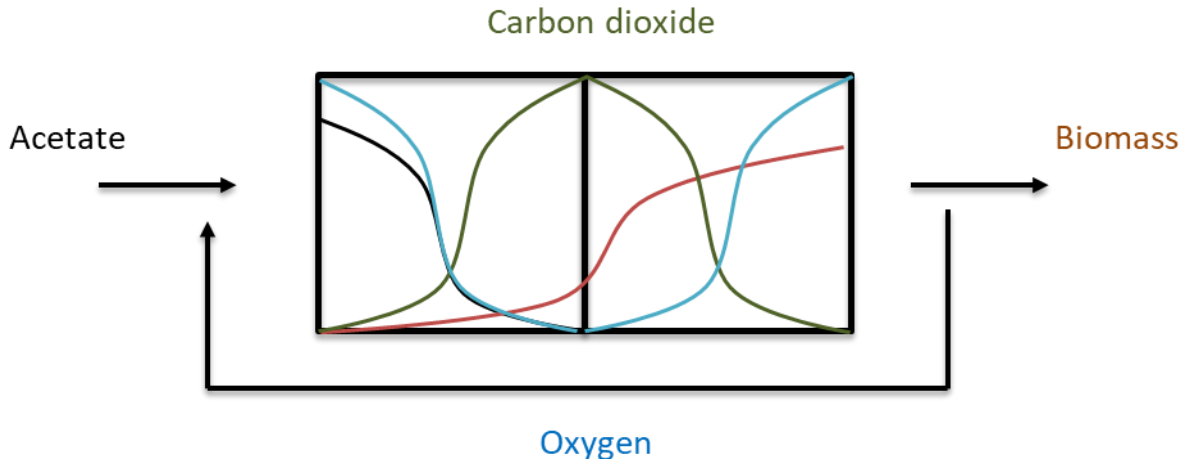

Figure 23: Qualitative graphic representation of the two-tanks in series system used to describe the metabolisms taking place in the photobioreactor. Acetate is fed through the influent, while part of the effluent is recirculated to the first tank. In the first tank, acetate and oxygen are depleted, while carbon dioxide and biomass are produced by photo- or chemo-organoheterotrophic metabolisms. In the second tank, carbon dioxide is consumed and oxygen and biomass are produced by photolithoautotrophic metabolism.

4.3.6 Acetate provided a better carbon source than lactose in batch photoorganoheterotrophic cultures, therefore pre-acidification of cheese whey may improve the phototrophic biomass harvesting

Batch cultivation using 40% demineralized cheese as the sole nutrient source was not suitable for the growth of phototrophs. Due to the high carbon content and the high acidification, cyanobacteria and microalgae were readily outcompeted by other types of microorganisms, as was clearly shown by the 16S (targeting prokaryotic ribosome) and 18S (targeting eukaryotic ribosome) rRNA gene amplicon sequencing. To make their growth viable, additional nutrients such as nitrogen, phosphorus and trace elements need to be included, and pH needs

to be kept above 6 for phototrophic biomass to be able to grow. However, this study showed that using demineralized cheese whey in combination with additional nutrients (nitrogen, phosphorus, and trace elements) sustained the growth of green phototrophs.

Acetate provided a higher phototrophic growth compared to lactose (170 mg VSS L^{-1} and 111 mg VSS $L^{-1,}$ respectively). Of the phototrophs identified by 16S and 18S rRNA gene sequencing, mixotrophic cultures were generally more productive when grown on glucose than on acetate (Bouarab *et al.*, 2004; Sijlil *et al.*, 2019). Lactose can be hydrolysed to glucose and galactose; however, this reaction requires specific enzymes (Zanette *et al.*, 2019). In our study, cultures grown on lactose did not show quantifiable production of the monosaccharides, suggesting that hydrolysis could be a limiting step. Moreover, strong acidification occurred in the cultures with lactose or cheese whey. Acidic pH can have an inhibitory effect on microalgal cultures (Kumar *et al.*, 2014), although tolerance is highly dependent on the algal species.

Another advantage is that, in anaerobic conditions, acetate can only be degraded by methanogens, which are characterized by low growth rates (μ_{max} = 0.12 d^{-1}) and are therefore generally outcompeted in batch conditions. Lactose, on the other hand, can be used as a carbon and energy source by fermenters, which are characterized by higher growth rates (μ_{max} = 2 d^{-1}). A small concentration of fermentation products (acetate and butyrate) were found in some samples of the $CWXA_{100}$ culture, suggesting the presence of fermenters. However, green phototrophs were not outcompeted in the cultures grown on lactose of demineralized cheese whey.

Therefore, the acidogenesis of cheese whey for the production of VFAs in the form of acetate can improve the assimilation of the original carbon source by photoorganoheterotrophic microorganisms. The acidogenic fermentation experiments performed showed that acetate was not the only VFA produced from 40% demineralized cheese whey. Acetate was primarily used as a model VFA in the subsequent phototrophic experiments. The use of the longer chain VFAs such as propionate, butyrate, and hexanoic acid as carbon source was not investigated. Additional experiments should be performed to evaluate the biomass growth on a more complex mixture of VFAs and other fermentation products, closer to the one obtained from cheese whey fermentation. Based on these results, the operational parameters of the acidification stage (such as pH) should be used to regulate the fraction of the VFA produced. Research by Fei *et al.* (2015) has informed that the microalga *Chlorella protothecoides* could grow photoorganoheterotrophically on a mixture of acetic, propionic, and butyric acids. The authors have shown that although the microalga could metabolise all VFAs, acetate was the preferred carbon source.

Green phototrophs were grown in mixed cultures using organic carbon sources derived from cheese whey. It was shown that green phototrophs could be selected using demineralized cheese whey, when providing a sufficient amount of N and P (106:101:1 and 36:101:1 C:N:P). High pH (7-10) and lower dissolved oxygen content proved to be more suitable. Acetate was a better organic substrate than lactose. These findings can all be used to improve the biological treatment and valorisation of cheese whey with the production of phototrophic biomass.

5. Conclusions

This study assessed that phototrophic microorganisms could be selected in mixed cultures using inorganic carbon and organics derived from cheese whey, such as lactose, acetate, and 40% demineralized cheese whey powder. The findings of this study can be used as a basis for the ecological engineering of acidogenic and photoorganoheterotrophic microbial metabolisms, for the valorisation of cheese whey.

This work resulted in the following six main conclusions:

1. VFA production during the acidogenic fermentation of the 40% demineralized cheese whey was impacted by the thermal pre-treatment of the inoculum and by the F/M ratio applied. The thermal pre-treatment of the sludge at 90°C disabled methanogenic microorganisms. The maximum degree of acidification (77±7%) was reached when the inoculum was thermally treated and combined with a F/M ratio of 0.5 g COD g VS^{-1}. The main VFA produced were acetate (49±9%), butyrate (16±11%), and hexanoic acid (24±3%). Higher alkalinity (1.66 mg $CaCO_3$ L^{-1}) resulted in a higher degree of acidification. As cheese whey is limited in alkalinity, lower F/M (<1 g COD g VS^{-1}) values are advised.

2. Photolithoautotrophic growth on BG-11 medium in batches resulted in a mixed culture composed by cyanobacteria such as *Synechocystis* and *Cyanobium*, and green microalgae such as *Chlorella* and *Micractinium*, and aerobic chemoorganoheterotrophs. Differentiation between the eukaryotic and prokaryotic genera was not possible neither by 16S and 18S rRNA gene amplicon sequencing nor by phase-contrast microscopy. Other methods, such as fluorescence in situ hybridization, should be applied to assess the selection within the green phototroph guild. The microbial population could use both nitrate and ammonium as nitrogen sources. The maximum growth, ranging between 0.12 and 0.97 d^{-1}, was affected by the inorganic carbon concentration and by the nitrogen source.

3. Sodium acetate, lactose, and 40% demineralized cheese whey powder proved to be adequate carbon sources for the cultivation of green phototrophs, provided the addition of mineral nutrients (ammonium, phosphate and trace elements, as in the BG-11 medium). Sealed systems in which no gas exchange was possible with the atmosphere provided a competitive advantage to phototrophic microorganisms, due to the limited presence of oxygen for aerobic heterotrophs. The reduced relative abundance of phototrophs was observed with the decreased amplitude of pigment-identifying absorbance peaks (440, 630, and 680 nm). C:N:P contents of 106:101:1 could sustain growth. However, higher nitrogen and phosphorus amounts (36:101:1 and 53:51:1 C:N:P) resulted in higher growth and pigment contents.

4. Maximum growth rates of 0.25, 0.29, and 0.56 d^{-1}, and maximum biomass concentrations of 170, 111, and 140 mg VSS L^{-1} were observed for the photoorganoheterotrophic cultures using sodium acetate, lactose, and demineralized whey respectively. The maximum pigment content (20.3, 13.8, and 5.3 μg mg VSS^{-1} of chlorophyll a, chlorophyll b, and total carotenoids, respectively) was observed when using sodium acetate as a carbon source in batches. Acetate was, therefore, the most efficient substrate for biomass and pigment production.

5. The growth of green phototrophs in a mixed culture was also possible in a chemostat PBR using acetate as a carbon source. The biomass concentration obtained in the reactor was 125 mg L^{-1}, and the biomass production was 45 mg VSS d^{-1}. The presence of green phototrophs was identifiable by pigment-identifying absorbance peaks (440, 630, and 680 nm), relating to chlorophyll a, chlorophyll b and carotenoids content. Oscillation in the carbon dioxide concentration in the off-gas indicated that this compound was both produced and consumed as a result of both heterotrophic and autotrophic metabolisms. These conditions can stimulate photomixotrophic growth.

6. Phase-contrast microscopy and absorbance wavelength scan did not identify a strong shift in the microbial populations when transitioning from the photolithoautotrophic to the photoorganoheterotrophic cultivation mode. Green phototrophs identified by 16S and 18S rRNA amplicon gene sequencing in the photolithoautotrophic cultures such as the microalgae Chlorella, Micractinium, Scenedesmus and Desmodesmus, and the cyanobacteria Synechocystis, have been proven to grow photoorganoheterotrophically in previous studies. 16S and 18S rRNA gene amplicon sequencing will determine more precisely how the communities changed (results pending).

Overall, photoorganoheterotrophic growth with green phototrophs selection was possible on all the cheese whey-based organics tested. Acetate, which can be derived from the acidogenic fermentation of cheese whey, was the most suitable substrate for the selection of green phototrophs, with successful growth in mixed cultures under both batch and continuous-flow regimes.

6. Recommendations

The following four recommendations are given for future research:

1. In mixed cultures, the fraction of organic carbon used by phototrophic microorganisms has not been defined. Methods for its determination should be applied, such as isotope labelling of the carbon source. This will enable to understand which metabolic processes (photoorganoheterotrophy, chemoorganoheterotrophy, or mixotrophy) are taking place inside the mixed culture.

2. Mechanisms driving the selection within the guild of green phototrophs, for example the competition between eukaryotic algae and cyanobacteria, should be investigated. It will help to understand what are the most suitable populations for this application and imposing the selective pressures necessary for the cultivation of the preferred strains.

3. The content of carbon, nitrogen, and phosphorus should be optimized to allow the maximum growth of phototrophs. Operational parameters, such as pH, temperature, and light intensity, should also be adjusted. Optimization is paramount in order to assess the economic feasibility of the process and for transitioning to large-scale implementation.

4. With the aim of large-scale applications, different regimes such as sequencing batch or fed-batch reactors should be considered. The regime that better selects for green phototrophs should be selected for further implementation. This will also provide a better understanding of the affinity for the substrate of the photoorganoheterotrophs selected.

7. References

Allen, M.M., Stanier, R.Y., (1968). *Growth and division of some unicellular blue-green algae*. Journal of General Microbiology, 51, 199-202. https://doi.org/10.1099/00221287-51-2-199

Alloul, A., Wuyts, S., Lebeer, S., Vlaeminck, S.E., (2019*). Volatile fatty acids impacting phototrophic growth kinetics of purple bacteria: Paving the way for protein production on fermented wastewater*, Water Research, 152, 138-147, ISSN 0043-1354, https://doi.org/10.1016/j.watres.2018.12.025.

Alves, M.P., Moreira, R. de O., Rodrigues Júnior, P.H., Martins, M. C. de F., Perrone, Í.T., Carvalho, A.F. de, (2014). *Whey: technologies for co-products production*. Revista do Instituto de Laticínios Cândido Tostes, 69(3), 212- 226.

Anderson, S. L., McIntosh, L., (1991). *Light-activated heterotrophic growth of the cyanobacterium Synechocystis sp. strain PCC 6803: A blue-light-requiring process.* Journal of Bacteriology, 173(9), 2761–2767. https://doi.org/10.1128/jb.173.9.2761-2767.1991

Arnon, D.I., (1949). *Copper enzymes in isolated chloroplasts. Polyphenoloxidase in Beta Vulgaris.* Plant Physiology, 4, 24, 1. https://doi.org/10.1104/pp.24.1.1

Bicas, J. L., Kleinegris, D. M.M., Barbosa, M.J., (2015). *Use of methylene blue uptake for assessing cell viability of colony-forming microalgae*, Algal Research, 8, 174-180, ISSN 2211-9264, https://doi.org/10.1016/j.algal.2015.02.004.

Blier, R., Laliberté, G., de la Noüe, J., (1995). *Tertiary treatment of cheese factory anaerobic effluent with Phormidium bohneri and Micractinium pusillum*, Bioresource Technology, 52(2), 151–155. https://doi.org/10.1016/0960-8524(95)00014-6

Bouarab, L., Dauta, A., Loudiki, M., (2004). *Heterotrophic and mixotrophic growth of Micractinium pusillum Fresenius in the presence of acetate and glucose: effect of light and acetate gradient concentration.* Water Research, 38 (11), 2706–2712. https://doi.org/10.1016/j.watres.2004.03.021

Bryant, D.A., Liu, Z., Li, T., Zhao, F., Garcia Costas, A.M., Klatt, C.G., Ward, D.M., Frigaard, N.U., Overmann, J., (2012). *Comparative and Functional Genomics of Anoxygenic Green Bacteria from the Taxa Chlorobi, Chloroflexi, and Acidobacteria*. In: Burnap R., Vermaas W. (eds) *Functional Genomics and Evolution of Photosynthetic Systems. Advances in Photosynthesis and Respiration*, vol 33. Springer, Dordrecht

Budinoff, C. R., Hollibaugh, J. T., (2007*). Ecophysiology of a Mono Lake picocyanobacterium.* Limnology and Oceanography, 52(6), 2484–2495. https://doi.org/10.4319/lo.2007.52.6.2484

Calero, R. R., Lagoa-Costa, B., Fernandez-Feal, M. M. del C., Kennes, C., Veiga, M. C., (2018). *Volatile fatty acids production from cheese whey: influence of pH, solid retention time and organic loading rate.* Journal of Chemical Technology and Biotechnology, 93(6), 1742–1747. https://doi.org/10.1002/jctb.5549

Chen, G., Zhao, L., Qi, Y., (2015). *Enhancing the productivity of microalgae cultivated in wastewater toward biofuel production: A critical review.* Applied Energy, 137, 282–291. https://doi.org/10.1016/j.apenergy.2014.10.032

Chen, J. H., Kato, Y., Matsuda, M., Chen, C. Y., Nagarajan, D., Hasunuma, T., Kondo, A., Dong, Cheng, D., Lee, D.J., Chang, J. S., (2019). *A novel process for the mixotrophic production of lutein with Chlorella sorokiniana MB-1-M12 using aquaculture wastewater.* Bioresource Technology, 290(July), 121786. https://doi.org/10.1016/j.biortech.2019.121786

Chew, K. W., Chia, S. R., Show, P. L., Yap, Y. J., Ling, T. C., Chang, J. S., (2018). *Effects of water culture medium, cultivation systems and growth modes for microalgae cultivation: A review.* Journal of the Taiwan Institute of Chemical Engineers, 91, 332–344. https://doi.org/10.1016/j.jtice.2018.05.039

Dahiya, S., Sarkar, O., Swamy, Y. V., Venkata Mohan, S., (2015). *Acidogenic fermentation of food waste for volatile fatty acid production with co-generation of biohydrogen*. Bioresource Technology, 182, 103–113. https://doi.org/10.1016/j.biortech.2015.01.007

Dauta, A., Devaux, J., Piquemal, F., Boumnich, L., (1990). *Growth rate of four freshwater algae in relation to light and temperature*. Hydrobiologia, 207(1), 221-226. https://doi.org/10.1007/BF00041459

De Kreuk, M., Martí, N., Tao, Y., Wang, H., (2012). *SMA Test. Laboratory Protocol (Unpublished material). Course CT 4485, Wastewater Treatment.* Department of Water Management, Faculty of Civil Engineering and Geosciences. TU Delft, The Netherlands.

Dragone, G., Mussatto, S. I., Almeida e Silva, J. B., Teixeira, J. A., (2011). *Optimal fermentation conditions for maximizing the ethanol production by Kluyveromyces fragilis from cheese whey powder.* Biomass and Bioenergy, 35(5), 1977–1982. https://doi.org/10.1016/j.biombioe.2011.01.045

DuBois, M., Gilles, K.A., Hamilton, J.K., Rebers, P.A., Smith, F., (1956). *Colorimetric Method for Determination of Sugars and Related Substances.* Analytical Chemistry, 28(3), 350-356. https://doi.org/10.1021/ac60111a017

D'Imporzano, G., Veronesi, D., Salati, S., Adani, F., (2018). *Carbon and nutrient recovery in the cultivation of Chlorella vulgaris: A life cycle assessment approach to comparing environmental performance*, Journal of Cleaner Production, 194, 685-694, ISSN 0959-6526. https://doi.org/10.1016/j.jclepro.2018.05.174.

Fei, Q., Fu, R., Shang, L., Brigham, C. J., Chang, H. N., (2015). *Lipid production by microalgae Chlorella protothecoides with volatile fatty acids (VFAs) as carbon sources in heterotrophic cultivation and its economic assessment*. Bioprocess and Biosystems Engineering, 38(4), 691–700. https://doi.org/10.1007/s00449-014-1308-0

Franchino, M., Comino, E., Bona, F., Riggio, V.A., (2013). *Growth of three microalgae strains and nutrient removal from an agro-zootechnical digestate*, Chemosphere, 92(6), 738-744, ISSN 0045-6535. https://doi.org/10.1016/j.chemosphere.2013.04.023.

Freyssinet, G., Nigon V., (1980). *Growth of Euglena gracilis on whey,* European Journal of Applied Microbiology and Biotechnology, 9(4), 295-303.

Garrity, G.M., Holt, J.G., Castenholz, R.W., Pierson, B.K., Keppen, O.I., Gorlenko, V.M., (2001). *Phylum BVI. Chloroflexi phy. nov.*. In: Boone D.R., Castenholz R.W., Garrity G.M. (eds) *Bergey's Manual® of Systematic Bacteriology*. Springer, New York, NY

Geider, R. J., La Roche, J., (2002). *Redfield revisited: Variability of C:N:P in marine microalgae and its biochemical basis*. European Journal of Phycology, 37(1), 1–17. https://doi.org/10.1017/S0967026201003456

Ghosh, S., Banerjee, S., Das, D., (2017). *Process intensification of biodiesel production from Chlorella sp. MJ 11/11 by single step transesterification.* Algal Research, 27(March), 12–20. https://doi.org/10.1016/j.algal.2017.08.021

Girard, J. M., Roy, M. L., Hafsa, M. Ben, Gagnon, J., Faucheux, N., Heitz, M., Deschênes, J. S., (2014). *Mixotrophic cultivation of green microalgae Scenedesmus obliquus on cheese whey permeate for biodiesel production.* Algal Research, 5(1), 241–248. https://doi.org/10.1016/j.algal.2014.03.002

Gonçalves, A. L., Pires, J. C. M., Simões, M., (2017). *A review on the use of microalgal consortia for wastewater treatment*. Algal Research, 24, 403–415. https://doi.org/10.1016/j.algal.2016.11.008

González-Fernández, C., Riaño-Irazábal, B., Molinuevo-Salces, B., Blanco, S., García-González, M.C., (2011). *Effect of operational conditions on the degradation of organic matter and development of microalgae–bacteria consortia when treating swine slurry*. Applied Microbiology and Biotechnology, 90(3), 1147-1153. https://doi.org/10.1007/s00253-011-3111-z

Gouveia, A. R., Freitas, E. B., Galinha, C. F., Carvalho, G., Duque, A. F., Reis, M. A. M., (2017). *Dynamic change of pH in acidogenic fermentation of cheese whey towards polyhydroxyalkanoates production: Impact on performance and microbial population.* New Biotechnology, 37, 108–116. https://doi.org/10.1016/j.nbt.2016.07.001

Griffiths, M. J., Garcin, C., van Hille, R. P., Harrison, S. T. L., (2011). *Interference by pigment in the estimation of microalgal biomass concentration by optical density.* Journal of Microbiological Methods, 85(2), 119–123. https://doi.org/10.1016/j.mimet.2011.02.005

Heijnen, J.J., (1997). *A thermodynamically based description of chemotrophic microbial growth stoichiometry and kinetics*, In *Encyclopedia of Bioprocess Technology: Fermentation, Biocatalysis and Bioseparation*, Flickinger, M.C., Drew, S.W., Eds.; John Wiley: New York.

Henrard, A.A., de Morais, M.G., Costa, J.A.V., (2011). *Vertical tubular photobioreactor for semicontinuous culture of Cyanobium sp*., Bioresource Technology, 102(7), 4897-4900, ISSN 0960-8524. https://doi.org/10.1016/j.biortech.2010.12.011.

Hu, J., Nagarajan, D., Zhang, Q., Chang, J., Lee, J., (2018). *Heterotrophic cultivation of microalgae for pigment production: A review*, Biotechnology Advances, 36(1), 54-67, ISSN 0734-9750. https://doi.org/10.1016/j.biotechadv.2017.09.009.

Imhoff, J.F., (1995). *Taxonomy and Physiology of Phototrophic Purple Bacteria and Green Sulfur Bacteria*. In: Blankenship R.E., Madigan M.T., Bauer C.E. (eds) *Anoxygenic Photosynthetic Bacteria. Advances in Photosynthesis and Respiration*, vol 2. Springer, Dordrecht

Jayakrishnan, U., Deka, D., Das, G., (2019). *Enhancing the volatile fatty acid production from agro-industrial waste streams through sludge pretreatment*. Environmental Science: Water Research and Technology, 5(2), 334–345. https://doi.org/10.1039/c8ew00715b

Jiang, Z., (2009). *Biomass production, chlorophyll A and carotenoid contents of spirulina maxima in mixed culture of lactose.* Proceedings - 2009 International Conference on Environmental Science and Information Application Technology, ESIAT 2009, 1, 542–544. https://doi.org/10.1109/ESIAT.2009.25

Kisaalita, W.S., Pinder, K.L., Lo, K.V., (1986). *Acidogenic fermentation of lactose.* Biotechnology and Bioengineering, 30, 88-95. https://doi.org/10.1002/bit.260300113

Kim, H. W., Vannela, R., Zhou, C., Rittmann, B. E., (2011). *Nutrient acquisition and limitation for the photoautotrophic growth of Synechocystis sp. PCC6803 as a renewable biomass source.* Biotechnology and Bioengineering, 108(2), 277–285. https://doi.org/10.1002/bit.22928

Krzycki, J. A., Wolkin, R. H., Zeikus, J. G., (1982). *Comparison of Unitrophic and Mixotrophic Substrate Metabolism by an Acetate-Adapted Strain of Methanosarcina barkeri*. Journal of Bacteriology, 149(1), 247–254.

Kumar, K., Dasgupta, C. N., Das, D., (2014). *Cell growth kinetics of Chlorella sorokiniana and nutritional values of its biomass.* Bioresource Technology, 167, 358–366. https://doi.org/10.1016/j.biortech.2014.05.118

Li, W., Xu, X., Fujibayashi, M., Niu, Q., Tanaka, N., Nishimura, O., (2016). *Response of microalgae to elevated CO 2 and temperature: impact of climate change on freshwater ecosystems.* Environmental Science and Pollution Research, 23(19), 19847–19860. https://doi.org/10.1007/s11356-016-7180-5

van Lier, J. B., Mahmoud, N., & Zeeman, G. (2008). *Anaerobic wastewater treatment*. In M. v. M. Henze, *Biological wastewater treatment* (pp. 415-456). London: IWA Publishing.

Liu, H., Wang, J., Liu, X., Fu, B., Chen, J., Yu, H. Q., (2012). *Acidogenic fermentation of proteinaceous sewage sludge: Effect of pH.* Water Research, 46(3), 799–807. https://doi.org/10.1016/j.watres.2011.11.047

Lopo, M., Montagud, A., Navarro, E., Cunha, I., Zille, A., de Córdoba, P.F., Moradas-Ferreira, P., Tamagnini, P., Urchueguía, J.F., (2012). *Experimental and Modeling Analysis of Synechocystis sp. PCC 6803 Growth,* Journal of Molecular Microbiology and Biotechnology, 22(2), 71-82. https://doi.org/10.1159/000336850

Madigan, M.T., Ormerod, J.G., (1995). *Taxonomy, Physiology and Ecology of Heliobacteria*. In: Blankenship R.E., Madigan M.T., Bauer C.E. (eds) *Anoxygenic Photosynthetic Bacteria. Advances in Photosynthesis and Respiration*, vol 2. Springer, Dordrecht

Marwaha, S.S., Kennedy, J.F., (1988). *Review: Whey – pollution problem and potential utilization*. International Journal of Food Science and Technology, 23, 323-336. https://doi.org/10.1111/j.1365-2621.1988.tb00586.x

Martínez, L., Morán, A., García, A. I., (2012). *Effect of light on Synechocystis sp. and modelling of its growth rate as a response to average irradiance.* Journal of Applied Phycology, 24(1), 125–134. https://doi.org/10.1007/s10811-011-9658-3

McCann, S. H., Boren, A., Hernandez-Maldonado, J., Stoneburner, B., Saltikov, C. W., Stolz, J. F., Oremland, R. S., (2017). *Arsenite as an electron donor for anoxygenic photosynthesis: Description of three strains of Ectothiorhodospira from Mono Lake, California and Big Soda Lake, Nevada*. Life, 7(1). https://doi.org/10.3390/life7010001

Melo de, R.G., Frazão de Andrade, A., Pedrosa Bezerra, R., Spindola Correia, D., de Souza, V.C., Brasileiro-Vidal, A.C., de Araújo Viana Marques, D., Figueiredo Porto, A.L., (2018). *Chlorella vulgaris mixotrophic growth enhanced biomass productivity and reduced toxicity from agro-industrial by-products*, Chemosphere, 204, 344-350, ISSN 0045-6535. https://doi.org/10.1016/j.chemosphere.2018.04.039.

Mockaitis, G., Ratusznei, S. M., Rodrigues, J. A. D., Zaiat, M., Foresti, E., (2006). *Anaerobic whey treatment by a stirred sequencing batch reactor (ASBR): Effects of organic loading and supplemented alkalinity*. Journal of Environmental Management, 79(2), 198–206. https://doi.org/10.1016/j.jenvman.2005.07.001

Mockaitis, G., Bruant, G., Guiot, S.R., Peixoto, G., Foresti, E., Zaiat, M., (2020). *Acidic and thermal pre-treatments for anaerobic digestion inoculum to improve hydrogen and volatile fatty acid production using xylose as the substrate*, Renewable Energy, 145, 1388-1398, ISSN 0960-1481. https://doi.org/10.1016/j.renene.2019.06.134.

Mondal, M., Ghosh, A., Sharma, A.S., Tiwari, O.N., Gayen, K., Mandal, M.K., Halder, G.N., (2016). *Mixotrophic cultivation of Chlorella sp. BTA 9031 and Chlamydomonas sp. BTA 9032 isolated from coal field using various carbon sources for biodiesel production*, Energy Conversion and Management, 124, 297-304, ISSN 0196-8904. https://doi.org/10.1016/j.enconman.2016.07.033.

Mooij, P. R., Stouten, G. R., Tamis, J., van Loosdrecht, M. C. M., Kleerebezem, R. (2016). *Survival of the fattest.* Journal of Cell Biology, 212(6), 3404–3406. https://doi.org/10.1083/jcb.2126if

Nielsen, S.L., (2006). *Size-dependent growth rates in eukaryotic and prokaryotic algae exemplified by green algae and cyanobacteria: comparison between unicells and colonial growth forms*. Journal of Plankton Research, 28 (5), 489-498. https://doi.org/10.1093/plankt/fbi134

Odjadjare, E. C., Mutanda, T., Olaniran, A. O., (2017). *Potential biotechnological application of microalgae: a critical review.* Critical Reviews in Biotechnology, 37(1), 37–52. https://doi.org/10.3109/07388551.2015.1108956

Overmann, J., Garcia-Pichel, F., (2013). *The Phototrophic Way of Life.* In Rosenberg, E., DeLong, E.F., Lory, S., Stackebrandt, E., Thompson, F., (eds.), *The Prokaryotes – Prokaryotic Communities and Ecophysiology* (pp. 203-258), Springer-Verlag Berlin Heidelberg. https://doi.org/10.1007/978-3-642-30194-0.

Patel, V. K., Maji, D., Pandey, S. S., Rout, P. K., Sundaram, S., Kalra, A., (2016). *Rapid budding EMS mutants of Synechocystis PCC 6803 producing carbohydrate or lipid enriched biomass.* Algal Research, 16, 36–45. https://doi.org/10.1016/j.algal.2016.02.029

Peeters, J.C.H., Eilers, P., (1978). *The relationship between light intensity and photosynthesis: a simple mathematical model*. Hydrological Bulletin, 12(2), 134–136. https://doi.org/10.1007/BF02260714

Posadas, E., García-Encina, P. A., Soltau, A., Domínguez, A., Díaz, I., Muñoz, R. (2013). *Carbon and nutrient removal from centrates and domestic wastewater using algal-bacterial biofilm bioreactors.* Bioresource Technology, 139, 50–58. https://doi.org/10.1016/j.biortech.2013.04.008

Prazeres, A.R., Carvalho, F., Rivas, J., (2012). *Cheese whey management: A review*, Journal of Environmental Management, 110, 48-68, ISSN 0301-4797. https://doi.org/10.1016/j.jenvman.2012.05.018.

Prest, E.I., Hammes, F., Kötzsch, S., van Loosdrecht, M.C.M., Vrouwenvelder, J.S., (2013). *Monitoring microbiological changes in drinking water systems using a fast and reproducible flow cytometric method*, Water Research, 47(19), 7131-7142, ISSN 0043-1354. https://doi.org/10.1016/j.watres.2013.07.051.

Pulz, O., Gross, W., (2004). *Valuable products from biotechnology of microalgae*. Applied Microbiology and Biotechnology, 65(6), 635–648. https://doi.org/10.1007/s00253-004-1647-x

Qu, Z., Duan, P., Cao, X., Liu, M., Lin, L., Li, M. (2019). *Comparison of monoculture and mixed culture (Scenedesmus obliquus and wild algae) for C, N, and P removal and lipid production.* Environmental Science and Pollution Research, 26(20), 20961–20968. https://doi.org/10.1007/s11356-019-05339-z

Qiao, H., Wang, G., Zhang, X., (2009). *Isolation and characterization of Chlorella sorokiniana GXNN01 (Chlorophyta) with the properties of heterotrophic and microaerobic growth.* Journal of Phycology, 45(5), 1153–1162. https://doi.org/10.1111/j.1529-8817.2009.00736.x

Ramanan, R., Kim, B.H., Cho, D.H., Oh, H.M., Kim, H.S., (2016). *Algae–bacteria interactions: Evolution, ecology and emerging applications*, Biotechnology Advances, 34 (1), 14-29, ISSN 0734-9750. https://doi.org/10.1016/j.biotechadv.2015.12.003.

Redfield, A.C., (1934). *On the proportions of organic derivatives in sea water and their relation to the composition of plankton*. In Daniel, R.J., (ed) *James Johnstone Memorial Volume*, 176–192. University of Liverpool.

Riaño, B., Blanco, S., Becares, E., García-González, M. C., (2016). *Bioremediation and biomass harvesting of anaerobic digested cheese whey in microalgal-based systems for lipid production*. Ecological Engineering, 97, 40–45. https://doi.org/10.1016/j.ecoleng.2016.08.002

Ríos, L. F., Martinez, A., Klein, B. C., Maciel, M. R. W., Filho, R. M., (2018). *Comparison of Growth and Lipid Accumulation at Three Different Growth Regimes with Desmodesmus sp.*, Waste and Biomass Valorization, 9(3), 421–427. https://doi.org/10.1007/s12649-016-9811-y

Rombouts, J. L., Mos, G., Weissbrodt, D. G., Kleerebezem, R., Van Loosdrecht, M. C. M., (2019). *Diversity and metabolism of xylose and glucose fermenting microbial communities in sequencing batch or continuous culturing.* FEMS Microbiology Ecology, 95(2), 1–12. https://doi.org/10.1093/femsec/fiy233

Salati, S., D'Imporzano, G., Menin, B., Veronesi, D., Scaglia, B., Abbruscato, P., Mariani, P., Adani, F., (2017). *Mixotrophic cultivation of Chlorella for local protein production using agro-food by-products.* Bioresource Technology, 230, 82–89. https://doi.org/10.1016/j.biortech.2017.01.030

Shah, F.A., Mahmood, Q., Shah, M.M., Pervez, A., Asad, S.A., (2014). *Microbial Ecology of Anaerobic Digesters: The Key Players of Anaerobiosis*, Scientific World Journal, DOI: 10.1155/2014/183752.

Shoaf, W. Thomas, Lium, Bruce W., (1976). *Improved extraction of chlorophyll a and b from algae using dimethyl sulfoxide*, Limnology and Oceanography, 6. https://doi.org/10.4319/lo.1976.21.6.0926

Sijil, P. V., Adki, V. R., Sarada, R., & Chauhan, V. S., (2019). *Strategies for enhancement of alpha-linolenic acid rich lipids in Desmodesmus sp. without compromising the biomass production*. Bioresource Technology, 294(September), 122215. https://doi.org/10.1016/j.biortech.2019.122215

Silva, F. C., Serafim, L. S., Nadais, H., Arroja, L., Capela, I,. (2013). *Acidogenic fermentation towards valorisation of organic waste streams into volatile fatty acids*, Chemical and Biochemical Engineering, Q. *27*(4), 467–476. https://hrcak.srce.hr/112368

Singh, G., Patidar, S. K., (2018). *Microalgae harvesting techniques: A review*. Journal of Environmental Management, 217, 499–508. https://doi.org/10.1016/j.jenvman.2018.04.010

Speziale, B. J., Schreiner, S. P., Giammatteo, P. A., Schindler, J. E., (1984). *Comparison of N,N-dimethylformamide, dimethyl sulfoxide, and acetone for extraction of phytoplankton chlorophyll.* Canadian Journal of Fisheries and Aquatic Sciences, 41(10), 1519–1522. https://doi.org/10.1139/f84-187

Stomp, M., Huisman, J., Stal, L. J., Matthijs, H. C. P., (2007). *Colorful niches of phototrophic microorganisms shaped by vibrations of the water molecule.* ISME Journal, 1(4), 271–282. https://doi.org/10.1038/ismej.2007.59

Suwan, D., Chitapornpan, S., Honda, R., Chiemchaisri, C., (2014). *Conversion of organic carbon in food processing wastewater to photosynthetic biomass in photo-bioreactors using different light sources.* Environmental Engineering Research, 19(3), 293–298. https://doi.org/10.4491/eer.2014.S1.009

Think USA Dairy, (2019). *Demineralized whey.* Retrieved from: https://www.thinkusadairy.org/products/whey-protein-and-ingredients/whey-categories/demineralized-whey

Ting, H., Haifeng, L., Shanshan, M., Zhang, Y., Zhidan, L., Na, D., (2017). *Progress in microalgae cultivation photobioreactors and applications in wastewater treatment: A review.* International Journal of Agricultural and Biological Engineering, 10(1), 1–29. https://doi.org/10.3965/j.ijabe.20171001.2705

Torres, P., (1992). *Desempenho de um reator anaeróbio de manta de lodo (UASB) de bancada no tratamento de substrato sintético simulando esgoto sanitário sob diferentes condições de operação*. Master Dissertation, SHS – EESC – USP, São Carlos.

Tsakali, E., Petrotos, K., Allessandro, A., Goulas, P., (2010). *A review on whey composition and the methods used for its utilization for food and pharmaceutical products.* 6th International Conference on Simulation and Modelling in the Food and Bio-Industry. FOODSIM

Tsolcha, O. N., Tekerlekopoulou, A. G., Akratos, C. S., Bellou, S., Aggelis, G., Katsiapi, M., Moustaka-Gouni, M., Vayenas, D. V., (2016). *Treatment of second cheese whey effluents using a Choricystis-based system with simultaneous lipid production.* Journal of Chemical Technology and Biotechnology, 91(8), 2349–2359. https://doi.org/10.1002/jctb.4829

Tsolcha, O. N., Tekerlekopoulou, A. G., Akratos, C. S., Antonopoulou, G., Aggelis, G., Genitsaris, S., Moustaka-Gouni, M., Vayenas, D. V., (2018). *A Leptolyngbya-based microbial consortium for agro-industrial wastewaters treatment and biodiesel production*. Environmental Science and Pollution Research, 25(18), 17957–17966. https://doi.org/10.1007/s11356-018-1989-z

Ullrich, W. R., Lazarová, J., Ullrich, C. I., Witt, F. G., Aparicio, P. J., (1998*). Nitrate uptake and extracellular alkalinization by the green alga Hydrodictyon reticulatum in blue and red light*. Journal of ExperimentalBotany, 49(324), 1157-1162, https://doi.org/10.1093/jxb/49.324.1157

UN, (2019). *Sustainable Development goals.* Retrieved from: https://www.un.org/sustainabledevelopment/development-agenda/ Accessed on 28/11/2019

FAO, (2005). *Field Guide on Salinity in Aceh*, © United Nations Food and Agriculture Organization. http://www.fao.org/ag/tsunami/docs/saltwater-guide.pdf

USDA, (2019). *Dairy: world markets and trade.* Retrieved from: https://www.fas.usda.gov/data/dairy-world-markets-and-trade Accessed on 28/11/2019

Wang, L., Min, M., Li, Y., Chen, P., Chen, Y., Liu, Y., Wang, Y., Ruan, R., (2010). *Cultivation of green algae Chlorella sp. in different wastewaters from municipal wastewater treatment plant.* Applied Biochemistry and Biotechnology, 162(4), 1174–1186. https://doi.org/10.1007/s12010-009-8866-7

Wang, Y., Li, Y., Shi, D., Shen, G., Ru, B., Zhang., S., (2002) *Characteristics of mixotrophic growth of Synechocystis sp. in an enclosed photobioreactor.* Biotechnology Letters, 24(19), 1593-1597. https://doi.org/10.1023/A:1020384029168

Wellburn, A.R., (1994). *The spectral determination of chlorophylls a and b, as well as total carotenoids, using various solvents with spectrophotometers of different resolution*. Journal of Plant Physiology, 144(3), 307-313. https://doi. org/10.1016/S0176-1617(11)81192-2

Xia, A., Cheng, J., Song, W., Su, H., Ding, L., Lin, R., Lu, H., Liu, J., Zhou, J., Cen, K., (2015). *Fermentative hydrogen production using algal biomass as feedstock*, Renewable and Sustainable Energy Reviews, 51, 209-230, ISSN 1364-0321. https://doi.org/10.1016/j.rser.2015.05.076.

Yamagishi, T., Katsumata, M., Yamaguchi, H., Shimura, Y., Kawachi, M., Koshikawa, H., Horie, Y., Tatarazako, N., (2016). *Rapid ecotoxicological bioassay using delayed fluorescence in the marine cyanobacterium Cyanobium sp. (NIES-981).* Ecotoxicology, 25(10), 1751–1758. https://doi.org/10.1007/s10646-016-1718-7

Yao, S., Lyu, S., An, Y., Lu, J., Gjermansen, C., Schramm, A., (2018). *Microalgae–bacteria symbiosis in microalgal growth and biofuel production: a review.* Journal of Applied Microbiology, 126(2), 359–368. https://doi.org/10.1111/jam.14095

Yen, H. W., Hu, I. C., Chen, C. Y., Ho, S. H., Lee, D. J., Chang, J. S., (2013). *Microalgae-based biorefinery - From biofuels to natural products.* Bioresource Technology, 135, 166–174. https://doi.org/10.1016/j.biortech.2012.10.099

Yu, Y., You, L., Liu, D., Hollinshead, W., Tang, Y. J., Zhang, F., (2013). *Development of synechocystis sp. PCC 6803 as a phototrophic cell factory.* Marine Drugs, 11(8), 2894–2916. https://doi.org/10.3390/md11082894

Zanette, C. M., Mariano, A. B., Yukawa, Y. S., Mendes, I., Rigon Spier, M., (2019). *Microalgae mixotrophic cultivation for β-galactosidase production.* Journal of Applied Phycology, 31(3), 1597–1606. https://doi.org/10.1007/s10811-018-1720-y

Appendix

A. Biogas measurements in the acidogenic fermentation experiments

Fractions of CO_2, CH_4, and H_2 in the gas samples measured in the acidogenic fermentation experiments are shown in Figure A.1. For the experiment testing the thermal pre-treatment of the inoculum, the content of CO_2, CH_4, and H_2 are shown in Figure A.1(a-b) for the triplicates of the control (C1-C3) and of the thermally pre-treated (T1-T3) batches. For the experiment testing the effect of the food-to-microorganism (F/M) ratio, the average CO_2 of the duplicates is shown in Figure A.1(c-d) for F/M 0.5, 1, 2, and 4 g COD g VS^{-1}. CH_4 and H_2 were not detected by the gas chromatographer in any of the F/M ratios.

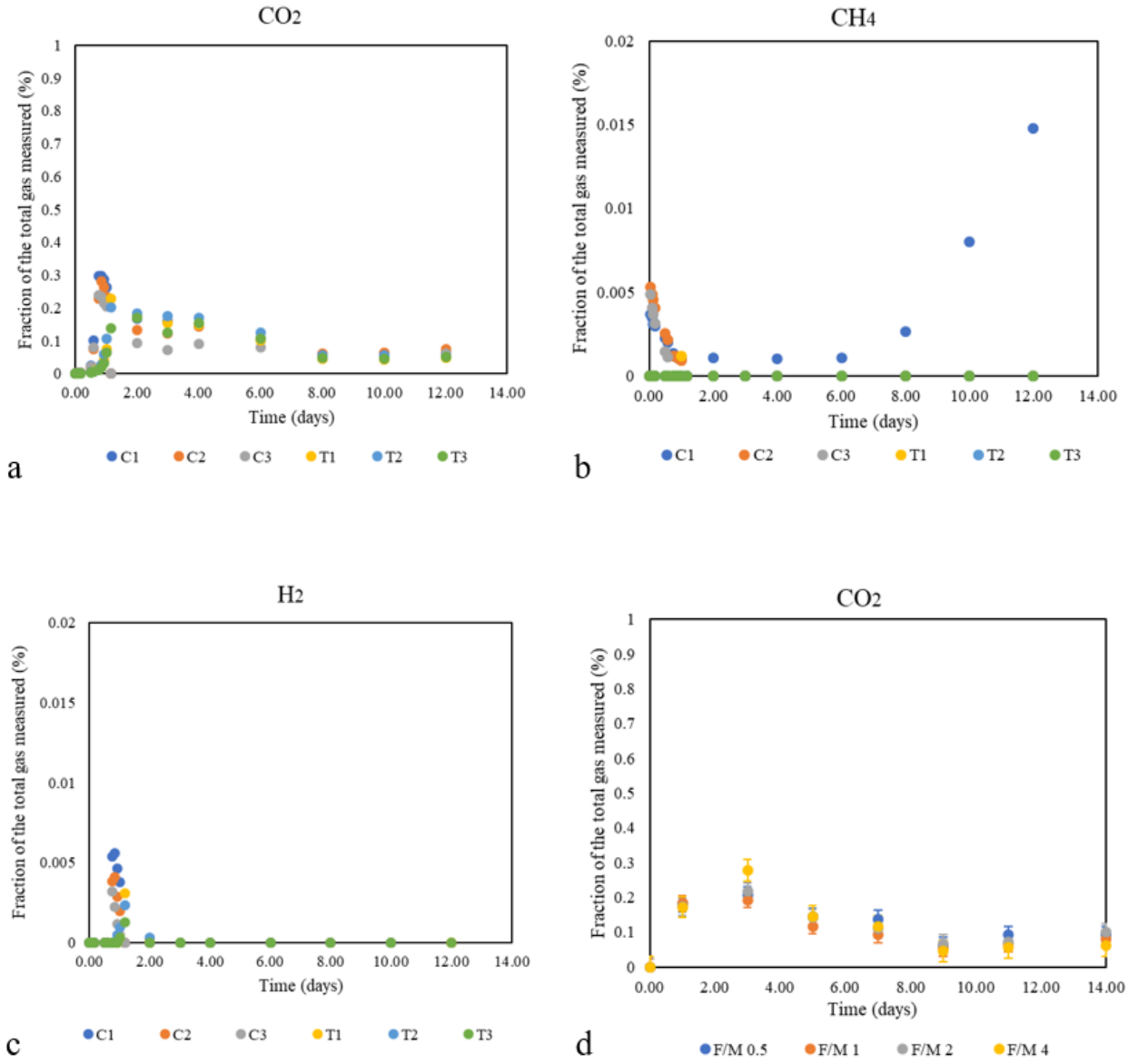

*Figure A.124: Concentration of carbon dioxide (**a**), methane (**b**), and hydrogen (**c**) in the control (C1-C3) and in the thermally pre-treated batches in the 10 mL gas sample, from day 0 to 12. In Figure **d**, the concentration of carbon dioxide in the gas samples taken from the different F/M ratios batches is shown. Methane and hydrogen gas were not detected in any of the gas samples from the F/M experiment.*

To test the efficiency of the thermal pre-treatment, the production of CH_4 was also measured with an Automatic Methane Potential Test System II (AMPTS II) (Bioprocess Control, Sweden). Bottles of 200 mL containing

untreated or thermally pre-treated inoculum (as in section 3.1) and demineralized cheese whey (as in section 3.1), with a F/M ratio of 0.5 g COD g VS^{-1}. A phosphate buffer (0.2 M $K_2HPO_4 \cdot 3H_2O$ and 0.2 M $NaH_2PO_4 \cdot 2H_2O$, dosed at 50 mL L^{-1} each) along with a macronutrients solution (NH^4Cl (170 g L^{-1}), $CaCl_2 \cdot 2H_2O$ (8 g L^{-1}) and $MgSO_4 \cdot 7H_2O$ (9 g L^{-1}), dosed at 6 mL L^{-1}) and a micronutrients solution as depicted in 3.1. The experiment was performed at 35°C, in triplicates (C1-3 for the control, T1-3 for the thermally pre-treated sludge). Moreover, blanks consisting of only inoculum, micronutrients, macronutrients, and buffer solutions were used (BC1-3 for the control, BT1-3 for the thermally pre-treated sludge).

All bottles were sparged with nitrogen gas. The volume of biogas produced was first flowed through a wash bottle containing 3 M NaOH, then measured in the flow array unit. The cumulative gas production is measured every 10 NmL of gas. The test lasted 85.5 hours. Cumulative gas productions are shown in Figure A.2.

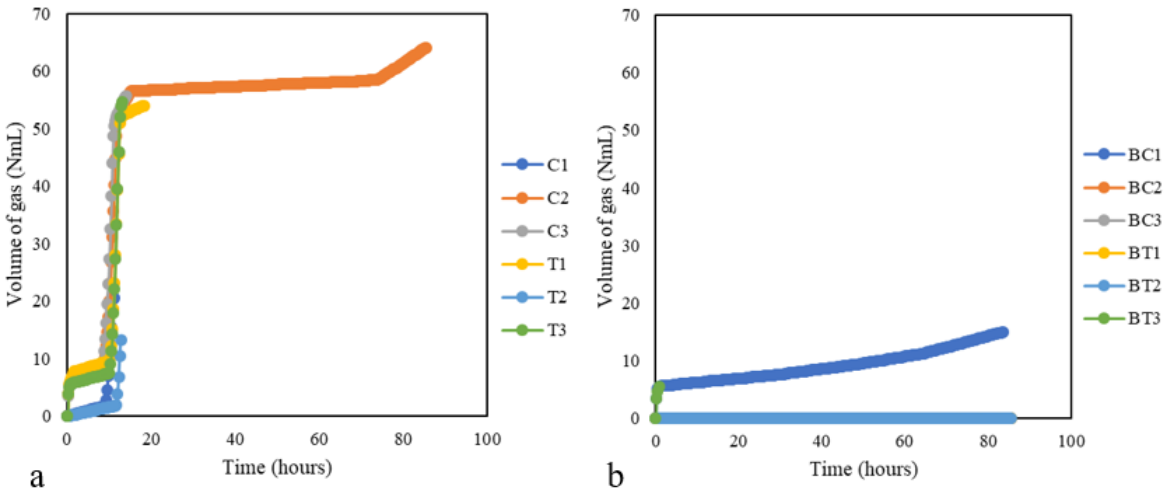

*Figure A.2:**a.** Methane produced in the AMPTS II experiment by the untreated (C1-C3) and treated (T1-T3) inoculums from demineralized cheese whey. **b.** Methane produced in the blanks of the untreated (BC1-BC3) and treated (BT1-BT3) inoculums, when no cheese whey was provided.*

Although the methane production was higher for the untreated sludge in both the experiment containing cheese whey and in the blank, the difference is minimal. The addition of a phosphate buffer could have determined the differences between the efficiency of the pre-treatment in the batches and in the AMPTS, the volume produced is still not completely understood. The biogas production from cheese whey reaches a maximum of ca. 65 NmL, which is still little compared to the COD available (400 mg COD, corresponding to 140 NmL of methane).

Due to the difficult interpretation of the results, the repetition of the experiment is strongly suggested.

B. COD consumption and VFA production in the acidogenic fermentation experiments

Figures B.1 and B.2 show the consumption of substrate, in the form of soluble COD and the total amount of sugars, and the production of volatile fatty acids.

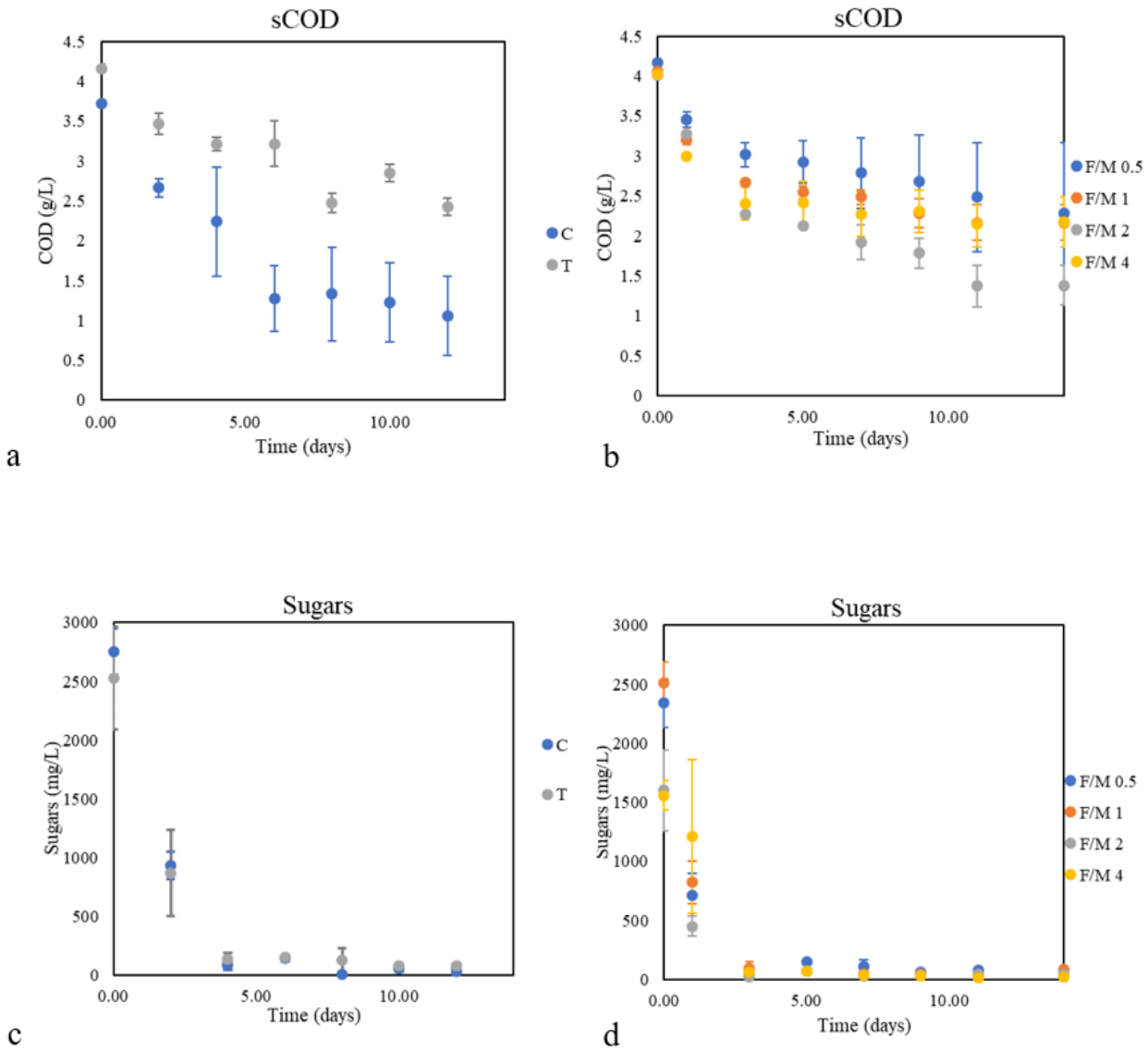

*Figure B.1: Figures **a** and **b** show the variation of sCOD over time in the first experiment (C: control, T: thermally pre-treated sludge) and in the second (F/M 0.5, 1, 2, and 4 g COD g VS^{-1}). Losses of sCOD are related to the production of biomass, biogas, and to the oxidation of organic matter.*

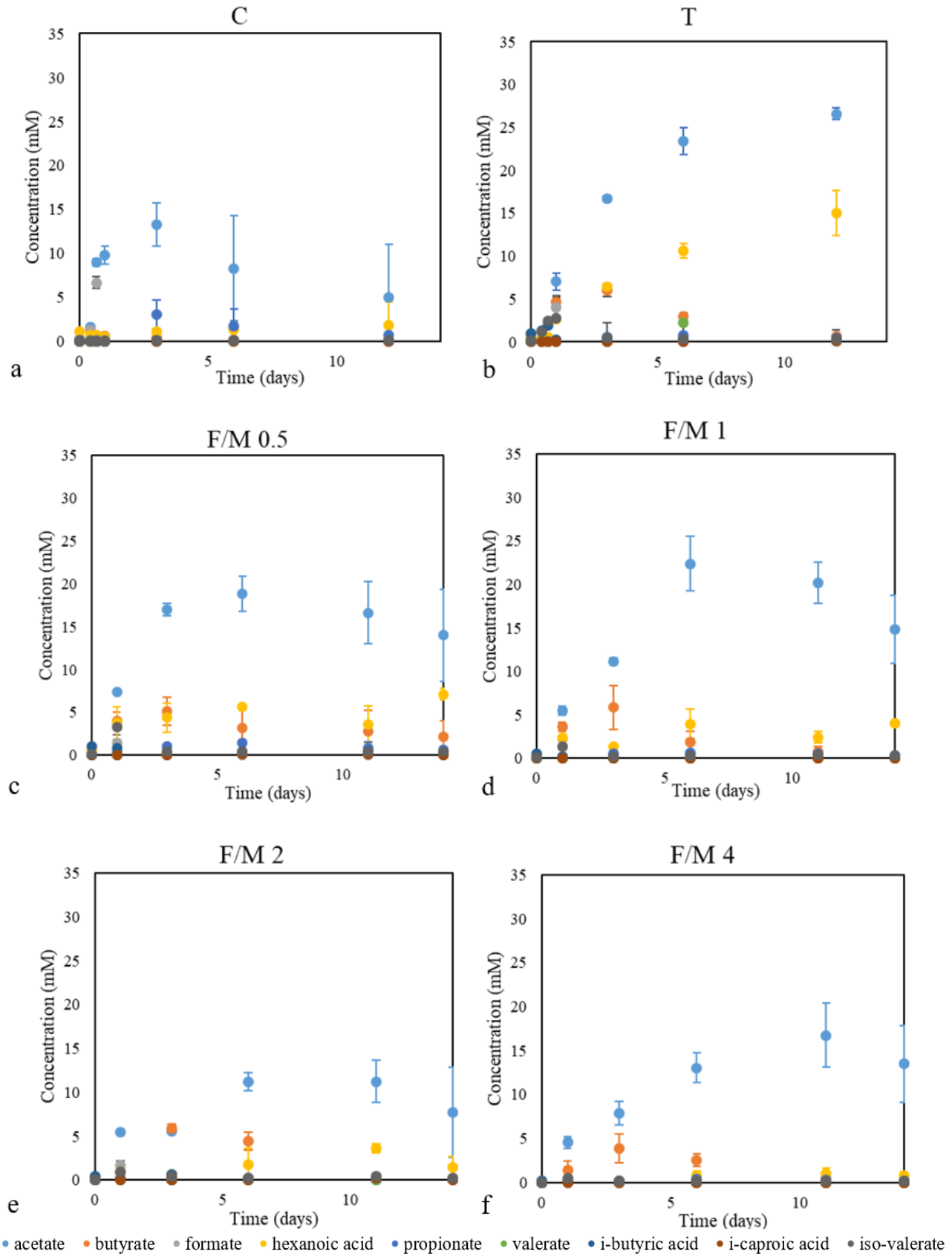

Figure B.2: ***a-b.*** *Volatile fatty acid production in the control (C) and in the thermally pre-treated (T) batches.* ***c-f.*** *Volatile fatty acid production in the batches with F/M ratio of 0.5, 1, 2, and 4 g COD g VS^{-1}. The major products are acetate, butyrate, and hexanoic acid.*

C. Cell counting and cell viability measurements

Cell viability was measured with both flow cytometry (FCM), by total and alive cells counting, and methylene blue (MB) adsorption. Raw data are shown in Table C.1 of the total cell count and alive cell count measured by FCM, and the absorbance at 664 nm (A_{664}) of the normal sample, the boiled sample, and the blank (solution containing MB) measured for the methylene blue adsorption.

Table C.1: Cell viability, determined as the percentage of alive cells in the FCM and MB experiments. For FCM, total and alive cell counts were measured and the alive fraction was calculated. For MB, A664 of the blank, the normal sample, and the boiled sample were measured, and the alive fraction was calculated. The alive fraction was adjusted when percentages were higher than 100% by setting them to 100%.

Day	**Flow Cytometry**			**Methylene blue adsorption**				
	Total cell count	Alive cell count	Alive fraction (%)	Normal sample A_{664}	Boiled sample A_{664}	Blank A_{664}	Alive fraction (%)	Adjusted alive fraction (%)
0	175170	35860	20.47	0.938	0.844	0.949	89.52	89.52
1	2562950	30520	1.19	0.947	0.732	0.943	101.90	100
2	24955000	1399000	5.61	0.879	0.759	0.877	101.69	100
3	19941000	1937000	9.71	0.846	0.728	0.853	94.4	94.4
4	27680000	2733000	9.87	0.911	0.78	0.867	150.57	100
7	32735000	11006000	33.62	0.857	0.667	0.866	95.48	95.48
8	35293000	3620000	10.26	0.934	0.808	0.865	221.05	100
9	38222000	5734000	15.00	/	/	/	/	/
10	37480000	11031000	29.43	0.833	0.67	0.85	90.56	90.56
11	38989000	15959000	40.93	0.821	0.679	0.859	78.89	78.89
13	42933000	5607000	13.06	0.762	0.605	0.844	65.69	65.69
14	42987000	12448000	28.96	/	/	/	/	/
17	55833000	8550000	15.31	0.667	0.493	0.834	51.03	51.03
23	47413000	2851000	6.01	0.386	0.244	0.835	24.03	24.03
25	40613000	13470000	33.17	0.391	0.26	0.834	22.82	22.82
31	88294000	38235000	43.30	0.307	0.199	0.826	17.22	17.22

The alive cell count measured by FCM was only considered reliable for day 25 and day 31. In these days, in fact, the SYBR green-Propidium Iodide dye used to detect viable cells was changed. As a result, the plots of alive cells measurements changed, as shown in Figure C.1. In these plots, cells were identified by the fluorescence intensity at Fl1 (533 ± 30 nm Band Pass Filter) and Fl3 (> 670 nm Band Pass Filter). To distinguish cells from other debris, a gate was defined according to Prest et al. (2013). The same perimeter should include total cells identified by SYBR green dye and living cells identified by SYBR green and Propidium Iodide mixture. On day 25, a new SYBR green – Propidium Iodide mixture was tested along with the previous one. As can be seen in Figure C.1, the new mixture was able to identify cells, as shown by the dots found inside the gate. The same sample showed different results using the old mixture. Therefore, it is likely that the old mixture had been degraded, possibly by light.

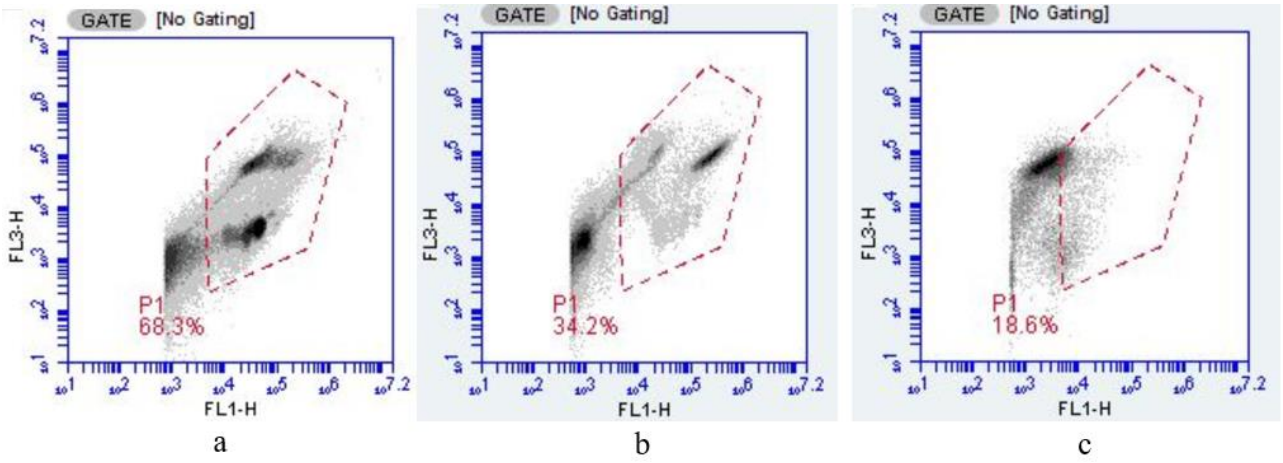

Figure C.1: The three plots show the cells identified by flow cytometry, with x-axis showing fluorescence intensity at Fl1 (533 ± 30 nm Band Pass Filter) and the y-axis showing fluorescence intensity at Fl3 (> 670 nm Band Pass Filter). The perimeter defined should include total cells and viable cells. ***a.*** *Total cell count measured by the SYBR green dye.* ***b.*** *Viable cell count measured by the new SYBR green – Propidium Iodide dye.* ***c.*** *Viable cell count measured by the old SYBR green – Propidium Iodide dye. The cells are not found within the gate.*

D. Biomass calibration line from A_{750}

Light absorbance at 750 nm (A750) was used to measure the biomass content of the phototrophic cultures. The calibration line is shown in Figure D.1.

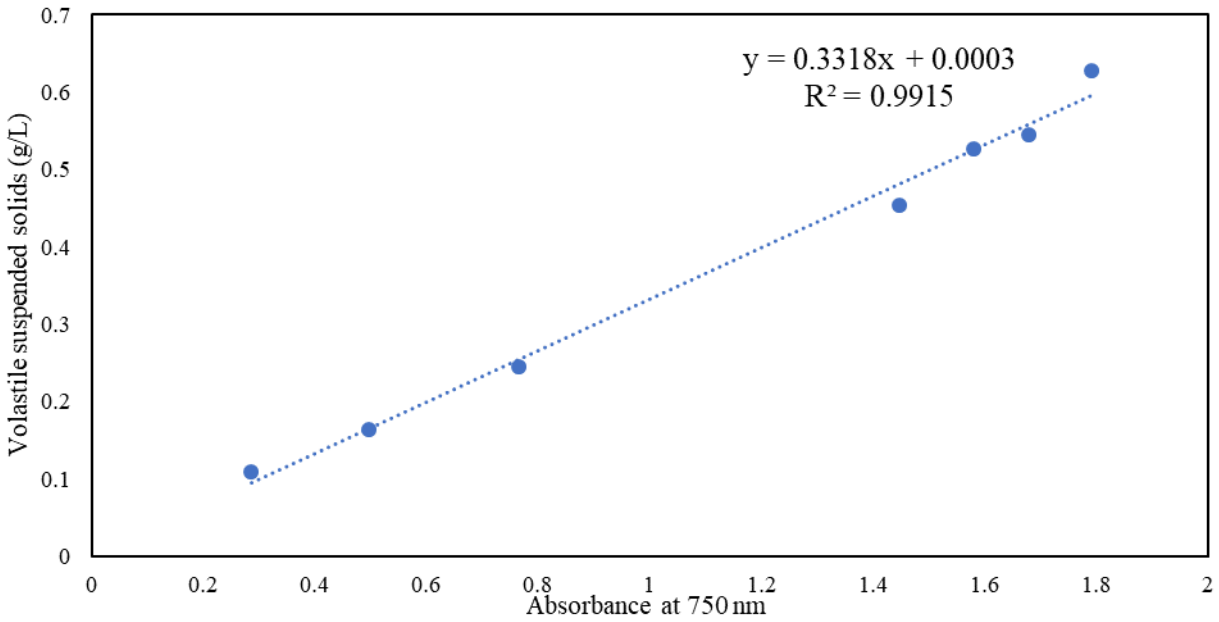

Figure D.1: Calibration line used to determine the biomass content (in terms of Volatile Suspended Solids) from the A_{750}.

E. Nutrient consumption in the photoorganoheterotrophic cultures

Nutrient consumption (carbon, nitrogen, and phosphorus) was tracked in the photoorganoheterotrophic cultures $AOAL_{100}$, $AXAL_{100}$, $LOAL_{100}$, $LXAL_{100}$, and $CWAL_{100}$ until stabilization of the biomass concentration was reached. Nutrient consumption and biomass growth are shown in Figure E.1.

The concentration of organic carbon dosed in the cultures was the same (ca. 225 mg C L^{-1}). The TOC measurement of the nutrient solutions used also showed similar concentrations, although lower than the amount dosed. (208 ± 1.5 mg C L^{-1}). HPLC measurements (displayed in the pictures) indicated lower concentrations of carbon in the acetate solutions (ca. 210 mg C L^{-1}), and higher concentrations in the lactose and demineralized cheese whey (ca. 250 mg C L^{-1}) solutions. This can be due to incorrect calibration, or to disturbances in the HPLC signal. For example, the injection dip (ca. 7.5 min) was close to the lactose peak (ca. 7.8 min); moreover, a peak was also observed in the acetate solution (ca. 7.6 min) likely related to a component of the BG-11 solution.

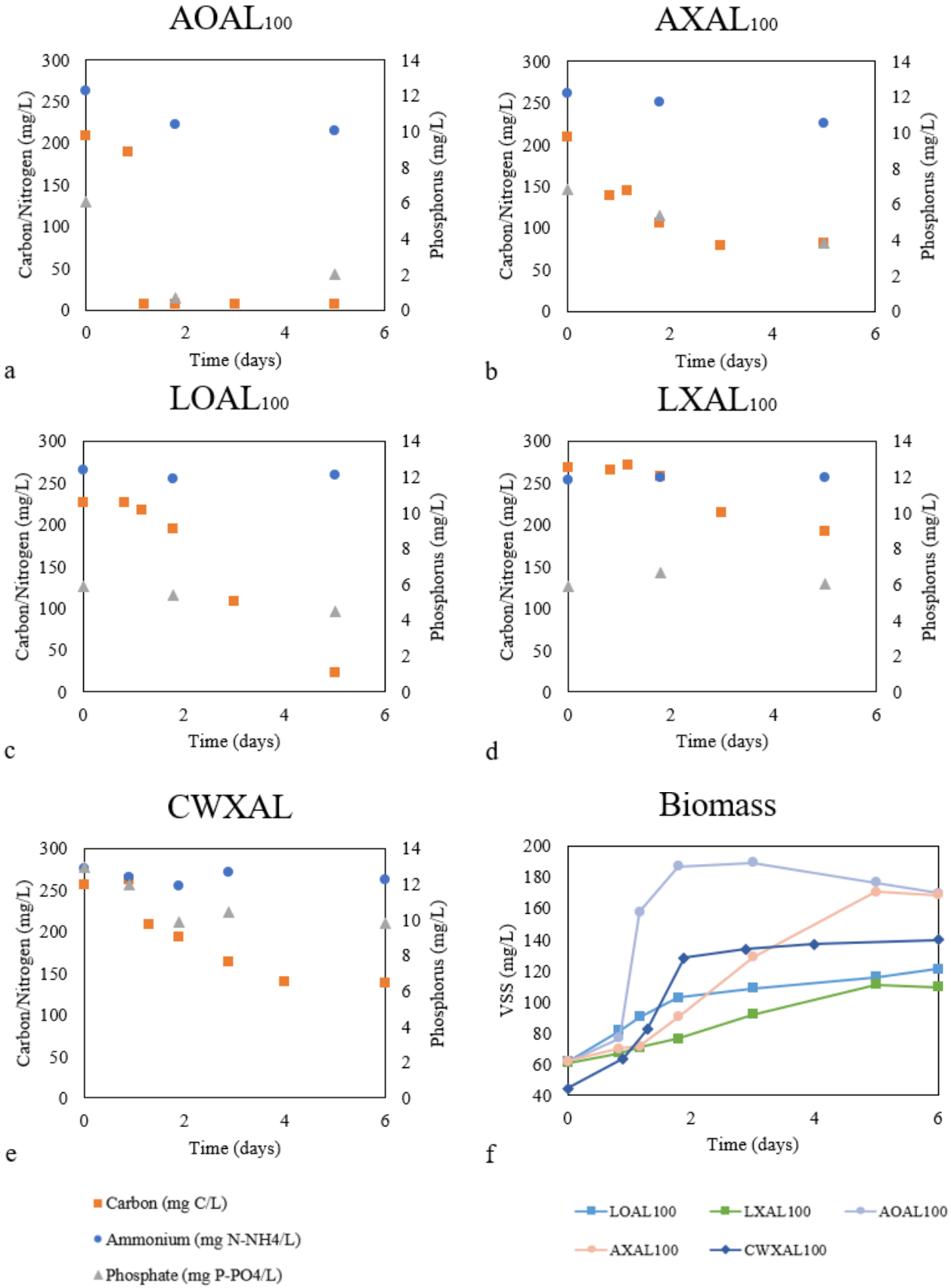

*Figure E.1: Nutrient consumption (carbon, nitrogen, and phosphorus) is shown from day 0 to day 6 in the photoorganoheterotrophic cultures AOAL$_{100}$ (**a**), AXAL$_{100}$ (**b**), LOAL$_{100}$ (**c**), LXAL$_{100}$ (**d**), and CWAL$_{100}$ (**e**). Biomass production in the same cultures is shown in Figure **f**.*

F. Carbon dioxide in the off-gas and dissolved oxygen in the Photobioreactor

Carbon dioxide and oxygen in the off-gas, as well as dissolved oxygen in the reactor, were continuously measured in the Photobioreactor. Oxygen in the off-gas, however, could not be calibrated in argon and was calibrated in compressed air. Therefore, this measurement only indicates a qualitative indication of the amount of oxygen in the off-gas. The measurement of dissolved oxygen was considered instead. The dissolved oxygen in the reactor and the carbon dioxide in the off-gas are shown in Figure F.1 and F.2. On day 9, the dilution rate was lowered from 0.24 to 0.17 d^{-1}. As a result, carbon dioxide in the off-gas decreased. Moreover, dissolved oxygen in the reactor increased once oxygenic phototrophs were able to grow inside the culture.

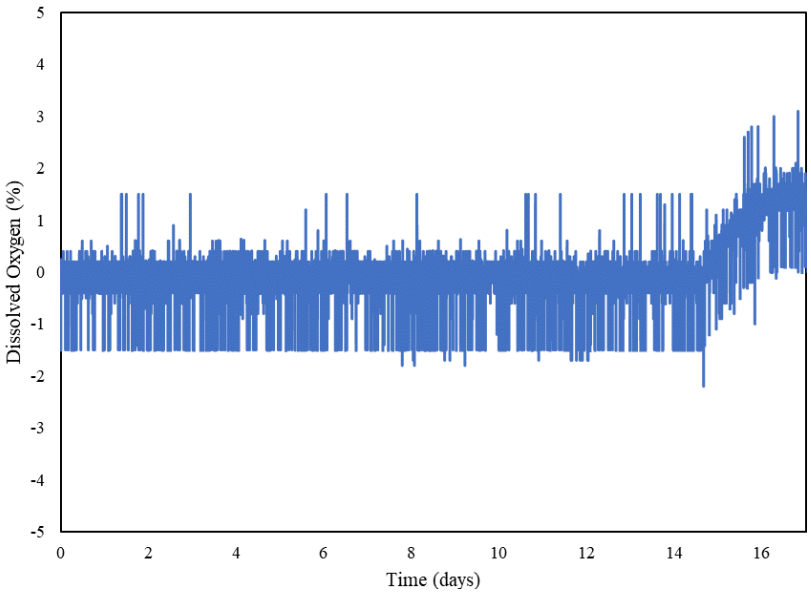

Figure F.1: Dissolved oxygen levels in the Photobioreactor. Dilution rate of 0.24 d^{-1} was applied between day 0 and 9, while 0.17 d^{-1} was applied from day 9 to 17. When phototrophs were able to grow inside the reactor, a higher oxygen concentration was found.

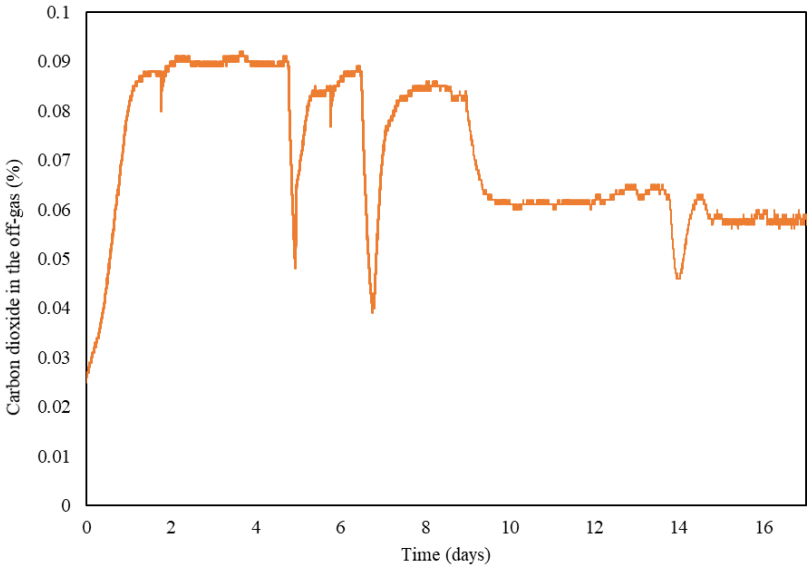

Figure F.2: Carbon dioxide concentration in the off-gas (argon, 100 mL min^{-1}). Dips in the concentration between day 0 and 9 were due to replacements of the medium bottle (biomass growth inside the bottle, due to inefficient sterilization, was observed). The strong decrease on day 9 was due to the lowering of the organic load. The dip around day 14 was not explained by changes of the set-up. However, it was concomitant with the increase in dissolved oxygen concentration.